

DYNAMICS OF MUSCLE BLOOD FLOW, O₂ UPTAKE AND MUSCLE
MICROVASCULAR OXYGENATION DURING EXERCISE

by

LEONARDO FRANKLIN FERREIRA

B.Sc., Universidade Estadual de Londrina, 2003

AN ABSTRACT OF A DISSERTATION

submitted in partial fulfillment of the requirements for the degree

DOCTOR OF PHILOSOPHY

Department of Anatomy and Physiology
College of Veterinary Medicine

KANSAS STATE UNIVERSITY
Manhattan, Kansas

2006

Abstract

The overall aim of this dissertation is to better understand the dynamic matching between O_2 delivery and uptake following the onset of exercise. The first study of this dissertation (Chapter 2) revealed that: i) the dynamics of muscle oxygenation were determined primarily by the $\dot{Q}O_2$ – $\dot{V}O_2$ interaction during the initial phase of $\dot{Q}O_2$ response (first 15-20 s); and ii) absolute values in the steady state used to calculate blood flow from $\dot{V}O_2$ and O_2 extraction did not affect the dynamics of blood flow response. Consistent with these predictions, using pulmonary gas exchange and near-infrared spectroscopy in humans (Chapter 3) we observed that the estimated kinetics of capillary blood flow (moderate exercise 25.4 ± 9.1 s and heavy exercise 25.7 ± 7.7 s) were not significantly different from the kinetics of muscle $\dot{V}O_2$ (moderate exercise 25.5 ± 8.8 s and heavy exercise 25.6 ± 7.2 s). In Chapter 4 we observed that nitric oxide (NO) is essential to maintain microvascular O_2 pressure ($PO_{2mv} \propto \dot{Q}O_2/\dot{V}O_2$) of contracting rat muscles. Blockade of NO synthase with L-NAME accelerated the kinetics [Δ Mean response time_(L-NAME-CONTROL) = -6.5 ± 6.6 s, $P < 0.05$] and reduced the contracting steady-state PO_{2mv} [ΔPO_{2mv} (L-NAME-CONTROL) = -5.0 ± 1.0 mmHg; $P < 0.05$] compared to control. In Chapter 5 we focused on the kinetics of bulk limb blood flow (LBF) to show that a low-pass filter (LP_{FILTER}) developed for LBF data improved the confidence of kinetic analysis by decreasing the standard error of the estimate ($SEE \propto 95\%$ confidence interval) for all kinetics parameters compared to the Beat-by-Beat method (e.g., time-constant phase 2: Beat-by-Beat = 16 ± 5 s; $LP_{\text{FILTER}} = 1.1 \pm 0.5$ s). In conclusion, the early increase in $\dot{Q}O_2$ is the main determinant of muscle oxygenation dynamics and NO is essential to maintain the tight coupling of $\dot{Q}O_2$ and $\dot{V}O_2$ kinetics during exercise. In this context, application of a LP_{FILTER} to LBF data provides the best confidence for kinetic analysis of bulk $\dot{Q}O_2$ that should facilitate investigations integrating bulk and microvascular $\dot{Q}O_2/\dot{V}O_2$ matching in a variety of settings in health and disease.

DYNAMICS OF MUSCLE BLOOD FLOW, O₂ UPTAKE AND MUSCLE
MICROVASCULAR OXYGENATION DURING EXERCISE

by

LEONARDO FRANKLIN FERREIRA

B.Sc., Universidade Estadual de Londrina, 2003

A DISSERTATION

submitted in partial fulfillment of the requirements for the degree

DOCTOR OF PHILOSOPHY

Department of Anatomy and Physiology
College of Veterinary Medicine

KANSAS STATE UNIVERSITY
Manhattan, Kansas

2006

Approved by:

Major Professor
Thomas J. Barstow

Abstract

The overall aim of this dissertation is to better understand the dynamic matching between O_2 delivery and uptake following the onset of exercise. The first study of this dissertation (Chapter 2) revealed that: i) the dynamics of muscle oxygenation were determined primarily by the $\dot{Q}O_2$ – $\dot{V}O_2$ interaction during the initial phase of $\dot{Q}O_2$ response (first 15-20 s); and ii) absolute values in the steady state used to calculate blood flow from $\dot{V}O_2$ and O_2 extraction did not affect the dynamics of blood flow response. Consistent with these predictions, using pulmonary gas exchange and near-infrared spectroscopy in humans (Chapter 3) we observed that the estimated kinetics of capillary blood flow (moderate exercise 25.4 ± 9.1 s and heavy exercise 25.7 ± 7.7 s) were not significantly different from the kinetics of muscle $\dot{V}O_2$ (moderate exercise 25.5 ± 8.8 s and heavy exercise 25.6 ± 7.2 s). In Chapter 4 we observed that nitric oxide (NO) is essential to maintain microvascular O_2 pressure ($PO_{2mv} \propto \dot{Q}O_2/\dot{V}O_2$) of contracting rat muscles. Blockade of NO synthase with L-NAME accelerated the kinetics [Δ Mean response time_(L-NAME-CONTROL) = -6.5 ± 6.6 s, $P < 0.05$] and reduced the contracting steady-state PO_{2mv} [$\Delta PO_{2mv(L-NAME-CONTROL)}$ = -5.0 ± 1.0 mmHg; $P < 0.05$] compared to control. In Chapter 5 we focused on the kinetics of bulk limb blood flow (LBF) to show that a low-pass filter (LP_{FILTER}) developed for LBF data improved the confidence of kinetic analysis by decreasing the standard error of the estimate ($SEE \propto 95\%$ confidence interval) for all kinetics parameters compared to the Beat-by-Beat method (e.g., time-constant phase 2: Beat-by-Beat = 16 ± 5 s; $LP_{FILTER} = 1.1 \pm 0.5$ s). In conclusion, the early increase in $\dot{Q}O_2$ is the main determinant of muscle oxygenation dynamics and NO is essential to maintain the tight coupling of $\dot{Q}O_2$ and $\dot{V}O_2$ kinetics during exercise. In this context, application of a LP_{FILTER} to LBF data provides the best confidence for kinetic analysis of bulk $\dot{Q}O_2$ that should facilitate investigations integrating bulk and microvascular $\dot{Q}O_2/\dot{V}O_2$ matching in a variety of settings in health and disease.

Table of Contents

List of Figures	vii
List of Tables	viii
Acknowledgements.....	ix
Preface.....	x
CHAPTER 1 - Introduction	1
CHAPTER 2 - Muscle blood flow - O ₂ uptake interaction and their relation to on-exercise dynamics of O ₂ exchange.....	4
Summary.....	5
Introduction.....	6
Methods	8
Results.....	11
Discussion.....	13
Conclusions.....	18
CHAPTER 3 - Muscle capillary blood flow kinetics estimated from pulmonary O ₂ uptake and near-infrared spectroscopy.....	30
Summary.....	31
Introduction.....	32
Methods	34
Results.....	38
Discussion.....	39
Conclusions.....	46
CHAPTER 4 - Effects of altered nitric oxide availability on rat muscle microvascular oxygenation during contractions.....	55
Summary.....	56
Introduction.....	57
Methods	59
Results.....	62
Discussion.....	63
Conclusions.....	68
CHAPTER 5 - Frequency domain characteristics and filtering of blood flow following the onset of exercise: implications for kinetics analysis	72

Summary.....	73
Introduction.....	74
Methods	76
Results.....	80
Discussion.....	82
Conclusion	88
CHAPTER 6 - Conclusions	102
References.....	103
Appendix A - Curriculum Vitae	115

List of Figures

Figure 2.1. Effects of altered venous O ₂ content and muscle O ₂ uptake parameters on muscle blood flow kinetics in Section I.	21
Figure 2.2. Effects of altered CvO ₂ time constant (τ) on blood flow kinetics.	22
Figure 2.3. Effects of CvO ₂ undershoot on blood flow kinetics.	23
Figure 2.4. Effects of CvO ₂ overshoot on blood flow kinetics.	24
Figure 2.5. Effects of altered phase 1 of blood flow on CvO ₂ kinetics.	25
Figure 2.6. CvO ₂ profile resulting from alterations in the phase 2 of blood flow.	26
Figure 2.7. CvO ₂ response to changes in the duration of phase 1 for blood flow.	27
Figure 2.8. CvO ₂ response to changes in amplitude of blood flow - phase 1 kinetics.	28
Figure 2.9. Dynamic coupling between muscle blood flow and oxygen consumption following the onset of exercise.	29
Figure 3.1. Schematic illustrating the estimation of muscle O ₂ uptake from pulmonary O ₂ uptake.	48
Figure 3.2. Representative data for moderate exercise.	49
Figure 3.3. Representative data for heavy exercise.	50
Figure 3.4. Estimated muscle capillary blood flow (moderate and heavy exercise).	51
Figure 3.5. Overall kinetics of deoxy-hemoglobin, O ₂ uptake and estimated capillary blood flow.	52
Figure 3.6. Relationship between kinetics of blood flow and O ₂ uptake.	53
Figure 4.1. Microvascular PO ₂ response from a representative animal.	69
Figure 4.2. Microvascular PO ₂ response normalized to mean arterial pressure.	70
Figure 4.3. Kinetics of microvascular PO ₂	71
Figure 5.1. Raw data during rest-to-exercise transition.	93
Figure 5.2. Time- and frequency-domain characteristics of simulated blood flow.	94
Figure 5.3. Effects of low-pass filtering on the kinetics of simulated blood flow.	95
Figure 5.4. Time- and frequency-domain characteristics of raw Doppler data.	96
Figure 5.5. Power spectral density of leg blood flow.	98
Figure 5.6. Representative leg blood flow response (5 transitions averaged).	99
Figure 5.7. Representative leg blood flow response (1 transition).	100
Figure 5.8. Results of SEE for each parameter describing the kinetics of blood flow.	101

List of Tables

Table 2.1 - Default values of the model parameters.	19
Table 2.2. Parameters used in Section I to simulate undershoots and overshoots of CvO_2	20
Table 3.1. Kinetic parameters of O_2 uptake, capillary blood flow and [HHb].	47
Table 5.1. Effects of simulated parameters on cutoff frequency for low pass filter.	89
Table 5.2. Kinetics parameters of leg blood flow for a single subject.....	90
Table 5.3. Parameter estimates describing the kinetics of blood flow for a single transition.	91
Table 5.4. Effects of cutoff frequency on kinetics parameters of leg blood flow for five transitions ensemble averaged.	92

Acknowledgements

Acquisition of the professional attributes and knowledge necessary to complete the Ph.D. degree is not limited to the years of graduate school, it goes beyond that and exceeds the boundaries of academic life. Therefore, many people will not be mentioned herein – it does not mean that I am not grateful to them or that they were not important, they definitely were, but I will limit to acknowledge those that had a direct impact on my life and academic career in the last five years. I would like to begin by thanking Prof. Thomas J. Barstow, my major Professor, Prof. David C. Poole and Prof. Timothy I. Musch, who were actively engaged in my education. Their teaching, guidance, kindness, understanding of my needs as a doctoral student and friendship were key for my progress as a scientist in-the-making. I also thank Drs. Craig A. Harms and Michael J. Kenney, Doctoral Committee members, for their support during the program. Next, I want to thank Ms. Sue Hageman, Dr. Brad. J. Behnke, Barbara J. Lutjemeier and Dana K. Townsend for their collaboration. However, I would not be at Kansas State University without the help of Drs. Brian J. Whipp, Janos Porszasz and Richard Casaburi from University of California at Los Angeles. Moreover, I would like to express my special thanks to Drs. Antonio F. Brunetto and Fabio O. Pitta from Universidade Estadual de Londrina – Brasil. On a personal note, I want to thank the Poole family – David, Katherine, Shayna, Connor and Kelton – it would not have been as much fun without you. My greatest gratitude and appreciation goes to my family: my beloved wife Mariane P. M. Ferreira, my father (Regis F. Ferreira), my mother (Greidinira M. Ferreira), my brothers (Jean F. Ferreira and Denis F. Ferreira) and my sister (Iane I. Ferreira). Uncle Milton C. Martins, who suggested academic career as a viable and interesting option, I am glad you were there when I needed you.

The continuous support, education, respect and consideration I have received from all of you (family, friends and Professors) were essential in my personal and academic life.

Preface

Each study of this dissertation has been published previously in physiology journals (citations below) and are reproduced here with permission from the publishers.

Ferreira, L.F., Poole, D.C., & Barstow, T.J. (2005). Muscle blood flow - O₂ uptake interaction and their relation to on-exercise dynamic of O₂ exchange. *Respir Physiol Neurobiol* **147**, 91-103.

Ferreira, L.F., Townsend, D.K., Lutjemeier, B.J., & Barstow, T.J. (2005). Muscle capillary blood flow kinetics estimated from pulmonary O₂ uptake and near-infrared spectroscopy. *J Appl Physiol* **98**, 1820-1828.

Ferreira, L.F., Padilla, D.J., Williams, J., Hageman, K.S., Musch, T.I., & Poole, D.C. (2006). Effects of altered nitric oxide availability on rat muscle microvascular oxygenation during contractions. *Acta Physiologica* **186**, 223-232.

Ferreira, L.F., Harper, A.H., & Barstow, T.J. (2006). Frequency-domain characteristics and filtering of blood flow following the onset of exercise: implications for kinetics analysis. *J Appl Physiol* **100**, 817-825.

CHAPTER 1 - Introduction

On a daily basis humans and animals perform activities that are of relatively short duration within a wide range of exertion intensity. These require an increase in oxygen uptake ($\dot{V}O_2$) to meet the metabolic demands of the contracting muscles. Specifically, following the onset of exercise, the requirement for adenosine triphosphate (ATP) increases immediately to a new (higher) steady state whereas muscle $\dot{V}O_2$ (oxidative phosphorylation) increases monoexponentially reaching a steady state within 30 to 300 s depending on the species, age, training and health status (Jones & Poole, 2005). The conventional wisdom is that the kinetics of $\dot{V}O_2$, by determining the size of the O_2 deficit and reliance on finite nonoxidative energy sources [e.g., glycolysis and phosphocreatine (PCr)], has a direct impact on exercise tolerance. Given the burden of chronic diseases characterized by severe exercise intolerance – diabetes, chronic obstructive lung disease, chronic heart failure and cancer to mention just a few – the understanding of what factors limit the kinetics of $\dot{V}O_2$ is of relevance not only to basic and applied physiology but also to medical practice and improvement of the quality of life of many patients (Jones & Poole, 2005).

The increase in $\dot{V}O_2$ depends on O_2 being delivered at a sufficient rate by adjustments that occur in the cardiovascular and pulmonary systems. Several studies have demonstrated that the kinetics of $\dot{V}O_2$ are not limited by bulk O_2 delivery ($\dot{Q}O_2$) in healthy young individuals and isolated muscles (e.g., Grassi *et al.* 1998; Bangsbo *et al.* 2000; Behnke *et al.* 2002; Burnley *et al.* 2002; Koga *et al.* 2005), but many investigators have been skeptical with regard to these conclusions because whole-limb/muscle measurements do not reflect events occurring at the capillary-to-myocyte interface where gas exchange takes place. In recent years technological advances facilitated assessment of $\dot{Q}O_2$ -to- $\dot{V}O_2$ matching in the skeletal muscle microcirculation of humans [near-infrared spectroscopy (Bellardinelli *et al.* 1997; DeLorey *et al.* 2003; Grassi *et al.* 2003)] and rats [phosphorescence quenching (Rumsey *et al.* 1988; Poole *et al.* 1995; Behnke *et al.* 2001)]. In general, investigation of the dynamic balance between $\dot{Q}O_2$ and $\dot{V}O_2$ in the microcirculation confirmed the predictions from bulk measurements, i.e., $\dot{Q}O_2$ did not limit the kinetics of $\dot{V}O_2$ following the onset of exercise. However, in chronic diseases and aging a different scenario emerged suggesting derangements in convective and diffusive O_2 transport as primary mediators of slowed $\dot{V}O_2$ kinetics (Diederich *et al.* 2002; Behnke *et al.* 2002b, 2005; DeLorey *et al.* 2004a). Thus, there has been growing interest in studying the dynamics of

muscle O₂ exchange to gain insights into the impact of diseases and the mechanisms of $\dot{Q}O_2$ - $\dot{V}O_2$ matching. However, advances in the field have been hindered by a poor understanding of how to interpret the dynamics of O₂ exchange. In this context, we developed the study described in Chapter 2 to clarify how $\dot{Q}O_2$ and $\dot{V}O_2$ interact to determine the dynamic profile of estimated O₂ extraction (near-infrared spectroscopy in humans) and microvascular O₂ pressures (PO_{2mv}; phosphorescence quenching in rats). Moreover, this study formed the theoretical basis for the investigation presented in Chapter 3, where we propose a new method to estimate noninvasively the kinetics of muscle capillary blood flow in humans. This method will permit large-scale assessment of microvascular $\dot{Q}O_2$ in exercising humans to examine dysfunction and effectiveness of therapies.

Several mechanisms have been proposed to explain the increase in blood flow following the onset of exercise including a muscle-pump effect, metabolite-induced vasodilation, nitric oxide (NO), prostaglandins and ATP among others (Clifford & Hellsten, 2004). Pathological profiles of PO_{2mv} have been demonstrated in conditions associated with diminished endothelial NO production suggesting an important role for NO on PO_{2mv}, which is directly proportional to the $\dot{Q}O_2$ -to- $\dot{V}O_2$ ratio. In the context of $\dot{Q}O_2$ - $\dot{V}O_2$ matching, as a support to oxidative phosphorylation, NO is a double-edged sword because it might simultaneously elevate muscle blood flow and inhibit mitochondrial oxidative phosphorylation. Human studies addressing this issue are controversial (Joyner & Dietz, 1997; Clifford & Hellsten, 2004), but, in many instances these are of limited scope because the distress caused by pharmacological and invasive interventions necessary to elucidate underlying mechanisms are unethical. In Chapter 4 we examined the role of NO in the dynamics and steady state of muscle oxygenation using the exposed rat spinotrapezius muscle.

The controversy surrounding the mechanisms of blood flow regulation is, in part, due to the fact that these studies have focused on the steady state of contractions. Since the various vasodilatory pathways are thought to be redundant, investigation in the steady state is not ideal (Laughlin & Korzick, 2001). Assessment of blood flow dynamics is relevant because it allows direct comparison with the kinetics of $\dot{V}O_2$ to examine the $\dot{Q}O_2$ - $\dot{V}O_2$ matching and could reveal important aspects of control of blood flow that are not evident in the steady state. For example, pharmacological blockade of a pathway essential for the increase in blood flow could slow the kinetics with achievement of similar steady states during control and blockade due to redundancy of regulatory mechanisms. However, the low signal-to-noise ratio of blood flow measurements with resolution sufficient for kinetics analysis in animals and humans (Doppler ultrasound) have limited the assessment of blood flow (and $\dot{Q}O_2$) kinetics with a confidence interval of parameter estimates narrow enough to draw definitive conclusions about blood flow regulation. In Chapter

5 we examined the validity and effectiveness of a filtering procedure to reduce the signal-to-noise ratio and accentuate the underlying kinetics of blood flow. This should facilitate development of studies aiming to elucidate the mechanisms controlling blood flow (kinetics) during exercise and derangements in aging and/or chronic diseases.

Therefore, the studies described herein were designed to further our understanding of the $\dot{Q}O_2$ - $\dot{V}O_2$ matching following the onset of exercise. Each chapter is self-contained following the standard journal article format (*Introduction, Methods, Results, Discussion and Conclusions*), whilst only one set of references was included in the end of the dissertation to avoid repetition.

**CHAPTER 2 - Muscle blood flow - O₂ uptake interaction and their
relation to on-exercise dynamics of O₂ exchange**

Summary

A computer model was developed to provide a theoretical framework for interpreting the dynamics of muscle capillary O₂ exchange in health and disease. We examined the effects of different muscle oxygen uptake ($\dot{V}O_{2m}$) and CvO₂ profiles on muscle blood flow (\dot{Q}_m) kinetics ($\dot{Q}_m = \dot{V}O_{2m}/[CaO_2 - CvO_2]$). Further, we simulated $\dot{V}O_{2m}$ and \dot{Q}_m responses to predict the CvO₂ profile and the underlying dynamics of capillary O₂ exchange ($CvO_2 = CaO_2 - \dot{V}O_{2m}/\dot{Q}_m$). Exponential equations describing $\dot{V}O_{2m}$, CvO₂ and \dot{Q}_m responses *in vivo* were used in the simulations. The results indicated that \dot{Q}_m kinetics were relatively insensitive to CvO₂ parameters, but directly associated with $\dot{V}O_{2m}$ kinetics. The biphasic \dot{Q}_m response produced a substantial fall in CvO₂ within the first 15-20 s of the exercise transition (phase 1 of \dot{Q}_m). These results revealed that the main determinant of CvO₂ (or O₂ extraction) kinetics was the dynamic interaction of \dot{Q}_m and $\dot{V}O_{2m}$ kinetics during phase 1 of \dot{Q}_m .

Introduction

Microvascular (phosphorescence quenching) and tissue (near-infrared spectroscopy, NIRS) oxygenation measurement techniques have revealed marked pathological alterations in capillary O₂ exchange within the muscle in disease states such as heart failure and diabetes (Belardinelli *et al.*, 1997; Diederich *et al.*, 2002; Behnke *et al.*, 2002b). However, interpretation of these findings is limited by a lack of understanding of the interrelationships among muscle oxygen uptake ($\dot{V}O_{2m}$), capillary blood flow (\dot{Q}_m), and O₂ extraction [\sim venous O₂ content (CvO₂), when CaO₂ is constant]. For instance, microvascular PO₂ profiles reported in diabetic rats (Behnke *et al.*, 2002b) and estimated capillary O₂ extraction in older human subjects (DeLorey *et al.*, 2004a) suggested a complex relationship between \dot{Q}_m and $\dot{V}O_{2m}$ that was not completely explained by assuming monoexponential \dot{Q}_m and $\dot{V}O_{2m}$ responses (Barstow *et al.*, 1990; Behnke *et al.*, 2002a; Diederich *et al.*, 2002). To date, the CvO₂ dynamics following the onset of exercise have not been systematically investigated to clarify how $\dot{V}O_{2m}$ and \dot{Q}_m are temporally associated to yield the profiles of O₂ exchange previously reported (Behnke *et al.*, 2002c; Behnke *et al.*, 2003; Diederich *et al.*, 2002).

Although recognizing that exercise hyperemia has two phases (Shoemaker & Hughson, 1999), the results from prior studies have been interpreted (Diederich *et al.*, 2002; Grassi *et al.*, 2003; DeLorey *et al.*, 2004a) and modeled (Barstow *et al.*, 1990; Behnke *et al.*, 2002a) considering \dot{Q}_m as a monoexponential response. However, the observed kinetics of muscle blood flow are biphasic during rest-exercise (MacDonald *et al.*, 1998; Shoemaker & Hughson, 1999; Kindig *et al.*, 2002b) and unloaded exercise-exercise transitions (Koga *et al.*, 2005). Interestingly, simulations of $\dot{V}O_{2m}$ and CvO₂ kinetics (similar to observed PO_{2mv} or O₂ extraction profiles) to predict the time course of \dot{Q}_m in the present study did not result in the noticeable two-exponential \dot{Q}_m response described in previous studies (see *Results* from Section I). Therefore, to investigate which CvO₂ (or O₂ extraction) profile would be associated with a biphasic \dot{Q}_m response (MacDonald *et al.*, 1998; Kindig *et al.*, 2002b; Koga *et al.*, 2005), we extended previous modeling studies (Barstow *et al.*, 1990) by simulating a two-exponential \dot{Q}_m response along with a monoexponential $\dot{V}O_{2m}$ (Section II). We predicted that this would yield new insights into those mechanisms underlying the dynamics of O₂ exchange in the microcirculation.

Thus, the present study was undertaken to provide a solid theoretical foundation from which to explore the mechanistic bases for physiologic and pathologic observations of microvascular PO₂ and tissue oxygenation. The study was divided into two sections. In the first section our aim was to estimate the \dot{Q}_m dynamics necessary to produce a given CvO₂ profile, as

implied from previous reports of PO_{2mv} and deoxyhemoglobin ([HHb], by NIRS) kinetics (Behnke *et al.*, 2002c; Diederich *et al.*, 2002; Grassi *et al.*, 2003; DeLorey *et al.*, 2004a). In addition, these simulations would provide the basis for estimating the kinetics of muscle capillary blood flow based on noninvasive estimates of $\dot{V}O_{2m}$ and microcirculatory O_2 extraction kinetics {i.e. [HHb] (t)}, which is an important step that has not, as yet, been performed (Grassi *et al.*, 2003; DeLorey *et al.*, 2004a). In the first section of this study a biphasic \dot{Q}_m response was not detected reliably by nonlinear regression analysis, therefore, the second part was designed to extend previous computer modeling studies (Barstow *et al.*, 1990; Behnke *et al.*, 2002a) by simulating a two-exponential \dot{Q}_m response in order to investigate the resulting CvO_2 (O_2 extraction) profile.

Methods

Model: In Section I the model was designed to simulate $\dot{V}O_{2m}$ and CvO_2 responses to study the independent effects of their kinetic parameters on \dot{Q}_m kinetics. Exponential equations describing $\dot{V}O_{2m}$ and O_2 extraction (Barstow *et al.*, 1990; Grassi *et al.*, 1996) or PO_{2mv} (Behnke *et al.*, 2002a) observed *in vivo* were used in the simulations. For $\dot{V}O_{2m}$ the equation was

$$\dot{V}O_{2m} = \dot{V}O_{2(BSL)} + A \cdot (1 - e^{-t/\tau}) \quad (1)$$

where BSL is baseline; A, amplitude and τ , time constant of response. Similarly, CvO_2 was described as

$$CvO_2 = CvO_{2(BSL)} - A \cdot (1 - e^{-(t-TD)/\tau}) \quad (2)$$

where TD is time delay and BSL, A, and τ are as defined above. A more complex equation was also included to generate CvO_2 profiles with overshoots (OS) and/or undershoots (US) to replicate patterns reported in health (Grassi *et al.*, 1996; Behnke *et al.*, 2002a) and disease conditions (Diederich *et al.*, 2002), respectively. To obtain smooth CvO_2 responses and closely approximate *in vivo* profiles we used a double exponential equation. Specifically,

$$\begin{aligned} CvO_2 = CvO_{2(BSL)} + A_u \cdot (1 - e^{-(t-TD)/\tau_u}) & \quad \text{upward component} \\ - A_d \cdot (1 - e^{-(t-TD)/\tau_d}) & \quad \text{downward component} \end{aligned} \quad (3)$$

where subscripts (u) and (d) represent the upward and downward components, respectively. Overshoots will be observed when the time course of the upward component is faster than the downward component ($\tau_u < \tau_d$) while undershoots will be determined by a downward component occurring faster than the upward response ($\tau_d < \tau_u$). For overshoots and undershoots, $A_d > A_u$ and the steady state amplitude will be equal to $A_d - A_u$ (see *Appendix* for exact values). The initial parameter values used in the simulations were obtained from published data. Specifically, baseline and steady state values of $\dot{V}O_{2m}$ and CvO_2 were taken from those reported by Richardson *et al.* (Table 2 in Richardson *et al.*, 1993) for knee extension exercise, whereas the kinetic parameters for $\dot{V}O_{2m}$ and CvO_2 (O_2 extraction) were equivalent to $\dot{V}O_{2p}$ (phase 2) and deoxy-Hb/Mb (or [HHb] as used herein) reported by Grassi *et al.* (2003). The values used for CvO_2 (TD and τ) are also consistent with the results obtained in a dog gastrocnemius preparation (Grassi *et al.*, 2002). The default values are shown in Table 2.1. Simulations were accomplished

by varying one kinetic parameter (τ or TD) of $\dot{V}O_2$ or CvO_2 while keeping the remaining values in the default condition. On the other hand, amplitudes (A in *Eq. 1* and 2) of $\dot{V}O_{2m}$ and CvO_2 were altered concurrently so that the steady state $\dot{V}O_{2m}$ to \dot{Q}_m relationship would reproduce the data reported for different work rates (Richardson *et al.*, 1993). Muscle blood flow was calculated from the resulting $\dot{V}O_{2m}$ and CvO_2 profiles by rearrangement of the Fick equation where $\dot{Q}_m = \dot{V}O_2 / (CaO_2 - CvO_2)$. For all situations CaO_2 was assumed to be $20 \text{ ml } O_2 \cdot 100 \text{ ml}^{-1}$ and constant. The resulting \dot{Q}_m response was fitted by a monoexponential model using nonlinear regression procedures (Sigma Plot 2001, Jandel Scientific) where

$$\dot{Q}_m = \dot{Q}_{m(BSL)} + A_1 \cdot (1 - e^{-(t-TD)/\tau}) \quad (4)$$

where BSL, A , τ and TD are defined above. A double exponential fitting was not justified because an exponential phase 1 response was not reliably discerned either by the curve fitting computer routine with analysis of residuals, or by visual inspection.

In Section II we simulated \dot{Q}_m and $\dot{V}O_{2m}$ to investigate the resulting CvO_2 profile. This section extended previous simulations (Barstow *et al.*, 1990; Behnke *et al.*, 2002a; Diederich *et al.*, 2002) by incorporating a physiologically relevant biphasic \dot{Q}_m response (Shoemaker & Hughson, 1999; Kindig *et al.*, 2002b). $\dot{V}O_{2m}$ was again modeled as a monoexponential response (*Eq. 1*) and the \dot{Q}_m response was simulated using a two exponential equation

$$\begin{aligned} \dot{Q} = \dot{Q}_{m(BSL)} + A_1 \cdot (1 - e^{-t/\tau_1}) & \quad \text{Phase 1} \\ + A_2 \cdot (1 - e^{-(t-TD_2)/\tau_2}) & \quad \text{Phase 2} \end{aligned} \quad (5)$$

where BSL is baseline; A , amplitude; τ , time constants and TD, time delay of each phase. Subscripts (1) and (2) refer to each phase of the response. Phase 1 was described up to TD_2 and its observed amplitude calculated as $A'_1 = A_1 \cdot (1 - e^{-TD_2/\tau_1})$. In turn, A'_1 was manipulated to simulate changes in the amplitude of phase 1. In this series $\tau\dot{V}O_{2m}$ and τ_1 , τ_2 , TD_2 and A'_1 (as a fraction of total amplitude, where $A_{tot} = A'_1 + A_2$) for \dot{Q}_m , were varied. The baseline, steady state values and default parameters of $\dot{V}O_{2m}$ and \dot{Q}_m are shown in Table 1. Slightly different values for \dot{Q}_m and CvO_2 , compared to Section I, were used so that a greater CvO_2 amplitude could be studied allowing better representation and analysis of the data. Unfortunately, detailed information regarding \dot{Q}_m kinetic parameters is limited and our choice for default τ_1 was based on average values of published data (MacDonald *et al.*, 1998; MacDonald *et al.*, 2000; Radegran & Saltin, 1998) while $\tau_2\dot{Q}_m$ was initially set equal to $\tau\dot{V}O_{2m}$ and $A'_1 = 0.4 A_{tot}$ based on visual inspection of Fig. 5 from Grassi *et al.* (1996). Although these values may not reflect universally

the underlying physiological responses, they do provide a standard condition for the modeling. Further, the simulations were designed to include the spectrum of conditions likely to be observed *in vivo*.

CvO₂ was calculated from the Fick equation solved for CvO₂ where,

$$CvO_2 = CaO_2 - \frac{\dot{V}O_{2m}}{\dot{Q}_m} \quad (6)$$

CaO₂ was the same as in Section I (i.e., 20 ml O₂·100 ml⁻¹). The resulting CvO₂ was then fitted by nonlinear regression procedures using *Eq. 2* to yield the τ and TD. The resulting CvO₂ profile was not always truly exponential (see *Results*), but *Eq. 2* provides quantitative information about the overall temporal profile. However, in some conditions an exponential model was not possible. In case of an initial overshoot the portion of the data corresponding to values above baseline were ignored in the nonlinear regression procedure.

For each of the simulations in Sections I and II we assumed a monoexponential increase in $\dot{V}O_{2m}$ from the onset of exercise and a homogeneous muscle compartment represented by a single set of parameters (amplitudes, time constants and time delays). Moreover, neither diffusion limitation nor the presence of anatomical or physiological shunts was incorporated in the simulations.

Results

Section I: The effects of varying the parameters describing CvO_2 and $\dot{V}O_{2m}$ on \dot{Q}_m kinetics are depicted in Figures 2.1-2.4. $\tau\dot{Q}_m$ was not affected (range 28.0 to 28.6 s) by the baseline values of CvO_2 (range 7.5 to 12 ml $O_2 \cdot 100 \text{ ml}^{-1}$; Fig. 2.1A). The effects of changes in the amplitude of CvO_2 (ΔCvO_2) were also small (Fig. 2.1B); $\tau\dot{Q}_m$ was 28.3 s when $\Delta CvO_2 = 3 \text{ ml } O_2 \cdot 100 \text{ ml}^{-1}$ and 26.6 s for $\Delta CvO_2 = 7 \text{ ml } O_2 \cdot 100 \text{ ml}^{-1}$. The effects of altered time-related parameters for CvO_2 are shown in Fig. 2.1C (TD- CvO_2) and Fig. 2.2 (τCvO_2). An increase in TD from 5 to 15 s led to a small decrease in $\tau\dot{Q}_m$ from 29 to 27 s, showing that the CvO_2 time delay had only a minor effect on the overall \dot{Q}_m kinetics. A 5 fold increase in τCvO_2 from 5 to 25 s resulted in only a ~ 4 s decrease in $\tau\dot{Q}_m$ (Fig. 2.2B and 2.2C). In contrast to the minor effects of CvO_2 parameter alterations on the resulting \dot{Q}_m kinetics, $\tau\dot{Q}_m$ was strongly dependent on, but ~ 2 s faster than, $\tau\dot{V}O_{2m}$ (Fig. 2.1D). An alternative interpretation for these results is that CvO_2 kinetics has little effect on the $\dot{V}O_{2m}$ kinetics, which is primarily affected by the dynamics of \dot{Q}_m (but see *Discussion*). This is consistent with measurements of $\dot{V}O_{2m}$ and \dot{Q}_m kinetics in humans (Grassi *et al.*, 1996) suggesting that $\dot{V}O_{2m}$ and \dot{Q}_m are closely linked following the onset of exercise.

In health and disease conditions, overshoots (OS) and undershoots (US) in CvO_2 (or PO_{2mv}) have been reported (Grassi *et al.*, 1996; Bangsbo *et al.*, 2000; Diederich *et al.*, 2002) and simulation of these responses yielded interesting results. As expected, undershoots were associated with progressively slower $\tau\dot{Q}_m$ relative to $\tau\dot{V}O_{2m}$ (Fig. 2.3). $\tau\dot{Q}_m$ for the deepest undershoot simulated was ~ 6 s slower than in the default condition (no undershoot). The surprising finding was that large changes in CvO_2 had relatively small effects on \dot{Q}_m kinetics. The US simulations included an 8 s time delay for CvO_2 and we acknowledge that if TD were 0 an even greater effect would have been observed (~ 2 s estimated from simulation of TD- CvO_2 ; see above). In contrast to what we anticipated, an OS (Fig. 2.4) did not lead to clear biphasic \dot{Q}_m responses, and only minor effects on $\tau\dot{Q}_m$ were again observed. $\tau\dot{Q}_m$ was only 1.5 s slower in the default condition (no overshoot) than when the amplitude of OS was 30% of the baseline CvO_2 (greatest values simulated; Fig. 2.4B). For this data set $\tau\dot{V}O_{2m}$ was 30 s and $\tau\dot{Q}_m = 27.1$ s (see Fig. 2.4C), demonstrating that an overshoot is not an indication that $\tau\dot{Q}_m$ is substantially (10-15 s) faster than $\tau\dot{V}O_{2m}$ (Barstow *et al.*, 1990). For comparison, in Fig. 2.4 this situation ($\tau\dot{Q}_m$ 15 s faster than $\tau\dot{V}O_{2m}$) is simulated (gray lines in panels B and C). The resulting overshoot, relatively long TD- CvO_2 (~ 40 s) and slow CvO_2 kinetics are not compatible with direct measurements of CvO_2 (Grassi *et al.*, 1996; Bangsbo *et al.*, 2000; Grassi *et al.*, 2002) or PO_{2mv} kinetics (Behnke *et al.*, 2002a). Altogether, these results suggest that \dot{Q}_m kinetics are relatively insensitive to CvO_2

(i.e., O₂ extraction) kinetics. However, stated in the alternative, more physiological direction (where CvO₂ is the dependent variable and $\dot{V}O_{2m}$ and \dot{Q}_m are considered independent variables, as in Eq. 6), CvO₂ is very sensitive to small changes in the relationship of \dot{Q}_m and $\dot{V}O_{2m}$ kinetics.

Section II: In this section a two-exponential muscle blood flow was coupled to the default monoexponential $\dot{V}O_{2m}$ to examine the determinants of CvO₂ kinetics. The most striking observation was the rapid fall in CvO₂ (~ 80%) occurring during phase 1 of the \dot{Q}_m response (Figs. 2.5-2.6) as a consequence of the continuing monoexponential increase in $\dot{V}O_{2m}$ at the time when \dot{Q}_m was initially plateauing. As observed in Section I, CvO₂ kinetics were very sensitive to changes in \dot{Q}_m kinetics, primarily during phase 1 (Fig. 2.5). During phase 2, the effects of \dot{Q}_m on the CvO₂ profile were most noticeably observed when $\tau_2\dot{Q}_m$ was slower than $\tau\dot{V}O_2$ (Fig. 2.6), which resulted in transient undershoots. When fitted by a monoexponential function the overall kinetics underwent only minor changes for $\tau_2\dot{Q}_m$ ranging from 30 to 45 s. When $\tau_2\dot{Q}_m$ was faster than $\tau\dot{V}O_2$ by only 5 s (25 vs. 30 s; Fig. 2.6) the CvO₂ profile was inconsistent with direct measurements (Grassi *et al.*, 1996; Behnke *et al.*, 2002a; Grassi *et al.*, 2002).

In general, as a consequence of the biphasic \dot{Q}_m , CvO₂ (or O₂ extraction) did not follow a ‘true’ exponential profile; however, physiological measurement noise, as in real data, would tend to mask this nonexponential characteristic of the response. In fact, direct measurements of PO_{2mv} (Behnke *et al.*, 2002a) and estimates of O₂ extraction (Grassi *et al.*, 2003) dynamics are relatively well described by exponential equations (as in Eq. 2).

Subsequent simulations revealed that the characteristics of the phase 1 of \dot{Q}_m response [time constant (τ_1), Fig. 2.5; time delay (TD₂), Fig. 2.7; and amplitude (A'_1), Fig. 2.8] were the main determinants of CvO₂ kinetics (both τ and TD). The effect of a slower $\tau_1\dot{Q}_m$ was that TD-CvO₂ became shorter and τ CvO₂ became slower (longer) while the equivalent of the mean response time ($\tau + TD$) remained reasonably constant (~ 13 s; Fig. 2.5). On the other hand, changes in the duration of phase 1 (TD₂; Fig. 2.7) had negligible effects on TD-CvO₂ but τ CvO₂ became progressively slower with decreases in TD₂, e.g, increasing the contribution of phase 2 to the overall response by 6 s (TD₂ from 15 to 9 s) resulted in a 15 s slower τ CvO₂. The effects of the amplitude of phase 1 were also appreciable (A'_1 ; Fig. 2.8). In the conditions simulated, when the amplitude at the end of phase 1 represented 30% of the overall increase in \dot{Q}_m (i.e., $A'_1 = 0.3 A_{tot}$) this resulted in a shorter TD and undershoot in CvO₂ which consequently led to faster apparent τ CvO₂. In contrast, $A'_1 = 0.5 A_{tot}$ produced a greater overshoot, longer TD and slower τ CvO₂ when compared to the default condition ($A'_1 = 0.4 A_{tot}$).

Discussion

The principal novel finding from Section I was that the \dot{Q}_m kinetics were relatively insensitive to alterations in the CvO_2 parameters but were sensitive to alterations in $\dot{V}O_{2m}$ kinetics. Conversely, from the more physiological perspective (where $\dot{V}O_{2m}$ and \dot{Q}_m are the independent variables, as in Eq. 6), CvO_2 kinetics were very sensitive to small changes in the relationship between \dot{Q}_m and $\dot{V}O_{2m}$ kinetics. The main observations from Section II were: 1) The fall in CvO_2 occurred predominantly during phase 1 of the \dot{Q}_m response (within 15-20 s of exercise onset); and consequently 2) Phase 1 parameters of \dot{Q}_m (time constant, amplitude and duration), as well as the parameters of $\dot{V}O_{2m}$, (i.e., interaction between $\dot{V}O_{2m}$ and \dot{Q}_m during phase 1 of \dot{Q}_m response) were the main determinants of CvO_2 (or O_2 extraction) kinetics.

Determination of \dot{Q}_m kinetics from $\dot{V}O_{2m}$ and CvO_2 responses (Section I): The simulations here showed that \dot{Q}_m kinetics were directly associated with $\dot{V}O_{2m}$ kinetics. This observation is consistent with a study using cycling as the exercise paradigm (Grassi *et al.*, 1996) suggesting that in the transition to cycling exercise the overall kinetics of \dot{Q}_m and $\dot{V}O_{2m}$ are temporally closely linked ($MRT \dot{Q}_m \sim \tau \dot{V}O_{2m}$). This close association may arise, by examination of the Fick equation, from the fact that \dot{Q}_m can increase 20-fold from rest (e.g. Radegran & Saltin, 1998) whereas over a similar range of metabolic rates O_2 extraction may increase only 50-60 % (e.g. Roach *et al.*, 1999). Thus, under normal physiological conditions increases in $\dot{V}O_{2m}$ through changes in O_2 extraction are relatively limited. However, this must not be misinterpreted to suggest that the rate of increase in \dot{Q}_m is the factor limiting $\dot{V}O_{2m}$ kinetics, as previously shown (Grassi *et al.*, 1998).

In investigations of $\dot{V}O_{2m}$ and \dot{Q}_m responses to exercise an overshoot in CvO_2 has been interpreted as a faster initial adjustment of O_2 delivery compared to utilization (Barstow *et al.*, 1990; Grassi *et al.*, 1996; Behnke *et al.*, 2002a). We incorporated the CvO_2 overshoot in the current model and the resulting overall \dot{Q}_m kinetics were indeed faster (~ 2 s) than $\tau \dot{V}O_{2m}$; nonetheless, as shown in Fig. 2.4, the CvO_2 profile resulting from $\tau \dot{Q}_m = \frac{1}{2} \tau \dot{V}O_{2m}$, as previously considered (Barstow *et al.*, 1990), was not consistent with direct measurements in humans (Grassi *et al.*, 1996; Bangsbo *et al.*, 2000) or animals (Behnke *et al.*, 2002a; Grassi *et al.*, 2002). In this circumstance the CvO_2 time delay (time from onset of exercise to where CvO_2 crossed baseline value) was ~ 40 s, whereas shorter time delays are observed in humans (6-10 s; Grassi *et al.*, 1996; Bangsbo *et al.*, 2000), dog gastrocnemius (~ 8 s; Grassi *et al.*, 2002) and rat spinotrapezius muscle (15-20 s; Behnke *et al.*, 2002a).

In the rat spinotrapezius (Behnke *et al.*, 2002a) and soleus muscle (Behnke *et al.*, 2003) as well as in the dog gastrocnemius (Piiper *et al.*, 1968; Grassi *et al.*, 2002) the \dot{Q}_m kinetics described by a monoexponential fitting is 6-10 s faster than $\dot{V}O_{2m}$ kinetics, while for the peroneal muscle \dot{Q}_m kinetics have been estimated as 3 s faster than $\dot{V}O_{2m}$ kinetics (Behnke *et al.*, 2003). In humans, the \dot{Q}_m kinetics were slightly (2-3 s), but not significantly faster than $\dot{V}O_{2m}$ kinetics (Grassi *et al.*, 1996), consistent with the results from the present study. Multiple factors could explain the dissimilarities between human and animal studies, including species differences, fibre type characteristics of the muscle investigated (Behnke *et al.*, 2003) and/or the experimental protocol which could result in different profiles of \dot{Q}_m phase 1. We used values for the kinetic parameters measured during cycling exercise; however, during knee-extension exercise (rest-exercise transitions), for instance, phase 1 amplitude may be as high as 0.8 A_{tot} (MacDonald *et al.*, 1998) and its time constant appears to be faster than for unloaded exercise-exercise transitions (Koga *et al.*, 2005). In the case of rest-exercise transition \dot{Q}_m kinetics (mean response time) were faster than $\dot{V}O_{2m}$ kinetics (estimated from $\dot{V}O_{2p}$ phase 2) (MacDonald *et al.*, 1998), possibly due to a greater muscle-pump effect on \dot{Q}_m phase 1 response.

Implications of biphasic \dot{Q}_m response (Section II): In the transitional phase exercise hyperemia is characterized by a biphasic response, with the initial fast phase lasting 15-20 s (Shoemaker & Hughson, 1999; Kindig *et al.*, 2002b). The faster O_2 delivery during the initial \dot{Q}_m phase is thought to result in a CvO_2 overshoot (Barstow *et al.*, 1990; Grassi *et al.*, 1996; Behnke *et al.*, 2002a). However, in the previous section simulation of CvO_2 overshoots did not lead to a clear exponential phase 1 of \dot{Q}_m (Fig. 2.4). The question then becomes “Which CvO_2 (or O_2 extraction) profile is associated with a biphasic \dot{Q}_m response?” To answer this question we extended previous modeling studies (Barstow *et al.*, 1990) by simulating a two-exponential \dot{Q}_m response along with the default monoexponential $\dot{V}O_{2m}$ to study the CvO_2 profile. The most striking result from this series of simulations was that the overshoot and predominant fall in CvO_2 occurred within the first 15-20 s (phase 1 of \dot{Q}_m response). In this instance, phase 1 parameters (amplitude, time constant and duration as TD_2) were the main determinants of CvO_2 kinetics (Figs. 2.5, 2.7 and 2.8). In addition, phase 2 kinetics of \dot{Q}_m appeared to be closely linked to $\dot{V}O_2$ kinetics.

Phase 1 of the exercise hyperemia has a fast time constant (Shoemaker & Hughson, 1999) that appears to be mediated by a muscle-pump mechanism (Sheriff *et al.*, 1993; Tschakovsky *et al.*, 1996; Sheriff & Hakeman, 2001), which may be potentiated by a rapid vasodilation (Hamann *et al.*, 2004b; Tschakovsky *et al.*, 2004); for review see (Tschakovsky & Sheriff, 2004). However, these two mechanisms do not explain the biphasic response *per se*, and

the nature of this phenomenon is not clear at present. In microcirculatory preparations, muscle contraction leads to localized arteriolar dilation consisting of two distinct phases (Gorczyński *et al.*, 1978). Further, a two-exponential increase in red blood cell (RBC) flux through skeletal muscle capillaries (Kindig *et al.*, 2002b) indicates that the biphasic response is not an event exclusive to large conduit vessels.

The effects of phase 1 kinetics of \dot{Q}_m on the CvO_2 profile were remarkable. A slower phase 1 of \dot{Q}_m (longer τ_1) resulted in shorter TD- CvO_2 (Fig. 2.5) whereas a prolonged duration (Fig. 2.7) and diminished amplitude (Fig. 2.8) of phase 1 \dot{Q}_m produced undershoots in CvO_2 . Endothelium-derived vasodilators (e.g. nitric oxide, Sheriff & Hakeman, 2001) and the muscle-pump are considered to represent important determinants of phase 1. Consistent with this notion, the profiles of CvO_2 undershoot observed in Figures 2.5, 2.7 and 2.8 are similar to those seen in older adults (Fig. 3 in DeLorey *et al.*, 2004a) and animal models of diabetes (Behnke *et al.*, 2002b) and heart failure (Diederich *et al.*, 2002) that are associated with compromised endothelial function (Drexler *et al.*, 1992; Taddei *et al.*, 1995; De Vriese *et al.*, 2000), muscle-pumping capacity (Shiotani *et al.*, 2002) and impaired capillary hemodynamics following the onset of exercise (Richardson *et al.*, 2003).

The \dot{Q}_m phase 2 response has been thought to involve integrated processes leading to vascular smooth muscle relaxation (Shoemaker & Hughson, 1999). In this study we observed that when \dot{Q}_m phase 2 began (or emerged), CvO_2 had already reached $\sim 85\%$ of the steady state exercise value (Fig. 2.6). Interestingly, the estimated capillary O_2 extraction kinetics ([HHb], by NIRS) in humans (Grassi *et al.*, 2003) and visual inspection of Fig. 2 from Grassi *et al.* (2002) for the dog gastrocnemius contracting at 65-70% $\dot{V}O_{2max}$ reveals a similar response, where more than 80% of the adjustment of O_2 extraction from the baseline to the exercise steady state was achieved within 20-25 s. From the Fick principle, a direct implication of this finding is that the kinetics of \dot{Q}_m phase 2 are closely related to the time course of $\dot{V}O_{2m}$ because under such circumstances $\dot{V}O_{2m}$ and \dot{Q}_m (phase 2) increase in parallel [N.B. As mentioned above, this does not mean that \dot{Q}_m is limiting $\dot{V}O_{2m}$ kinetics (Grassi *et al.*, 1998)]. A different representation of this concept is shown in Figure 2.9 by the linear relationship between $\dot{V}O_{2m}$ and \dot{Q}_m during phase 2. This figure qualitatively resembles Fig. 5 from Grassi *et al.* (1996) for moderate cycling exercise and, within the parameters of this simulation, indicates that $\tau_2 \dot{Q}_m$ is similar to ($\pm 2-3$ s) $\tau \dot{V}O_{2m}$. From this figure it is possible to analyze the $\dot{V}O_{2m}$ -to- \dot{Q}_m coupling in the transitional phase especially when distinction between phase 1-2 is difficult or not justified by the curve fitting routine as a result of sampling strategies [e.g., one data point at each 3-5 s in the first 30 s and every 15-30 s from 30 s to the end of exercise (Behnke *et al.*, 2002a; Grassi *et al.*, 2002)].

Contracting skeletal muscle blood flow is controlled by a complex interplay among mechanical (muscle pump), neural and chemical stimuli [rev. (Laughlin & Korzick, 2001; Clifford & Hellsten, 2004; Thomas & Segal, 2004)]. Rigorous investigation of the role of each potential hyperemic mediator on the kinetics of \dot{Q}_m remains to be undertaken. However, the theoretical analysis presented herein, as well as inspection of the microvascular PO_2 profiles in diabetes (Behnke *et al.*, 2002b) and heart failure (Diederich *et al.*, 2002) reveals that the \dot{Q}_m increase between ~ 10 and 30 s (i.e., across the transition between phase 1 and phase 2) is of crucial importance. As apparent in Figures 2.3, 2.6-2.8, this is when the venous O_2 content (and microvascular PO_2) typically fall to their lowest points (below the subsequent steady-state values in diabetes and heart failure) and O_2 flux is most likely to become diffusion limited thereby increasing the size of the O_2 deficit. Consequently, crucial insights into the mechanistic bases for the slowed VO_2 kinetics, high O_2 deficit and exercise intolerance in diabetes (Regensteiner *et al.*, 1998) and heart failure (e.g. Hepple *et al.*, 1999) will depend on rapid, high-fidelity \dot{Q}_m measurements in the phase 1-phase 2 transition, i.e., ~ 10 - 30 s following the onset of contractions.

Model limitations and assumptions: A potential confounding factor in the interpretation of predictions from the current simulations is that we used baseline and steady state values of $\dot{V}O_{2m}$, \dot{Q}_m and CvO_2 determined for knee-extension exercise (Richardson *et al.*, 1993), while the kinetic parameters were obtained from cycling exercise (Grassi *et al.*, 2003). However, the results from Section I suggest that, within physiological limits, the effects of baseline and amplitude of response (or steady state values) for the three variables included in the modeling have negligible effects on the kinetics of the response. It is important to note that the default time constant of phase 1 of \dot{Q}_m for the simulations of Section II were taken from knee-extension exercise where rest-exercise transitions were investigated (MacDonald *et al.*, 1998; MacDonald *et al.*, 2000) and phase 1 kinetics are potentially faster ($\tau_1 \sim 4$ s) than for unloaded exercise-exercise transitions ($\tau_1 \sim 8$ s; Koga *et al.*, 2005); however, this does not limit the predictions of the modeling to rest-exercise transitions because we have performed simulations of τ_1 ranging from 2 to 8 s (Fig. 5).

In this study we assumed a monoexponential increase in $\dot{V}O_{2m}$ following the onset of exercise and a homogeneous muscle compartment without addressing the effects of O_2 conductance (DO_2) on PO_{2mv} dynamics, where DO_2 is a lumped coefficient which includes all impediments to the flux of O_2 from capillaries to mitochondria [from Fick's Law $\dot{V}O_2 = DO_2 \cdot (PO_{2capillary} - PO_{2mito})$]. In isolated single myocytes (Kindig *et al.*, 2003) and rat skeletal muscle with preserved blood supply (Behnke *et al.*, 2002a) $\dot{V}O_2$ has been shown to increase

immediately (no time delay) following the onset of contraction. In humans, phosphocreatine kinetics (presumably reflecting $\dot{V}O_{2m}$) are monoexponential with no delay (Rossiter *et al.*, 1999). These studies support our assumption of monoexponential increase in $\dot{V}O_{2m}$ without a time delay following the onset of exercise. In contrast, skeletal muscle is heterogeneous regarding blood flow (Laughlin & Armstrong, 1982) and O_2 exchange profile (Behnke *et al.*, 2003). Blood flow and \dot{Q}_m -to- $\dot{V}O_{2m}$ heterogeneity (Whipp *et al.*, 1995) and diffusion limitation (Roca *et al.*, 1989) are important determinants of venous O_2 content and pressure, while muscle O_2 conductance (DO_2) may affect microvascular PO_2 kinetics (Geer *et al.*, 2002). Thus, we acknowledge that the current assumptions are likely oversimplifications of the real physiology, but they are a starting point to conceptually understand the mechanisms underlying the physiological and pathological responses observed in previous investigations.

Conclusions

Our computer simulations have demonstrated that the time course (kinetics) of \dot{Q}_m estimated from CvO_2 (i.e., O_2 extraction) and $\dot{V}O_{2m}$ dynamics (Section I) is relatively insensitive to alterations of CvO_2 parameters, mainly baseline and steady state values, but is closely related to $\dot{V}O_{2m}$ kinetics confirming empirical observations (Grassi *et al.*, 1996). Interpreted in a physiological sense (where $\dot{V}O_{2m}$ and \dot{Q}_m are considered independent variables), the kinetics of CvO_2 were very sensitive to minor changes in the relationship between \dot{Q}_m and $\dot{V}O_{2m}$ kinetics. Modeling a biphasic \dot{Q}_m response (Section II) resulted in an initial overshoot and subsequent rapid fall in CvO_2 . This temporal characteristic of CvO_2 was the obligatory consequence of an ongoing monoexponential increase in $\dot{V}O_{2m}$ in the presence of an initial rapid increase in \dot{Q}_m with subsequent transient plateau at a value inferior to its final steady state response towards the end of phase 1 (15-20 s). In this context, the CvO_2 response was almost complete (>80%) within the first 15-20 s of exercise and the resulting relatively constant CvO_2 during phase 2 implied a close dynamic coupling of $\dot{V}O_{2m}$ and \dot{Q}_m in this second phase of the blood flow response up to the steady state. It is important to note, however, that the dynamics of muscle oxygen uptake and blood flow will affect the temporal characteristics of O_2 extraction, whereas the steady state value of $(CaO_2 - CvO_2)$ will be determined by the steady state relationship between $\dot{V}O_{2m}$ and \dot{Q}_m .

Future directions: This study predicts that in the transition to exercise, CvO_2 (or O_2 extraction) is very sensitive to subtle changes in the dynamic balance between \dot{Q}_m and $\dot{V}O_{2m}$. In this context, the [HHb] signal from NIRS (a proxy of O_2 extraction; Grassi *et al.*, 2003), and PO_{2mv} by phosphorescence quenching (Rumsey *et al.*, 1988; Behnke *et al.*, 2002a) are promising techniques to aid in the investigation of \dot{Q}_m kinetics. Specifically, our results lead to the following questions: What mechanism(s) determine the amplitude and time constant of phase 1 of \dot{Q}_m ? Are phase 2 and phase 1 distinct responses, i.e., does phase 2 start or emerge at the observed time delay of phase 2? What are the mechanisms underlying the time delay of phase 2? What dictates the apparent tight coupling between phase 2 \dot{Q}_m and $\dot{V}O_{2m}$? and, finally, Which specific parameters of the \dot{Q}_m response are changed by interventions such as exercise training and pharmacological blockade of vasodilator/vasoconstrictor pathways? The answers to these questions are imperative to understanding the control of blood flow following the onset of exercise and the \dot{Q}_m , $\dot{V}O_{2m}$ and O_2 extraction profiles observed in states of health and disease.

Table 2.1 - Default values of the model parameters.

	$\dot{V}O_{2m}$	\dot{Q}_m	CaO ₂	CvO ₂
Section I				
Baseline	50	400	20	7.5
Exercise	810	5226	20	4.5
TD	-	-	-	8
τ	30	-	-	10
Section II				
Baseline	50	500	20	10
Exercise	810	5400	20	5
τ	30	-	-	-
τ_1	-	4	-	-
A' ₁	-	1960	-	-
TD ₂	-	15	-	-
τ_2	-	30	-	-
A ₂	-	2940	-	-

$\dot{V}O_{2m}$, muscle oxygen consumption ($ml \cdot min^{-1}$); \dot{Q}_m , muscle blood flow ($ml \cdot min^{-1}$); CaO₂, arterial oxygen concentration ($ml O_2 \cdot 100 ml^{-1}$); CvO₂, venous oxygen concentration ($ml O_2 \cdot 100 ml^{-1}$); TD, time delay (s); τ , time constant (s); A, amplitude (see units for each variable).

Subscripts 1 and 2 denote the phase of \dot{Q}_m response. *Dash*, parameter not applicable for the given variable. Model parameters of Section I were obtained from Richardson et al. (1993) (baseline and steady state values) and Grassi et al. (2003) (time delay and time constants). For Section II the \dot{Q}_m parameters were estimated from published data (Grassi *et al.*, 1996; MacDonald *et al.*, 1998; MacDonald *et al.*, 2000). See text for further details.

Appendix – Chapter 2

Table 2.2. Parameters used in Section I to simulate undershoots and overshoots of CvO_2 .

	Undershoot			Overshoot		
TD (s)	8	8	8	0	0	0
τ_u (s)	40	90	200	5	5	5
τ_d (s)	10	10	10	10	10	10
A_u (ml $O_2 \cdot 100 \text{ ml}^{-1}$)	2	2	2	6	10	14
A_d (ml $O_2 \cdot 100 \text{ ml}^{-1}$)	5	5	5	9	13	17

TD, time delay. τ , time constant; and A, amplitude. Subscripts (u) and (d) refer to upward and downward components of Eq. 3. Baseline and steady state values of CvO_2 and $\dot{V}O_{2m}$ parameters are shown in Table 2.1 (Methods). From left to right the parameters will yield a progressively greater amplitude of undershoot or overshoot.

Figure 2.1. Effects of altered venous O₂ content and muscle O₂ uptake parameters on muscle blood flow kinetics in Section I.

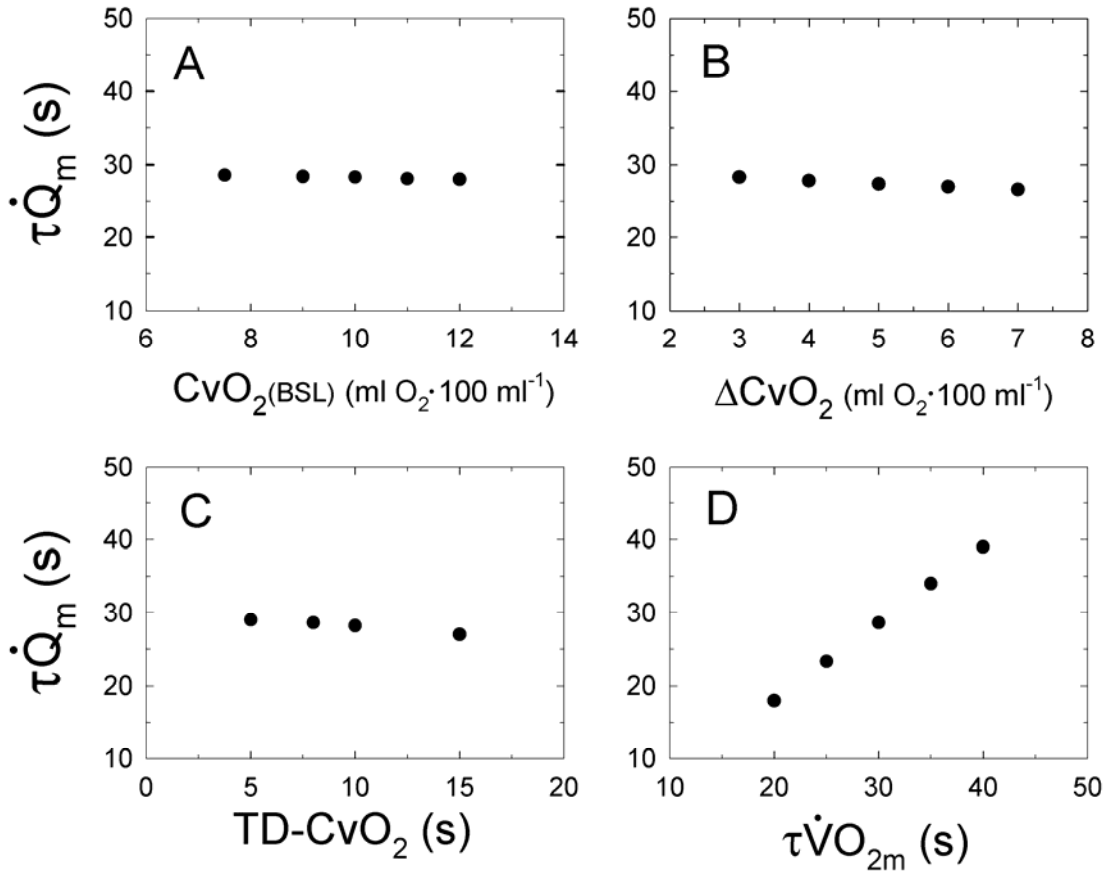


Figure 2.1. Effects of altered venous O₂ content (CvO_2) and muscle oxygen uptake ($\dot{V}O_{2m}$) parameters on muscle blood flow (\dot{Q}_m) kinetics in Section I. τ , time constant; TD, time delay; BSL, baseline; ΔCvO_2 , amplitude of change from BSL. In (B) baseline CvO_2 was 10 ml O₂·100 ml⁻¹, otherwise the parameters are as shown in Table 2.1. $\tau\dot{Q}_m$ is shown on the same scale in A-D to facilitate comparison among conditions. See text for further details. Note the strong dependency of $\tau\dot{Q}_m$ on muscle $\dot{V}O_2$ kinetics (D), but otherwise relative independency of the parameters of the CvO_2 response (A-C).

Figure 2.2. Effects of altered CvO_2 time constant (τ) on blood flow kinetics.

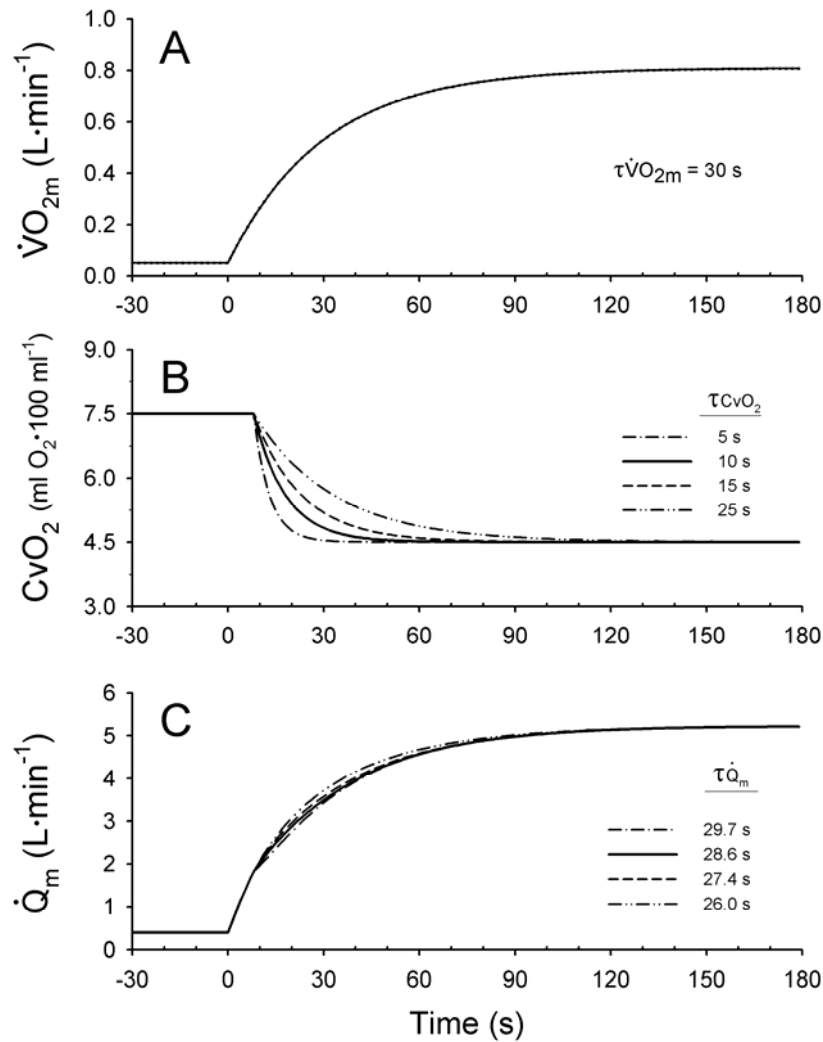


Figure 2.2. Effects of altered CvO_2 time constant (τ) on \dot{Q}_m kinetics. In this figure \dot{Q}_m (shown in C) was determined from simulation of $\dot{V}O_{2m}$ and CvO_2 using the Fick principle. The parameters used in A and B (except for τCvO_2 ; given in B) are shown in Table 1. The time constants shown in C were obtained by monoexponential fitting. *Solid line* represents the default condition for section I. Note that $\tau\dot{Q}_m$ is slightly faster than, but similar to $\tau\dot{V}O_{2m}$ despite large differences in τCvO_2 .

Figure 2.3. Effects of CvO₂ undershoot on blood flow kinetics.

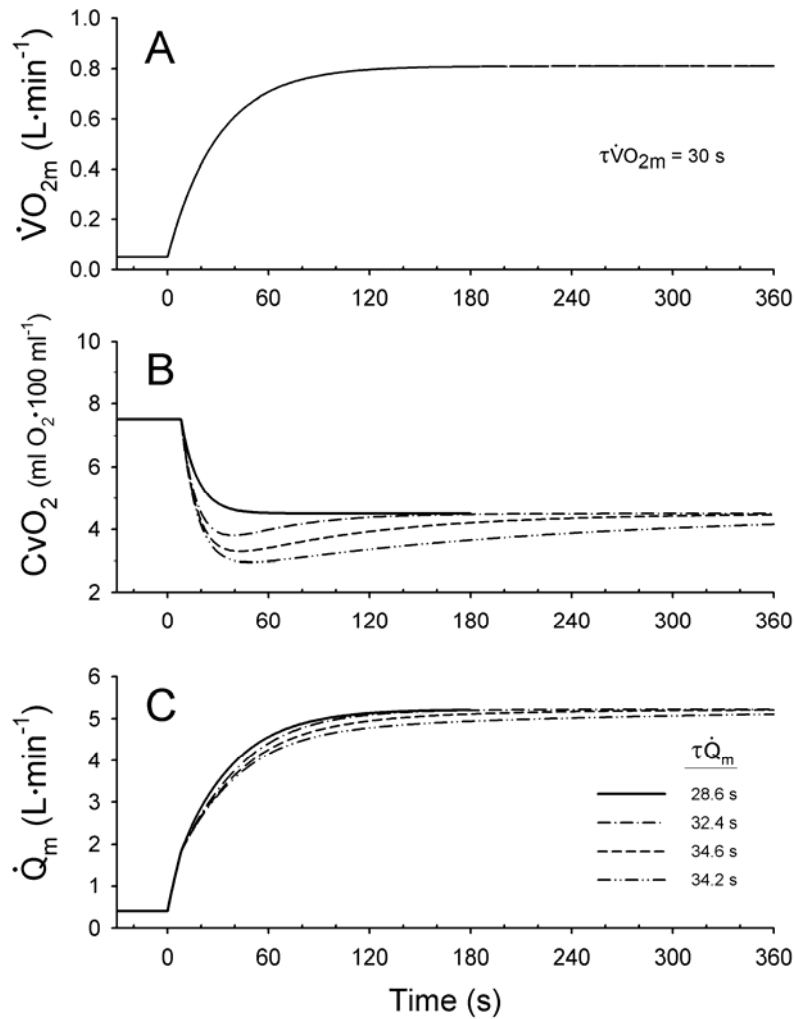


Figure 2.3. Effects of CvO₂ undershoot on \dot{Q}_m kinetics. The parameters used to simulate the responses shown in *A* and *B* are given in Table 2.1 (Methods) and Table 2.2 (*Appendix – Chapter 2*), respectively. See legend in Fig. 2.2 for further details. Note that compared to Fig. 2.2, undershoots in CvO₂ are associated with \dot{Q}_m kinetics being slower than $\dot{V}O_{2m}$ kinetics.

Figure 2.4. Effects of CvO_2 overshoot on blood flow kinetics.

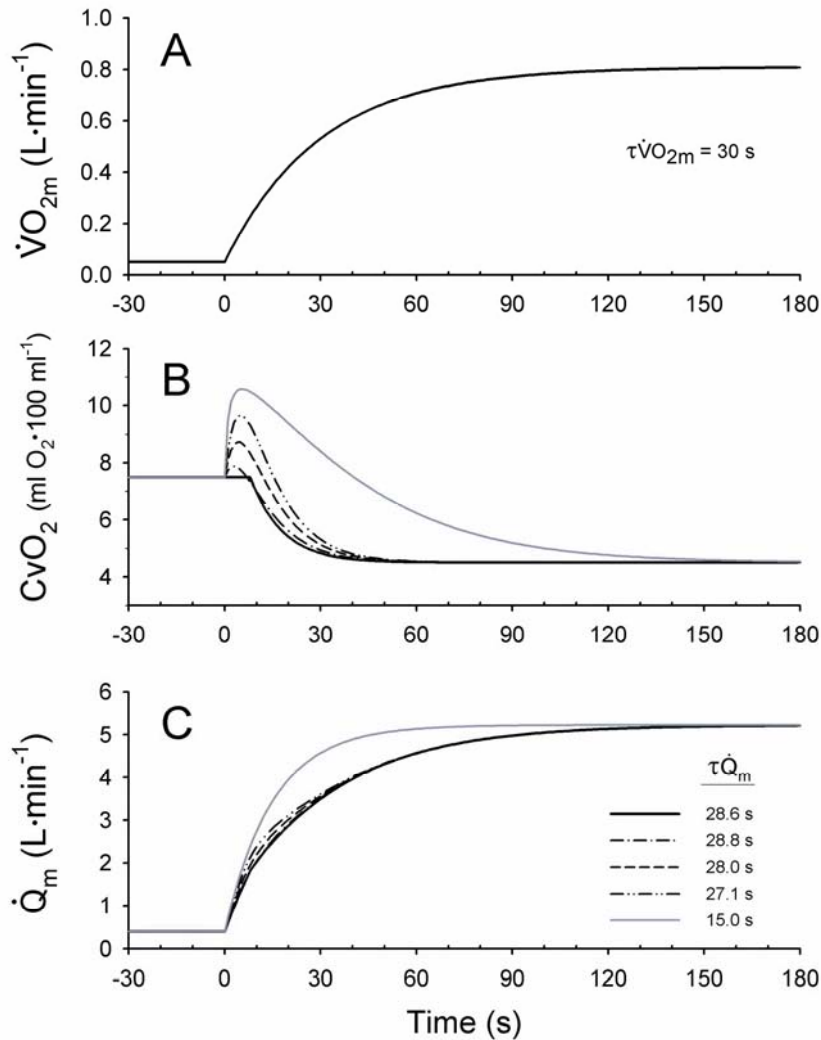


Figure 2.4. Effects of CvO_2 overshoot on \dot{Q}_m kinetics. The parameters used to simulate the responses shown in *A* and *B* are given in Table 2.1 (Methods) and Table 2.2 (*Appendix-Chapter 2*), respectively. *Solid lines (gray)* in *B* and *C* were obtained from modeling both \dot{Q}_m and $\dot{V}O_{2m}$ as monoexponential increases at the onset of exercise where $\tau\dot{V}O_{2m} = 30$ s and $\tau\dot{Q}_m = 15$ s to illustrate the effects of faster \dot{Q}_m on the CvO_2 profile (Barstow *et al.*, 1990; Grassi *et al.*, 1996). In this situation CvO_2 values below baseline were not observed until ~ 40 s. See Fig. 2.2 for further details.

Figure 2.5. Effects of altered phase 1 of blood flow on CvO₂ kinetics.

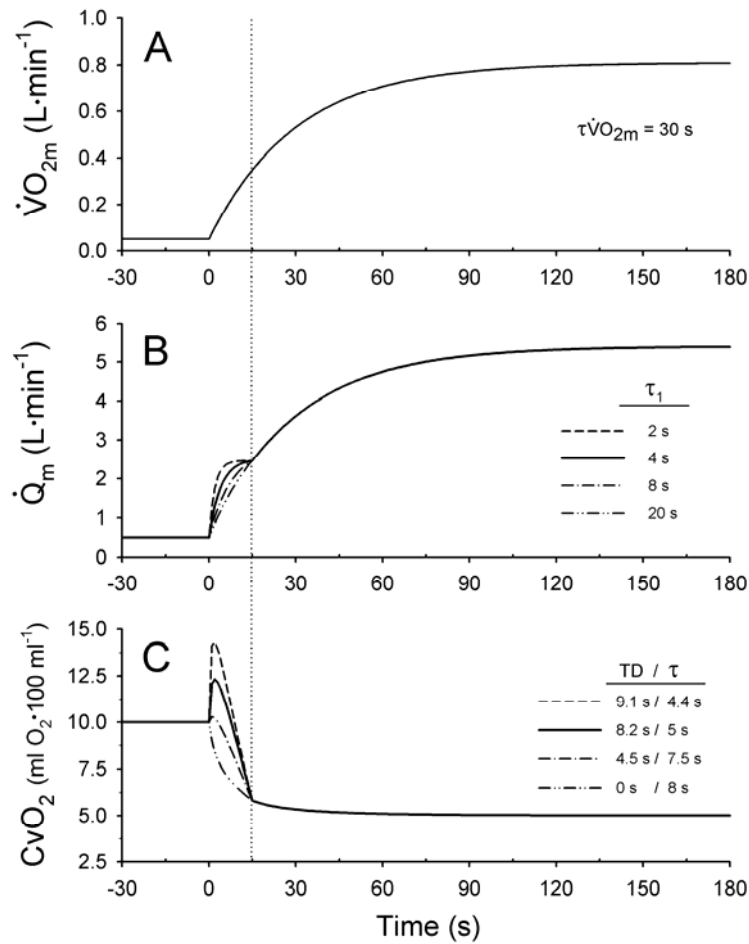


Figure 2.5. Effects of altered \dot{Q}_m phase 1 time constant (τ_1) on CvO₂ kinetics. CvO₂ was determined from simulation of $\dot{V}O_{2m}$ and \dot{Q}_m using Eq. 6. The parameters used to simulate $\dot{V}O_{2m}$ and \dot{Q}_m (except τ_1) are given on Table 1, while τ_1 values are shown in B. In C the time delay (TD) and time constant (τ) were determined by fitting the response with Eq. 2 (Methods). The response is not exponential but TD and τ provide quantitative values with which to analyze the effects of \dot{Q}_m phase 1 (B) on CvO₂ kinetics. Note that the faster the τ_1 for \dot{Q}_m , the greater the initial overshoot in CvO₂. Solid line represents the default condition for Section II.

Figure 2.6. CvO₂ profile resulting from alterations in the phase 2 of blood flow.

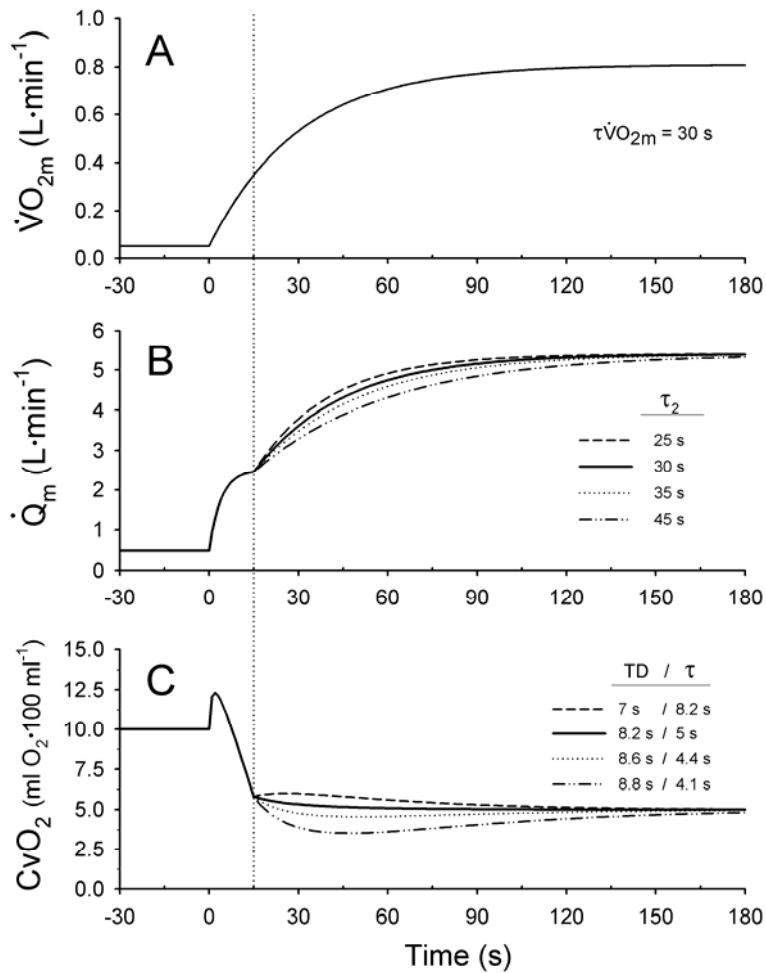


Figure 2.6. CvO₂ profile resulting from simulation of a biphasic \dot{Q}_m response with varying phase 2 time constant (τ_2). Note that when τ_2 for \dot{Q}_m is greater than $\tau\dot{V}O_{2m}$ there is a slight undershoot in CvO₂. Also, note that most of the fall in CvO₂ occurs within the phase 1 time period (15 s in this data set). *Solid line* represents the default condition for Section II. See *Fig. 2.5* and text for further details.

Figure 2.7. CvO₂ response to changes in the duration of phase 1 for blood flow.

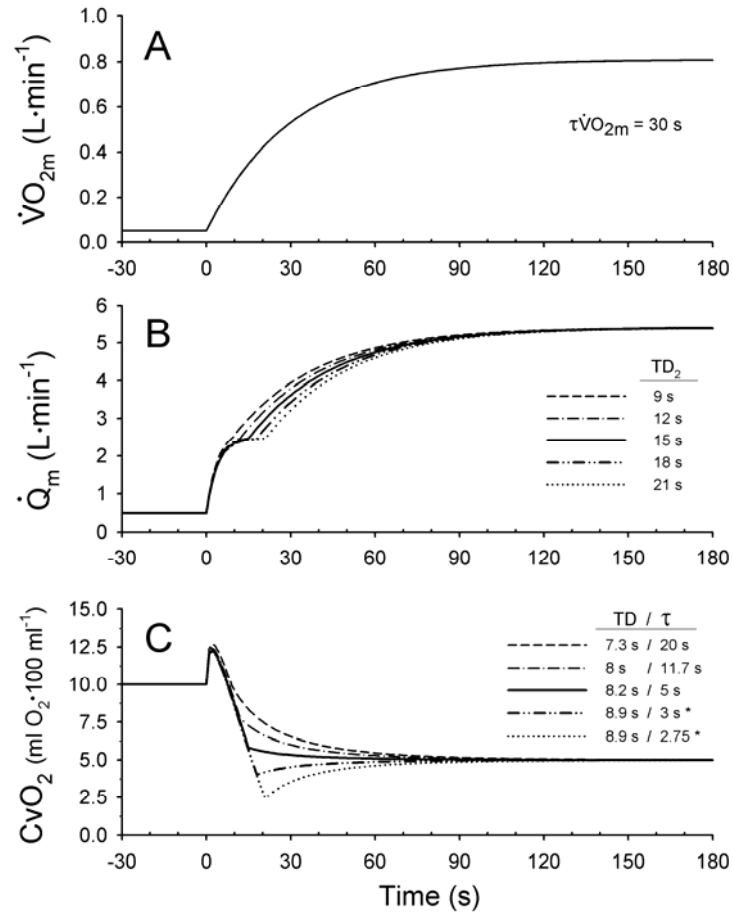


Figure 2.7. CvO₂ response to changes in the duration of phase 1 for \dot{Q}_m . * curve fitting did not follow the undershoot (below steady state) portion of CvO₂ (monoexponential fitting, Eq. 2), but the results are shown to demonstrate the effects likely to be observed when fitting is done on “real” data under similar conditions. Solid line represents the default condition for Section II. For further details and abbreviations see Fig. 2.5.

Figure 2.8. CvO₂ response to changes in amplitude of blood flow - phase 1 kinetics.

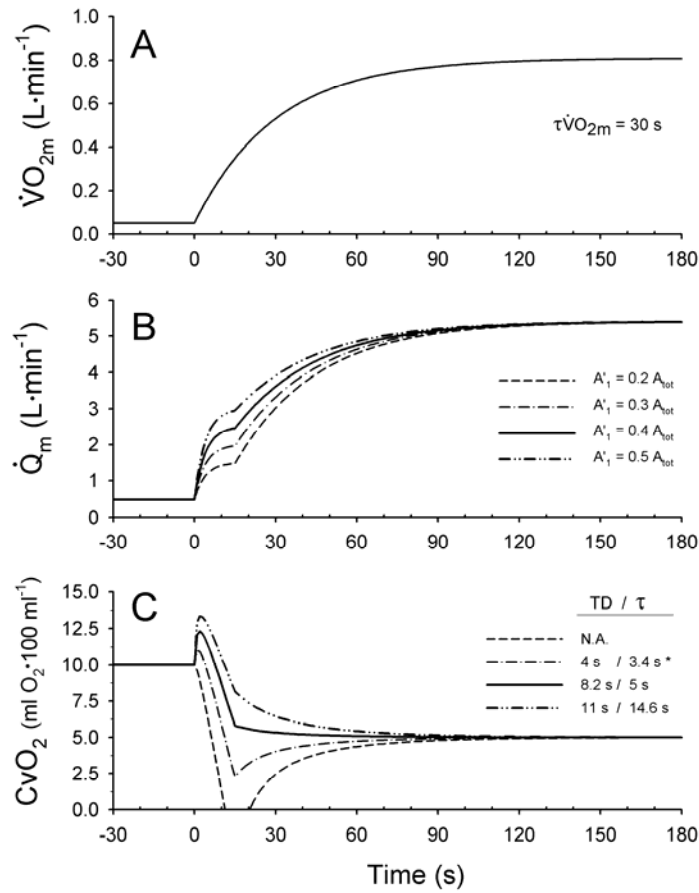


Figure 2.8. CvO₂ response to changes in amplitude of \dot{Q}_m phase 1 (A'_1) kinetics. * curve fitting did not follow the undershoot (below steady state) portion of CvO₂ (single-exponential fitting, Eq. 2). For $A'_1 = 0.2 A_{tot}$ curve fitting became unfeasible. N.A., not applicable for the reasons stated. *Solid line* represents the default condition for Section II. For further details and abbreviations see *Fig. 2.5*.

Figure 2.9. Dynamic coupling between muscle blood flow and oxygen consumption following the onset of exercise.

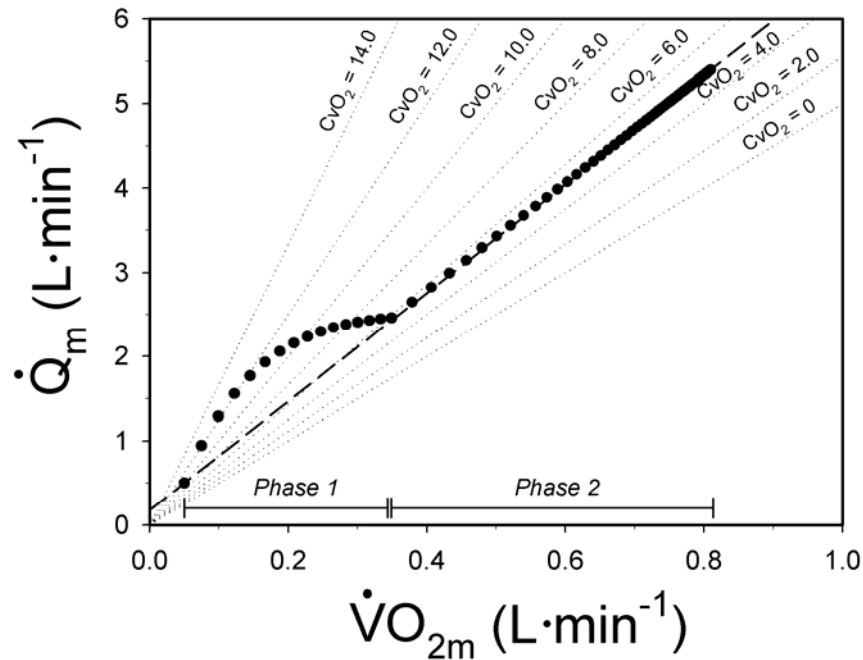


Figure 2.9. Dynamic coupling between muscle blood flow (\dot{Q}_m) and oxygen consumption ($\dot{V}O_{2m}$) from exercise onset to the steady state. 1) *Dotted lines*, isopleths of different CvO_2 values (in $\text{ml O}_2 \cdot 100 \text{ ml}^{-1}$), assuming $CaO_2 = 20 \text{ ml O}_2 \cdot 100 \text{ ml}^{-1}$; 2) *Dashed line*, expected values for monoexponential $\dot{V}O_{2m}$ and \dot{Q}_m increase from the onset of exercise, both with a time constant of 30 sec (baseline and steady state values as for default condition); 3) *Closed circles*, simulated response (default condition for Section II, Table 2.1; represented by a solid line in Figs. 2.5-2.8); *Phase 1* and *2* refers to the \dot{Q}_m response but its boundaries are shown on the $\dot{V}O_{2m}$ axis for clarity. This figure qualitatively resembles Fig. 5 from Grassi et al. (1996), where the overall \dot{Q}_m kinetics (mean response time) were ~ 2 s faster than $\dot{V}O_{2m}$ kinetics. Note that the CvO_2 response is nearly complete during Phase 1. Based on the Fick principle a direct implication of this is that \dot{Q}_m phase 2 is closely related to $\dot{V}O_{2m}$ (as shown by their linear relationship) because under such circumstances further increases in $\dot{V}O_{2m}$ are almost entirely due to increments in \dot{Q}_m , since O_2 extraction (as CvO_2) has almost reached its steady state change by the end of Phase 1.

**CHAPTER 3 - Muscle capillary blood flow kinetics estimated from
pulmonary O₂ uptake and near-infrared spectroscopy**

Summary

The near-infrared spectroscopy (NIRS) signal (deoxy-hemoglobin concentration; [HHb]) reflects the dynamic balance between muscle capillary blood flow (\dot{Q}_{cap}) and muscle oxygen uptake ($\dot{V}O_{2\text{m}}$) in the microcirculation. The purposes of the present study were to estimate the time course of \dot{Q}_{cap} from the kinetics of the primary component of pulmonary $\dot{V}O_2$ ($\dot{V}O_{2\text{p}}$) and [HHb] throughout exercise, and compare the \dot{Q}_{cap} kinetics with the $\dot{V}O_{2\text{p}}$ kinetics. Nine subjects performed moderate- (M; below Lactate Threshold, LT) and heavy-intensity (H, above LT) constant work rate tests. $\dot{V}O_{2\text{p}}$ ($\text{L}\cdot\text{min}^{-1}$) was measured breath-by-breath and [HHb] (μM) was measured by NIRS during the tests. The time course of \dot{Q}_{cap} was estimated from the rearrangement of the Fick equation [$\dot{Q}_{\text{cap}} = \dot{V}O_{2\text{m}}/(\text{CaO}_2 - \text{CvO}_2)$] using $\dot{V}O_{2\text{p}}$ (primary component) and [HHb] as proxies of $\dot{V}O_{2\text{m}}$ and $(\text{CaO}_2 - \text{CvO}_2)$, respectively. The kinetics of [HHb] ($\tau + \text{TD}$ [HHb]; M = 17.8 ± 2.3 s and H = 13.7 ± 1.4 s) were significantly ($P < 0.001$) faster than the kinetics of $\dot{V}O_2$ (τ_{p} ; M = 25.5 ± 8.8 s and H = 25.6 ± 7.2 s) and \dot{Q}_{cap} (mean response time, MRT; M = 25.4 ± 9.1 s and H = 25.7 ± 7.7 s). However, there was no significant difference between MRT- \dot{Q}_{cap} and $\tau_{\text{p}}-\dot{V}O_2$ for both intensities ($P = 0.99$), and these parameters were significantly correlated (M and H; $r = 0.99$; $P < 0.001$). In conclusion, we have proposed a new method to noninvasively approximate \dot{Q}_{cap} kinetics in humans during exercise. The resulting overall \dot{Q}_{cap} kinetics appeared to be tightly coupled to the temporal profile of $\dot{V}O_{2\text{m}}$.

Introduction

Insights on the control of exercising muscle blood flow (\dot{Q}_m) can be gained from the investigation of its response in the transitional phase (i.e., kinetics) (Laughlin & Korzick, 2001; Hughson, 2003), but due to methodological constraints the kinetics of \dot{Q}_m in humans have been studied primarily in larger vessels (Shoemaker *et al.*, 1996b; Shoemaker *et al.*, 1997; Hughson *et al.*, 1996; Grassi *et al.*, 1996; MacDonald *et al.*, 1998; Bangsbo *et al.*, 2000; Radegran & Saltin, 1998).

The difficulty in obtaining measurements with a time resolution that allows reliable kinetic analysis during large muscle mass exercise (e.g., cycling or running) has led to a predominant use of knee-extensor or forearm exercise with measurements of blood flow made by Doppler ultrasound (Shoemaker *et al.*, 1996b; Shoemaker *et al.*, 1997; Hughson *et al.*, 1996; MacDonald *et al.*, 1998; Fukuba *et al.*, 2004; Radegran & Saltin, 1998). These investigations have shown that the \dot{Q}_m response is biphasic with an initial fast phase determined by the combined effects of muscle contraction (muscle pump) (Sheriff & Hakeman, 2001) and possibly rapid vasodilation (Tschakovsky *et al.*, 2004) followed by a second slower phase that appears to match O_2 delivery and utilization (Shoemaker & Hughson, 1999).

Several studies have addressed the relationship between \dot{Q}_m and muscle $\dot{V}O_{2m}$ ($\dot{V}O_{2m}$) kinetic response following the onset of exercise (Hughson *et al.*, 1996; MacDonald *et al.*, 1998; Grassi *et al.*, 1996; Grassi *et al.*, 1998; Grassi *et al.*, 2000; Behnke *et al.*, 2002a). Although Grassi *et al.* (1996) and Koga *et al.* (2005) demonstrated a similar time course for $\dot{V}O_{2m}$ and \dot{Q}_m during moderate exercise, other human (Hughson *et al.*, 1996; MacDonald *et al.*, 1998) and animal studies (Grassi *et al.*, 1998; Grassi *et al.*, 2002; Behnke *et al.*, 2002a) have shown that \dot{Q}_m reaches a steady state level sooner than $\dot{V}O_{2m}$ (i.e., 5-10 s faster time constant). However, it is possible that the adjustment of \dot{Q}_m in the microcirculation of active skeletal muscles may differ from that measured in larger conduit arteries (Laughlin & Korzick, 2001). To date, for technical and ethical reasons, assessing the kinetics of muscle capillary blood flow (\dot{Q}_{cap}) in humans has been problematic. Resolution of this discrepancy in \dot{Q}_m kinetics relative to those of $\dot{V}O_{2m}$ is crucial to advancing our understanding of the mechanisms which govern the control of both \dot{Q}_m and $\dot{V}O_{2m}$ in health and disease.

Near-infrared spectroscopy (NIRS) provides a noninvasive measure of muscle oxygenation (or O_2 extraction) in the microcirculation. Although distinction between hemoglobin and myoglobin with regard to absorption of the near-infrared light cannot be made, the deoxygenated hemoglobin/myoglobin (deoxy-Hb/Mb) signal obtained by NIRS has been used as an index of local O_2 extraction reflecting the $\dot{V}O_{2m}$ to \dot{Q}_m ratio in the capillaries (Grassi *et al.*,

2003; DeLorey *et al.*, 2003). The time course of deoxy-Hb/Mb following the onset of exercise resembles qualitatively and quantitatively the arteriovenous O₂ difference (CaO₂ – CvO₂) observed in separate investigations (Grassi *et al.*, 1996; Grassi *et al.*, 1998; Grassi *et al.*, 2000). Although these studies have not directly compared the kinetics of deoxy-Hb/Mb and (CaO₂ – CvO₂), collectively these observations suggest that the contribution of myoglobin to the NIRS signal does not distort the similarity between deoxy-Hb/Mb and (CaO₂ – CvO₂) kinetics. In fact, inferences about \dot{Q}_m kinetics have been made based on the deoxy-Hb/Mb profile following the onset of exercise (Grassi *et al.*, 2003; DeLorey *et al.*, 2003; DeLorey *et al.*, 2004b).

Based on the above review, we propose that the kinetics of \dot{Q}_{cap} could be estimated noninvasively by solving the Fick equation for blood flow ($\dot{Q}_{cap} = \dot{V}O_{2m}/[CaO_2 - CvO_2]$), using the primary component of $\dot{V}O_{2p}$ and deoxy-hemoglobin ([HHb]) kinetics as surrogates of $\dot{V}O_{2m}$ and (CaO₂ – CvO₂) kinetics, respectively. Results from computer simulations suggest that the amplitude of the $\dot{V}O_{2m}$ and (CaO₂ – CvO₂) responses have little influence on the calculated \dot{Q}_m kinetics (Chapter 2). Thus, assuming that the relative contributions of arterial and venous blood to the [HHb] signal remain constant, so that the proportionality of [HHb](*t*) to (CaO₂ – CvO₂)(*t*) also remains relatively constant, the temporal (kinetic) characteristics of \dot{Q}_{cap} should be preserved. Therefore, the aims of the present study were to estimate the kinetics of \dot{Q}_{cap} from the time course of $\dot{V}O_{2p}$ (primary component) and [HHb] following the onset of exercise and compare the overall kinetics of the estimated \dot{Q}_{cap} with the estimated $\dot{V}O_{2m}$ kinetics. As the preponderance of studies investigating the temporal association between \dot{Q}_m and $\dot{V}O_{2m}$ have shown that blood flow adjusted at a faster rate than O₂ uptake (Hughson *et al.*, 1996; MacDonald *et al.*, 1998; Grassi *et al.*, 1998; Behnke *et al.*, 2002a), we hypothesized that the estimated \dot{Q}_{cap} kinetics would also be faster than the $\dot{V}O_{2m}$ kinetics.

Methods

Subjects: Nine healthy subjects (7 men, 2 women) with mean \pm S.D. age 24.7 ± 6.3 years, body weight 67.9 ± 12.2 kg and height 175.4 ± 13.1 cm participated in this study. After explanation of all procedures and possible risks and benefits of participation, each subject signed an informed consent form. The experimental protocol was approved by the Institutional Review Board for Research Involving Human Subjects at Kansas State University.

Protocol: Subjects performed the exercise protocol on three separate days within a period of 2 wks, and were instructed to avoid strenuous exercise for at least 24 hr preceding each visit to the laboratory. On the first visit seat height and handlebar position on the cycle ergometer were recorded and these were reproduced on subsequent tests.

The first visit was used to familiarize the subjects with testing procedures and to determine the peak oxygen uptake ($\dot{V}O_{2\text{peak}}$), estimated lactate threshold (LT) and work rates for the constant work rate tests. All exercise tests were performed on an electronically-braked cycle ergometer (Corival 400, Lode, The Netherlands). The incremental exercise test involved 4 min of baseline cycling at 60 rpm followed by a progressive (ramp) increase in exercise intensity ($15\text{-}30 \text{ W}\cdot\text{min}^{-1}$) to volitional exhaustion. $\dot{V}O_{2\text{peak}}$ was defined as the highest $\dot{V}O_2$ achieved during the test averaged over a 15 s interval. The LT was estimated from gas exchange measurements using the V-slope method, ventilatory equivalents and end-tidal gas tensions (Beaver *et al.*, 1986; Wasserman *et al.*, 1973). The work rates calculated to elicit 90% of the LT $\dot{V}O_2$ (90% LT) and a $\dot{V}O_2$ half way between the LT and $\dot{V}O_{2\text{peak}}$ ($50\% \Delta = \dot{V}O_2 \text{ LT} + 0.5 \cdot [\dot{V}O_{2\text{peak}} - \dot{V}O_2 \text{ LT}]$), were determined. Over the next two visits, the subjects performed a total of 4-6 bouts of constant work rate exercise at 90% LT (6 min each) interspersed by 6 min at 20W, and 2 bouts at 50% Δ (8 min duration). The first bout was preceded by 4 min of baseline pedaling at 20W. Pulmonary $\dot{V}O_2$ and muscle oxygenation were measured continuously in all subjects and transitions.

Pulmonary gas exchange ($\dot{V}O_2$ and $\dot{V}CO_2$) and minute expired ventilation ($\dot{V}E$) were measured breath-by-breath by an "open-circuit" method (CardiO₂, Medical Graphics Corp., St. Paul, MN). Before each exercise test the volume signal was calibrated by pumping a 3-liter syringe at flow rates spanning the range expected during the exercise studies, while the O₂ and CO₂ analyzers were calibrated with gases of known concentration. Heart rate was recorded from the electrocardiogram using a modified lead I configuration and stored in the breath-by-breath file.

Muscle oxygenation was evaluated by a frequency-domain multi-distance (FDMD) near-infrared spectroscopy system (OxiplexTS, ISS, Champaign, IL). The principles of operation and

algorithms utilized by the equipment have been described in detail elsewhere (Gratton *et al.*, 1997). In this study we used a single channel consisting of eight laser diodes operating at two wavelengths (690 and 830 nm, four at each wavelength) and a photomultiplier tube (PMT). The laser diodes and PMT are connected to a lightweight plastic probe by optical fibers consisting of two parallel rows of emitter fibers and one detector fiber bundle comprising source-detector separations of 2.0, 2.5, 3.0 and 3.5 cm for both wavelengths. The frequency modulation of laser intensity was 110 MHz and the heterodyne detection was performed at a 5 KHz cross-correlation frequency. The output frequency was selected as 31.25 Hz. The probe was positioned longitudinally on the belly of the vastus lateralis muscle ~15 cm above the patella. To minimize motion artifacts and contamination of the signal by ambient light, the margins of the probe were bound to the thigh with a skin cement (Skin-Bond, Smith & Nephew, Largo, FL) after carefully shaving and drying the area, and secured with Velcro straps around the thigh. The probe position was marked to check for any sliding and for accurate repositioning on subsequent test days. No movement (sliding) was observed in any exercise test. The near-infrared spectrometer was calibrated on each test day after a warm-up period of at least 30 min. The calibration was done with the optical probe placed on a calibration block (phantom) with absorption and reduced scattering coefficients previously measured, and correction factors were determined and automatically implemented by the equipment's software for the calculation of the absorption coefficient (μ_A) and reduced scattering coefficient (μ'_s) for each wavelength during the data collection (Hueber *et al.*, 2001).

The FDMD method provides continuous measurement of absolute concentration of oxyhemoglobin ([HbO₂]), deoxyhemoglobin ([HHb]) (expressed in μM) and μ'_s (1/cm). The [HHb] reported in the present study was calculated incorporating the continuous measurement of μ'_s made throughout the exercise test, i.e., without assuming a constant value for scattering.

Kinetics Analysis: The breath-by-breath $\dot{V}O_2$ and NIRS-oxygenation data were converted to second-by-second values. For each subject, the $\dot{V}O_{2p}$ and NIRS-oxygenation were time-aligned to the start of exercise and ensemble-averaged to generate a single data set for each variable, at each exercise intensity, to improve the signal-to-noise ratio and confidence of fitting procedures. The kinetics of $\dot{V}O_{2p}$, [HHb] and \dot{Q}_{cap} (see below) were determined by nonlinear regression using a least squares technique (Marquadt-Levenberg, SigmaPlot 2001, Jandel Scientific). The model used for fitting the [HHb] response consisted of a single-exponential with a time delay (primary component of *Eq. 1*) or, a two-exponential term (primary and slow component of *Eq. 1*) when an additional "slow component" was observed

$$\begin{aligned}
[\text{HHb}]_{(t)} &= [\text{HHb}]_{(b)} + A_P \cdot (1 - e^{-(t-\text{TD}_P)/\tau_P}) && \text{(Primary component)} && (1) \\
&+ A_S \cdot (1 - e^{-(t-\text{TD}_S)/\tau_S}) && \text{(Slow component)}
\end{aligned}$$

The $\dot{V}O_{2p}$ response was fitted by conventional equations (Eq. 2) with two- (Phases 1-2) and three- (Phases 1-3) exponential terms for exercise below and above the LT, respectively

$$\begin{aligned}
\dot{V}O_{2(t)} &= \dot{V}O_{2(b)} + A_I \cdot (1 - e^{-(t-\text{TD}_I)/\tau_I}) && \text{(Phase 1)} && \text{(Initial component)} \\
&+ A_P \cdot (1 - e^{-(t-\text{TD}_P)/\tau_P}) && \text{(Phase 2)} && \text{(Primary component)} && (2) \\
&+ A_S \cdot (1 - e^{-(t-\text{TD}_S)/\tau_S}) && \text{(Phase 3)} && \text{(Slow component)}
\end{aligned}$$

where in *Equations (1) and (2)* the subscript *b* refers to baseline unloaded cycling; A_I , A_P and A_S are the amplitudes; TD_I , TD_P and TD_S are the time delays; and τ_I , τ_P and τ_S are the time constants of the exponential responses of interest for each variable. The initial (cardiodynamic) component of $\dot{V}O_{2p}$ was described up to TD_P and the amplitude of the response at TD_P (A'_I) calculated as $A'_I = A_I \cdot (1 - e^{-\text{TD}_P/\tau_I})$. The relevant amplitude of the primary component was calculated as $A'_P = A'_I + A_P$. The 95% confidence limits for τ_P of $\dot{V}O_2$ kinetics were on average $\tau_P \pm 17\%$ (moderate exercise) and $\tau_P \pm 35\%$ (heavy exercise).

Muscle Capillary Blood Flow: The design used to investigate the kinetics of muscle capillary blood flow (\dot{Q}_{cap}) in this study is conceptually similar to that applied in modeling studies (Barstow *et al.*, 1990) and, more recently, in rat muscle preparations (Behnke *et al.*, 2002a). The \dot{Q}_{cap} response to exercise was derived from the kinetics of $\dot{V}O_{2p}$ and [HHb]. The kinetics of the primary component of $\dot{V}O_{2p}$ during constant work rate exercise has been shown to approximate the muscle $\dot{V}O_2$ ($\dot{V}O_{2m}$) kinetics (Barstow & Mole, 1987; Barstow *et al.*, 1990; Grassi *et al.*, 1996; Rossiter *et al.*, 1999), whereas [HHb] measured by NIRS is thought to be a function of the muscle oxygen uptake-to-blood flow ratio ($\dot{V}O_{2m}/\dot{Q}_m$) (Grassi *et al.*, 2003; DeLorey *et al.*, 2004b). The [HHb] signal has been shown to be less sensitive than [HbO₂] to changes in blood volume under the field of interrogation, thus better representing the muscle oxygenation status during steady- and nonsteady-state situations (Ferrari *et al.*, 1997; Grassi *et al.*, 2003). Hence, assuming that arterial oxygen saturation did not change appreciably during moderate and heavy exercise in the present subjects, the [HHb] response was considered to be proportional to oxygen extraction ($\text{CaO}_2 - \text{CvO}_2$). Therefore, by rearranging the Fick equation, the temporal characteristic of \dot{Q}_{cap} could be estimated from the ratio of $\dot{V}O_{2m}$ to [HHb], specifically,

$$\dot{Q}_{\text{cap}}(t) = \frac{\dot{V}O_{2m}(t)}{(\text{CaO}_2 - \text{CvO}_2)(t)} \alpha \frac{\dot{V}O_{2p}(\text{phase 2})(t)}{[\text{HHb}](t)} \quad (3)$$

In this circumstance, the amplitude of \dot{Q}_{cap} is quantitatively uncertain because the precise proportional contribution of arterial and venous blood to the [HHb] signal are unknown for skeletal muscle. However, if this distribution remains constant from baseline to exercise in a given subject, the temporal (kinetic) characteristic of [HHb], and thus \dot{Q}_{cap} , should be preserved. Consistent with this, the results from computer simulations have shown that the amplitude of $\dot{V}O_2$ and $(\text{CaO}_2 - \text{CvO}_2)$ responses have little influence on the calculated blood flow kinetics (see Chapter 1). The $\dot{V}O_{2m}$ kinetics were estimated using the kinetic parameters of $\dot{V}O_{2p}$ obtained from the curve fitting, i.e., by assuming that $\dot{V}O_{2m}$ rose exponentially at time zero with the time constant and amplitude determined for the primary component of the $\dot{V}O_{2p}$ response (e.g., Fig. 3.1). The resulting estimated $\dot{V}O_{2m}$ kinetics was used to estimate the \dot{Q}_{cap} kinetics (see Figs. 3.2-3.3). The time course of \dot{Q}_{cap} was analyzed with exponential equations as described above (Eq. 2), where \dot{Q}_{cap} is substituted for $\dot{V}O_2$. At present we do not know if simple exponential equations provide the best mathematical description of the \dot{Q}_{cap} response; however, we used methods similar to those previously employed to investigate the kinetics of muscle blood flow (Hughson *et al.*, 1996; MacDonald *et al.*, 1998; Radegran & Saltin, 1998; Shoemaker *et al.*, 1996b). The mean response time (MRT) for \dot{Q}_{cap} , which approximates the time to reach 63% of the response, was calculated as

$$\text{MRT} = \frac{A'_I}{A'_P} \cdot (\text{TD}_I + \tau_I) + \frac{A_P}{A'_P} \cdot (\text{TD}_P + \tau_P) \quad (4)$$

where the parameters are from Eq. 2 and subsequent text.

Statistical analysis: To determine significant differences between two means, a two-tailed Student's paired t-test was performed. A repeated-measures analysis of variance was performed to compare more than two means and the Tukey-Kramer's *post hoc* test was used for pairwise comparisons. The relationship between two variables was analyzed by the Pearson's product-moment correlation. Significance was accepted when $P < 0.05$. All tests were conducted using a commercial statistical software (NCSS 2000, NCSS Statistical Software, Kaysville, UT). Values were reported as mean \pm S.D., unless otherwise specified.

Results

The subjects' $\dot{V}O_{2\text{peak}}$ was $48.8 \pm 7.0 \text{ ml}\cdot\text{kg}^{-1}\cdot\text{min}^{-1}$ and the estimated LT occurred at $56.3 \pm 8.5 \% \dot{V}O_{2\text{peak}}$. The work rates for the constant work rate tests were $115.0 \pm 35.6 \text{ W}$ (90% LT) and $205.7 \pm 55.7 \text{ W}$ (50% Δ).

Preliminary analysis showed no main effect for the order of the moderate exercise bout averaged for visits 2 and 3 on \dot{Q}_{cap} kinetics (MRT $\dot{Q}_{\text{cap}} = 25.9 \pm 6.4 \text{ s}$, $25.1 \pm 6.9 \text{ s}$ and $25.6 \pm 7.2 \text{ s}$ for bouts 1, 2 and 3 respectively; $P = 0.73$). Therefore, \dot{Q}_{cap} kinetics during exercise at 90% LT was estimated based on [HHb] (and $\dot{V}O_{2p}$) response from the 4-6 transitions ensemble-averaged to yield a single data set for each subject.

The estimated $\dot{V}O_{2m}$, [HHb] and estimated \dot{Q}_{cap} response of a representative subject are shown in Fig. 3.2 (90% LT) and 3.3 (50% Δ), while Fig. 3.4 depicts the best regression fit through the \dot{Q}_{cap} presented in Figs. 3.1-3.2. The kinetic parameters of \dot{Q}_{cap} and [HHb] during moderate and heavy intensity exercise are presented in Table 1. As previously shown (Grassi *et al.*, 2003), the TD_1 of [HHb] for heavy exercise was shorter than for moderate exercise ($P < 0.001$) while no significant difference was observed for τ_1 of [HHb].

The results of the overall kinetics of $\dot{V}O_2$, [HHb] and \dot{Q}_{cap} are shown in Fig. 3.5. The MRT of [HHb] ($TD_p + \tau_p$) was significantly faster than \dot{Q}_{cap} and $\dot{V}O_2$ kinetics for moderate and heavy exercise (Fig. 3.5). However, the overall kinetics of \dot{Q}_{cap} was similar to the estimated $\dot{V}O_2$ kinetics for both exercise intensities, i.e., $MRT-\dot{Q}_{\text{cap}}$ was not significantly different from $\tau_p\dot{V}O_{2p}$ (Fig. 3.5). No exercise intensity effect was observed for either the $MRT-\dot{Q}_{\text{cap}}$ or $\tau_p\dot{V}O_{2p}$. Finally, there were significant correlations between $MRT-\dot{Q}_{\text{cap}}$ and the estimated $\tau\dot{V}O_{2m}$ ($\tau_p\dot{V}O_{2p}$) for moderate ($r = 0.99$; $P < 0.001$) and heavy exercise ($r = 0.99$; $P < 0.001$) (Fig. 3.6).

Discussion

In the present study we sought to estimate the kinetics of muscle capillary blood flow, noninvasively, from the kinetics of pulmonary $\dot{V}O_2$ and deoxy-hemoglobin, and to test the hypothesis that the resulting \dot{Q}_{cap} kinetics were faster than muscle $\dot{V}O_2$ kinetics. The main novel finding was that the estimated temporal profile of muscle blood flow in the microcirculation was tightly coupled to $\dot{V}O_{2m}$ kinetics. To the best of our knowledge this is the first study to noninvasively estimate, in humans, the time course of on-transient muscle blood flow in the microcirculation. Although the [HHb] signal from NIRS has been used to investigate the balance between blood flow and O_2 uptake in the microcirculation under various experimental conditions (DeLorey *et al.*, 2003; DeLorey *et al.*, 2004b; Grassi *et al.*, 2003), the kinetics of \dot{Q}_{cap} itself have not previously been estimated as in the present study.

Validity of Assumptions: Two primary assumptions were made in order to estimate the temporal profile of \dot{Q}_{cap} from the Fick principle. These involved the use of pulmonary $\dot{V}O_2$ (primary component) and [HHb] kinetics as surrogates of $\dot{V}O_{2m}$ and O_2 extraction kinetics, respectively. Therefore the validity of these assumptions should be addressed before discussing the \dot{Q}_{cap} profile observed herein.

Pulmonary $\dot{V}O_2$ as muscle $\dot{V}O_2$: The $\dot{V}O_{2m}$ was determined based on the kinetics of the primary component of $\dot{V}O_{2p}$. The $\dot{V}O_{2p}$ on-transient is characterized by two (moderate intensity) or three phases (heavy intensity) (Whipp *et al.*, 1982), where the initial component has a cardiodynamic origin (“cardiodynamic hyperpnea”) (Whipp *et al.*, 1982). The time course of the primary component of $\dot{V}O_{2p}$ has generally been shown or predicted to closely reflect (within 10%) the $\dot{V}O_{2m}$ response (Barstow & Mole, 1987; Barstow *et al.*, 1990; Grassi *et al.*, 1996; Rossiter *et al.*, 1999). Grassi *et al.* (1996) directly measured leg $\dot{V}O_2$ and pulmonary $\dot{V}O_2$ during cycling exercise and found that kinetics of the primary component of $\dot{V}O_{2p}$ were similar to, and consequently a good approximation of, the $\dot{V}O_{2leg}$ kinetics. In a different modality (knee-extension exercise), it has been demonstrated that phosphocreatine (PCr) breakdown (from ^{31}P -NMR) followed a similar dynamic profile to that of the primary component of $\dot{V}O_{2p}$ during moderate intensity (below LT) exercise (Rossiter *et al.*, 1999). Regarding the heavy exercise intensity domain (50% Δ , present study), approximately 86% of the pulmonary $\dot{V}O_2$ slow component comes from the exercising legs (Poole *et al.*, 1991). Therefore, based on experimental and theoretical studies (Barstow *et al.*, 1990), it is reasonable to assume that the

primary and slow component of $\dot{V}O_{2p}$ approximates the time course of the muscle $\dot{V}O_2$ response during moderate and heavy exercise.

Deoxy-hemoglobin as arteriovenous oxygen difference: Hemoglobin and myoglobin have similar absorption spectra that at present cannot be distinguished by near-infrared spectroscopy devices incorporating 2-4 wavelengths. There is ongoing controversy as to what extent the NIRS signal contains qualitatively significant information from Mb (Tran *et al.*, 1999; Mancini *et al.*, 1994; Seiyama *et al.*, 1988). It has been generally accepted that the NIRS signal evolves predominantly from changes in oxy- or deoxy-Hb (McCully & Hamaoka, 2000); however, for its relevance to the present study this issue deserves further consideration.

In rat thigh muscles perfused with perfluorocarbon to eliminate the NIRS signal arising from Hb, an interference from Mb of less than 10% was observed (Seiyama *et al.*, 1988). These results were confirmed in human muscle by use of $^1\text{H-NMR}$ (Mancini *et al.*, 1994). In contrast, Tran *et al.* (1999), also using $^1\text{H-NMR}$, showed that in the human gastrocnemius the deoxy-Mb kinetics matched the NIRS oxygenation profile during cuff occlusion suggesting that the latter signal originated from Mb. It is noteworthy that the $^1\text{H-NMR}$ studies (Mancini *et al.*, 1994; Tran *et al.*, 1999) analyzed the tissue oxygen saturation ($\% \text{StO}_2 = [\text{HbO}_2]/\text{Total}[\text{Hb}]$), while recent studies (Grassi *et al.*, 2003; DeLorey *et al.*, 2003) have emphasized the use of $[\text{HHb}]$ as an index of O_2 extraction (see below). The deoxy-Mb signal from the quadriceps muscle did not change from 50-60% to 100% WRmax (Richardson *et al.*, 1995) whereas $[\text{HHb}]$ continued to demonstrate a WR-dependency above 50-65% $\dot{V}O_{2\text{max}}$ (Grassi *et al.*, 1999). Collectively, these observations suggest that NIRS light absorption in the quadriceps muscle is mainly associated with hemoglobin during exercise.

The NIRS output has often been used to describe a global tissue O_2 saturation ($\% \text{StO}_2$) and comparisons with direct measurements of venous O_2 saturation during exercise have been made (MacDonald *et al.*, 1999; Costes *et al.*, 1996). There are two shortcomings to these studies that are relevant to the present one. First, as discussed by DeLorey *et al.* (2003) femoral venous oxygen saturation includes blood flow through both active and inactive muscles, whereas the StO_2 was obtained from the m. vastus lateralis (active) only. To this point, Wilson *et al.* (1989) found good agreement between StO_2 from NIRS of the contracting dog gracilis muscle and direct measurements of the isolated venous effluent O_2 saturation from the same muscle. Second, changes in blood volume under the area of tissue sampled by the probe (cf. Fig. 4 MacDonald *et al.*, 1999) will affect the $[\text{HbO}_2]$ and StO_2 signals, independent of any changes in O_2 extraction. On the other hand, the $[\text{HHb}]$ is insensitive to blood volume changes (Ferrari *et al.*, 1997) and has been used to assess variations in muscle O_2 extraction (DeLorey *et al.*, 2003; DeLorey *et al.*,

2004b). Indeed, Grassi et al. (2003) pointed out the striking similarity of [HHb] kinetics during moderate and heavy exercise with the time course of $(CaO_2 - CvO_2)$. Specifically, in the dog gastrocnemius (Grassi *et al.*, 2002), where venous outflow is isolated and, thus, errors due to multiple vessels draining the exercising muscle and muscle-to-sampling site transit delay are minimized, the O_2 extraction kinetics ($TD \sim 7.5$ s and $\tau \sim 8$ s, Grassi *et al.*, 2002) were similar to those found for [HHb] in the present (Table 1) and other studies in exercising humans (DeLorey *et al.*, 2003; Grassi *et al.*, 2003). These findings provide a framework supporting the assumption of [HHb] as a noninvasive surrogate of $(CaO_2 - CvO_2)$ to estimate the temporal profile of muscle capillary blood flow by the Fick principle. However, to our knowledge no study has directly compared the kinetics of [HHb] with those of $(CaO_2 - CvO_2)$ for a single muscle and its entire venous outflow in exercising humans. Thus, this assumption must await direct validation.

Since the \dot{Q}_{cap} kinetics were estimated from indirect measures of $\dot{V}O_{2m}$ and $(CaO_2 - CvO_2)$ kinetics, the estimated \dot{Q}_{cap} kinetics will have some error when compared with the “true” \dot{Q}_{cap} kinetics. Inasmuch as the error introduced by the assumption that $[HHb](t) \propto (CaO_2 - CvO_2)(t)$ is not known, we cannot predict the extent of error that will be present in the estimated \dot{Q}_{cap} kinetics. However, since the kinetics of $\dot{V}O_{2p}$ (primary component) reflects the $\dot{V}O_{2m}$ kinetics with a $\pm 10\%$ error (see above), we might predict that the estimated \dot{Q}_{cap} kinetics will represent the true \dot{Q}_{cap} kinetics within $\geq 10\%$ (or ≥ 2.5 s for the $MRT-\dot{Q}_{cap}$ observed herein). Nevertheless, based on the relationship between \dot{Q}_m vs. $\dot{V}O_{2m}$ kinetics resulting from computer simulations of $\dot{V}O_{2m}$ and $(CaO_2 - CvO_2)$ response to exercise (Chapter 2), and the estimated $MRT-\dot{Q}_{cap}$ vs. $\tau_p \dot{V}O_{2p}$ (Fig. 3.6), it appears that the error due to the assumptions made are not much greater than 10%.

Kinetics of muscle blood flow: The muscle hemodynamic response following the onset of moderate exercise is characterized by two phases (for review see Shoemaker & Hughson, 1999). In the present investigation the estimated muscle \dot{Q}_{cap} response was also better described by a two-exponential model (three-exponential for heavy exercise) with the initial phase (phase 1) lasting ~ 15 -20 sec. These results are in concert with the kinetics of bulk blood flow determined in larger human vessels (Shoemaker *et al.*, 1997; MacDonald *et al.*, 1998) and those of red blood cells (RBC) in capillaries of contracting rat spinotrapezius muscle (Kindig *et al.*, 2002b).

The rapid phase 1 response of \dot{Q}_m is thought to be due to a mechanical effect of muscle contraction (i.e., muscle-pump) and possibly rapid vasodilation (Tschakovsky & Sheriff, 2004). Pharmacological interventions (Wunsch *et al.*, 2000) and theoretical predictions (Kindig *et al.*, 2002b) suggest a lack of vasodilation during phase 1; however, recent studies have indirectly

pointed to the presence of a rapid vasodilation sufficient to elevate blood flow in conduit arteries (Tschakovsky *et al.*, 2004; Hamann *et al.*, 2004a). It is noteworthy that the kinetics of phase 1 appear to be faster, with a greater contribution to the overall response, in rest-to-exercise transitions (Shoemaker *et al.*, 1997; MacDonald *et al.*, 1998; Kindig *et al.*, 2002b) compared to exercise-to-exercise transitions (present study; Grassi *et al.*, 1996). This response may reflect a greater muscle-pump effect as contraction frequency is an important determinant of the muscle-pump (Sheriff & Hakeman, 2001). Our results, within the constraints of the assumptions made to estimate \dot{Q}_{cap} kinetics (see above), suggest that a biphasic capillary blood flow response (Kindig *et al.*, 2002b) is also present in the human muscle microcirculation.

The second, slower phase of blood flow adjustment has been associated with feedback metabolic control, and several vasodilators have been proposed to mediate the response (Shoemaker & Hughson, 1999; Laughlin & Korzick, 2001; Hughson, 2003). The time constant of the primary component (or Phase 2) of \dot{Q}_{cap} in the present study (~ 26 s, Table 3.1) was faster than those reported for the femoral artery (40 s, MacDonald *et al.*, 1998 and 59 s, Koga *et al.*, 2005). The cause of this disparity is not clear, but it is important to emphasize that a different exercise modality (knee-extension) was utilized in these studies compared to cycling in the present study. Also, in the current study \dot{Q}_{cap} kinetics were estimated based on assumptions that would introduce some error in the estimated vs. “true” time constant of \dot{Q}_{cap} (discussed above). However, it is unlikely that the potentially random error introduced by our assumptions would account for the ~ 14 -25 s systematic difference with these previous studies. The overall blood flow response estimated in the current study by the mean response time was slower than some (Hughson *et al.*, 1996; MacDonald *et al.*, 1998) but similar to other (Grassi *et al.*, 1996; Koga *et al.*, 2005) studies on larger human vessels, when the relationship between \dot{Q}_{m} and $\dot{V}O_{2\text{m}}$ kinetics is considered (Figure 3.4A). In general, our results differ from those studies that investigated rest-to-exercise transitions (Hughson *et al.*, 1996; MacDonald *et al.*, 1998), but agree with results from studies using exercise-to-exercise protocols (Grassi *et al.*, 1996; Koga *et al.*, 2005). Therefore, the inconsistency of results could be related to differences in the phase 1 profile of \dot{Q}_{m} and its relative contribution to the overall response (see above).

For heavy exercise, comparison of MRT or τ_p of blood flow with previous investigations in humans is not straightforward because we chose to truncate the MRT so as to reflect the primary component of the response while others have included the blood flow increase associated with the $\dot{V}O_2$ slow component (Radegran & Saltin, 1998; Bangsbo *et al.*, 2000; Fukuba *et al.*, 2004). The rationale for limiting the calculation of the heavy exercise MRT was that we were interested in determining the relationship between the primary components of the estimated \dot{Q}_{cap} and $\dot{V}O_{2\text{m}}$ kinetics. Further, it is not clear if the time course of [HHb]

approximates the dynamics of $(CaO_2 - CvO_2)$ during the slow component phase of $\dot{V}O_2$ (Poole *et al.*, 1991) which technically limited us from determining the MRT for the total response (primary and slow component). Based on the relationship presented in Figure 4B, our results for \dot{Q}_{cap} kinetics are in agreement with the primary component of \dot{Q}_m kinetics in the dog gastrocnemius muscle preparation contracting at $\dot{V}O_{2peak}$ (Grassi *et al.*, 2000).

Dynamic coupling of \dot{Q}_m to $\dot{V}O_{2m}$: In the present study the estimated temporal profile of \dot{Q}_{cap} was directly related to the $\dot{V}O_{2m}$ kinetics. As seen in Fig. 3.4, the association between blood flow and $\dot{V}O_2$ kinetics has been demonstrated by a number of investigators (MacDonald *et al.*, 1998; Hughson *et al.*, 1996; Grassi *et al.*, 1996; Grassi *et al.*, 2002; Koga *et al.*, 2005). Some studies have shown that the time constants for adjustment of blood flow were 5-10 s faster than those of $\dot{V}O_2$ during moderate exercise (Hughson *et al.*, 1996; MacDonald *et al.*, 1998; Grassi *et al.*, 2002), while others have found similar kinetics for \dot{Q}_m and $\dot{V}O_2$ (Grassi *et al.*, 1996; Koga *et al.*, 2005) for moderate exercise. Our results are in agreement with the latter studies, and suggest that in the human muscle microcirculation, under the experimental conditions and assumptions of this investigation, the dynamic adjustment of blood flow is intimately coupled to the time course of $\dot{V}O_{2m}$. As noted above, rest-to-exercise transitions were associated with overall \dot{Q}_m kinetics faster than $\dot{V}O_{2m}$ kinetics (Hughson *et al.*, 1996; MacDonald *et al.*, 1998) while exercise-to-exercise transitions (“unloaded” to exercise) demonstrated \dot{Q}_m kinetics similar to $\dot{V}O_2$ kinetics (Grassi *et al.*, 1996; Koga *et al.*, 2005). This could be the result of differences in the initial phase of the \dot{Q}_m response, possibly due to a greater muscle-pump effect during rest-to-exercise transitions (see above). Collectively, this raises an interesting question: Does the muscle-pump induced increase in blood flow alter the coupling between \dot{Q}_m and $\dot{V}O_{2m}$ during rest-to-exercise transitions? The mechanisms underlying the close association between \dot{Q}_m and $\dot{V}O_{2m}$ kinetics are not presently clear because studies of muscle blood flow in the microcirculation during the transitional phase of exercise are scarce. Pharmacological blockade of vasodilator pathways did not change the overall time course of bulk blood flow adjustment (e.g., Shoemaker *et al.*, 1997), but the possibility of different effects on the microcirculation cannot be excluded (Laughlin & Korzick, 2001).

In this context, it has been suggested that the time constant of phase 2 should be used to investigate the control of muscle blood flow because phase 1 may have a mechanical origin which increases blood flow indiscriminately to active and nonactive muscle fibers (Hughson, 2003). In the current model we chose to evaluate the temporal association between the MRT for \dot{Q}_{cap} and τ_p of $\dot{V}O_{2p}$. As discussed above, $\tau_p \dot{V}O_{2p}$ is a reasonable approximation of muscle $\dot{V}O_2$ kinetics, whilst the MRT was selected to reflect the overall kinetics of blood flow due to the

present uncertainty about the mechanism(s) of \dot{Q}_{cap} phase 1. In fact, recent studies have indicated the presence of a rapid vasodilation that is related to muscle metabolism (Tschakovsky *et al.*, 2004). Therefore, based on current knowledge of the blood flow response to exercise, it is our contention that the mean response time gives a better representation of the overall temporal profile of blood flow. Using this analysis, the kinetics of \dot{Q}_{cap} were found to be similar to $\dot{V}O_2$ kinetics during moderate and heavy exercise. From these results alone, it is difficult to make inferences about the potential role of O_2 delivery to determine the kinetics of $\dot{V}O_{2m}$ during upright cycling exercise (present study). $\dot{V}O_{2m}$ kinetics reflects the interaction between O_2 delivery and metabolic inertia (Tschakovsky & Hughson, 1999). If \dot{Q}_{cap} (and presumably O_2 delivery) kinetics had been clearly faster than $\dot{V}O_2$ kinetics it would suggest that O_2 delivery was not the limiting factor to $\dot{V}O_{2m}$ kinetics. Conversely, if the kinetics of \dot{Q}_{cap} were slower than O_2 uptake kinetics it might suggest an O_2 delivery limitation to $\dot{V}O_{2m}$ kinetics. However, our results lie between these two extremes. It is important to note that similar kinetics for \dot{Q}_{cap} and $\dot{V}O_{2m}$ does not necessarily mean that \dot{Q}_{cap} (and by inference O_2 delivery) limits $\dot{V}O_{2m}$ kinetics. To this point, augmented O_2 delivery in the transitional phase of moderate exercise did not change significantly the kinetics of $\dot{V}O_2$ (MacDonald *et al.*, 1997; Grassi *et al.*, 1998). In contrast, during heavy exercise, enhanced O_2 delivery resulted in faster $\dot{V}O_2$ kinetics in some [pump-perfused muscle (Grassi *et al.*, 2000); prior exercise (Tordi *et al.*, 2003)], but not all studies (prior exercise, Wilkerson *et al.*, 2004). In our study, estimated $\dot{V}O_{2m}$ and \dot{Q}_{cap} kinetics were similar for both exercise intensities (Fig. 3.6). Therefore, it cannot be ascertained, from our data only, how O_2 delivery and metabolic inertia interact to determine $\dot{V}O_{2m}$ kinetics (for further discussion on this topic see Tschakovsky & Hughson, 1999; Tordi *et al.*, 2003; Wilkerson *et al.*, 2004).

Methodological considerations: The basic assumptions made to estimate the temporal profile of \dot{Q}_{cap} were discussed in detail above. It is important to recognize, however, that possible subtle changes in the exponential characteristic of $\dot{V}O_{2m}$ response occurring in the transitional phase will be masked by the breath-by-breath noise of pulmonary $\dot{V}O_2$, which prevents statistical justification of higher-order models, but has important physiological implications (Hughson *et al.*, 2001); however, resolution of this limitation is not possible at present. In addition, we have assumed that $\dot{V}O_{2m}$ and $(CaO_2 - CvO_2)$, estimated locally from NIRS, were proportionately distributed among the exercising muscles. However, the skeletal muscles recruited are not homogeneous, either with respect to their relative contribution to the work of cycling, or with regard to muscle fiber type, recruitment pattern and distribution of blood flow (Laughlin & Armstrong, 1982). At present, resolution of both the intra- and inter-muscular heterogeneity of

$\dot{Q}/\dot{V}O_2$ during cycling is not possible and must await further advances in methods such as those recently reported (Mizuno *et al.*, 2003).

Two inherent limitations of NIRS are the small tissue volume sampled by the probe and the relatively shallow light penetration depth. In this study we used the m. vastus lateralis based on electromyography (EMG) activity, which indicates that the m. vastus lateralis provides a good representation of muscle recruitment during cycling (Li & Caldwell, 1998). Contribution from other muscles (by EMG) during heavy exercise may become important during the period corresponding to the slow component of $\dot{V}O_{2p}$ (Burnley *et al.*, 2002), but this is expected to have minor effects on our results because we restricted our analysis to the primary component of $\dot{V}O_{2p}$, [HHb] and estimated \dot{Q}_{cap} . Regarding the light penetration depth, the predominance of type II fibers in superficial muscle areas (Lexell *et al.*, 1983) could result in slower estimated \dot{Q}_{cap} kinetics, if the lower endothelium-dependent vasodilator response of type II fibers demonstrated in animal muscles (Woodman *et al.*, 2001) is observed in human muscles. The potential influence of fiber type regionalization on the NIRS estimated \dot{Q}_{cap} kinetics must await further studies. Finally, we assumed that the relative contribution of arterioles, capillaries and venules to the [HHb] signal remained constant during the exercise period. This is a technical limitation of NIRS in general that cannot be solved at present. However, based on the similarity between the temporal profile of [HHb] observed in the present study and recently reported by others (Grassi *et al.*, 2003; DeLorey *et al.*, 2003), and the dynamics of O_2 extraction measured in other studies (Grassi *et al.*, 1996; Grassi *et al.*, 1998; Grassi *et al.*, 2000) a possible shift in the vessels contributing to the [HHb] signal would not invalidate our assumption.

Conclusions

In summary, this study introduced a new method to noninvasively estimate the time course of muscle capillary blood flow (\dot{Q}_{cap}) from the kinetics of pulmonary $\dot{V}O_2$ and deoxy-hemoglobin ([HHb]) from NIRS. The resulting estimated \dot{Q}_{cap} kinetics were similar to $\dot{V}O_{2p}$ (phase 2) kinetics indicating that in the microcirculation muscle blood flow is tightly coupled to muscle oxygen uptake following the onset of exercise. Moreover, the temporal profile of the estimated \dot{Q}_{cap} response suggests that in human muscles the kinetics of capillary blood flow is biphasic, as previously shown in the rat muscle (Kindig *et al.*, 2002b).

Table 3.1. Kinetic parameters of O₂ uptake, capillary blood flow and [HHb].

Parameter	\dot{Q}_{cap}		[HHb]	
	Moderate	Heavy	Moderate	Heavy
Baseline	33.8 ± 10.6	38.4 ± 11.8 *	23.4 ± 8.8	21.4 ± 8.4 *
A' _I	15.7 ± 6.6	18.8 ± 7.5 *		
τ _I (s)	6.7 ± 2.7	3.3 ± 1.6 *		
A _P	14.4 ± 9.1	30.2 ± 13.9 *		
A' _P	30.1 ± 13.5	49.0 ± 18.7 *	6.06 ± 4.57	11.0 ± 7.5 *
TD _P (s)	18.9 ± 4.6	13.6 ± 4.8 *	8.5 ± 1.8	5.1 ± 1.5 *
τ _P (s)	28.3 ± 5.8	25.7 ± 5.0	9.3 ± 3.1	8.6 ± 1.9

Values are mean ± SD. A, amplitude. TD, time delay and τ, time constant of each component. I, initial component; P, primary component. A'_P, amplitude of primary component of response (A'_I + A_P, for \dot{Q}_{cap}). * Significantly different from moderate exercise ($P < 0.05$).

Figure 3.1. Schematic illustrating the estimation of muscle O₂ uptake from pulmonary O₂ uptake.

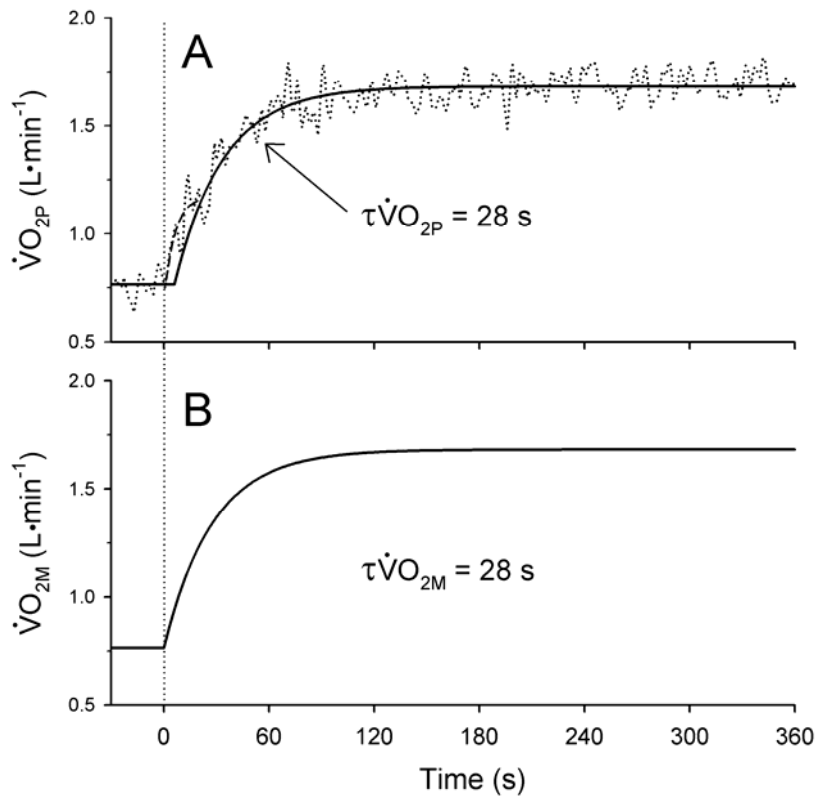


Figure 3.1. Schematic illustrating the procedure used to estimate, from the time constant (τ) and amplitude of the primary component (A'_1) of the pulmonary $\dot{V}O_2$ ($\dot{V}O_{2p}$) response (*A*), and the kinetics of muscle $\dot{V}O_2$ ($\dot{V}O_{2m}$) (*B*). *A*) *Dashed line*, best regression fit through the $\dot{V}O_{2p}$ corresponding to the cardiodynamic phase; *Solid line*, best regression fit through the primary component of $\dot{V}O_{2p}$ response extended back to the baseline value, to illustrate how $\dot{V}O_{2m}$ kinetics were estimated from the $\dot{V}O_{2p}$ response. $\dot{V}O_{2m}$ kinetics shown in (*B*) (*Solid line*) depicts the solid line shown in (*A*), but with $\dot{V}O_{2m}$ rising exponentially from time zero. The resulting $\dot{V}O_{2m}$ kinetics (as shown in *B*), were then used to estimate the \dot{Q}_{cap} kinetics (Figs. 3.2-3.3).

Figure 3.2. Representative data for moderate exercise.

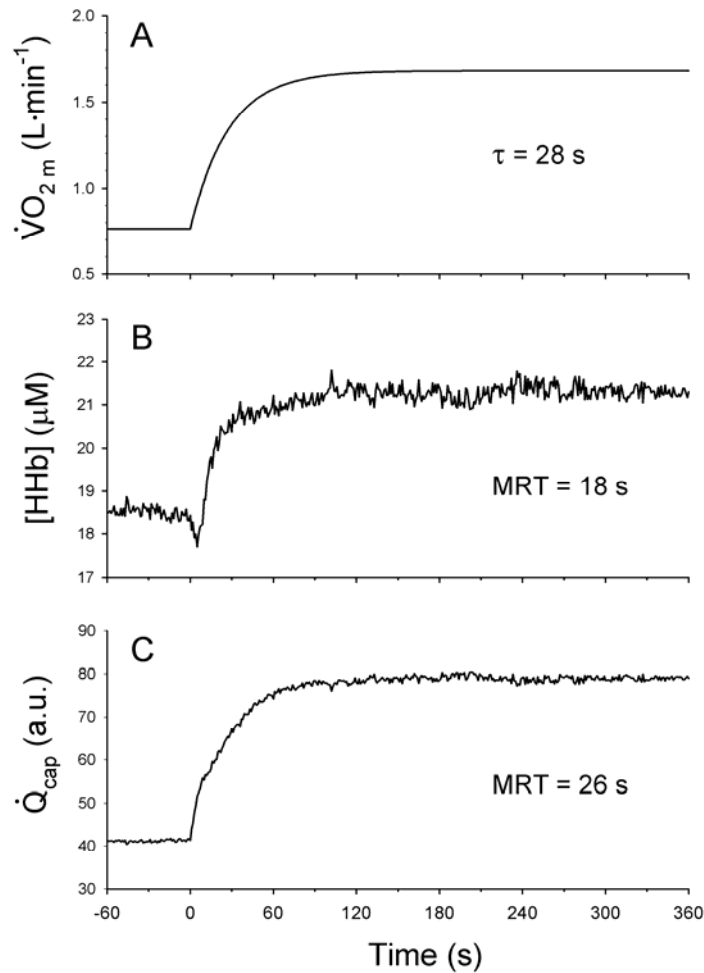


Figure 3.2. Representative data for constant moderate work rate exercise (90% LT) of one subject. *A)* muscle $\dot{V}O_2$ ($\dot{V}O_{2m}$, L·min⁻¹) estimated from the kinetics parameters of pulmonary $\dot{V}O_2$ (as shown in Fig. 1); τ , time constant of $\dot{V}O_{2p}$ (primary component, Eq. 2), *B)* deoxy-hemoglobin concentration ([HHb], μM); MRT, mean response time (time delay plus time constant) and *C)* estimated temporal profile of muscle capillary blood flow (\dot{Q}_{cap}) obtained as $\dot{V}O_{2m}$ divided by [HHb]; MRT was determined as in Eq. 5. The amplitude observed in *C* does not reflect the ‘true’ amplitude of blood flow; however, the kinetics should be robust (see text). Note that in this subject (and also in two other subjects) [HHb] temporarily decreased in the first seconds of exercise, indicating that \dot{Q}_{cap} initially (first 5-10 s) increased faster than $\dot{V}O_{2m}$. Other possible causes of this early decrease in [HHb] has been discussed in detail by DeLorey et al. (2003) and Grassi et al. (2003).

Figure 3.3. Representative data for heavy exercise.

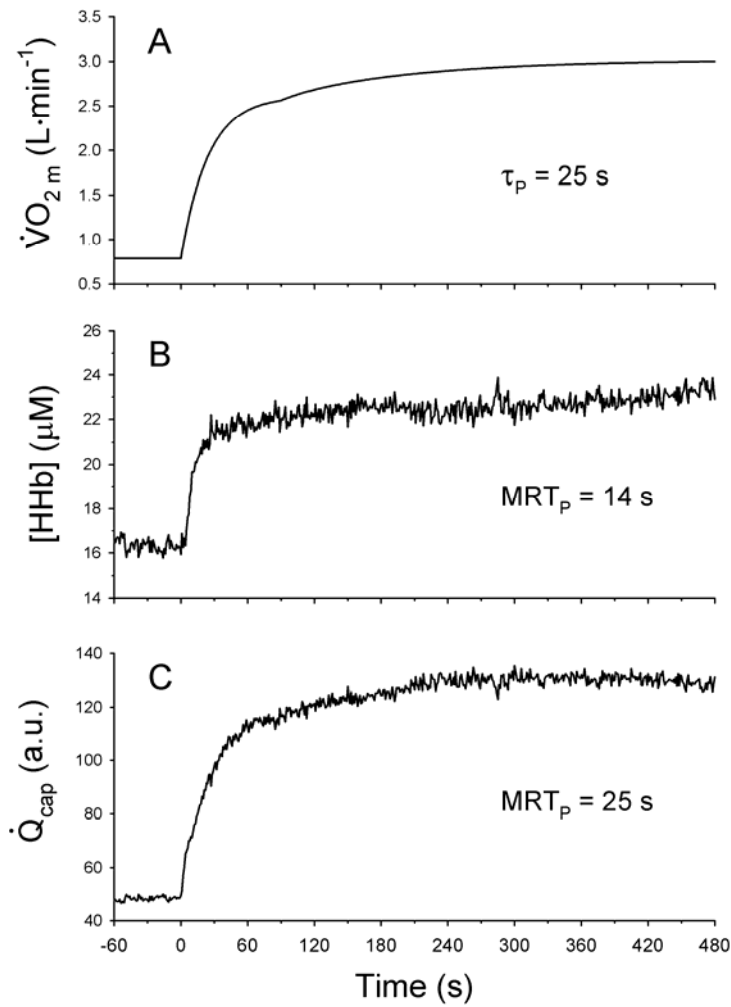


Figure 3.3. Representative data for heavy exercise (50% Δ) from the subject presented in Fig. 3.2. τ_p , time constant of primary component. MRT_p , mean response time of primary component. See Fig. 3.2 for abbreviations and further details on panels *A*, *B* and *C*.

Figure 3.4. Estimated muscle capillary blood flow (moderate and heavy exercise).

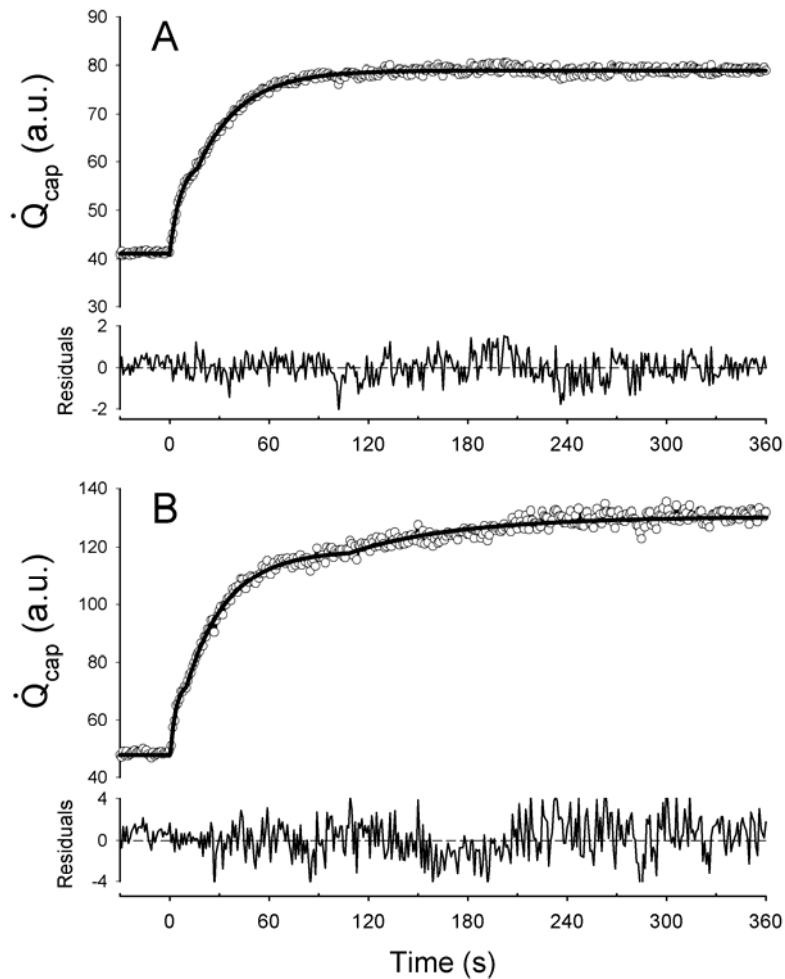


Figure 3.4. Estimated muscle capillary blood flow (\dot{Q}_{cap} ; *open circles*) for moderate exercise (*A*, from Fig. 3.2C) and heavy exercise (*B*, from Fig. 3.3C). *Solid line* represents the best fit using Eq. 2. Note the presence of an early ‘phase 1’ for both moderate (*A*) and heavy exercise (*B*). Note that in *B* the last 120 s of data (360-480 s) are not shown so as to facilitate visualization of the primary component of the \dot{Q}_{cap} response.

Figure 3.5. Overall kinetics of deoxy-hemoglobin, O₂ uptake and estimated capillary blood flow.

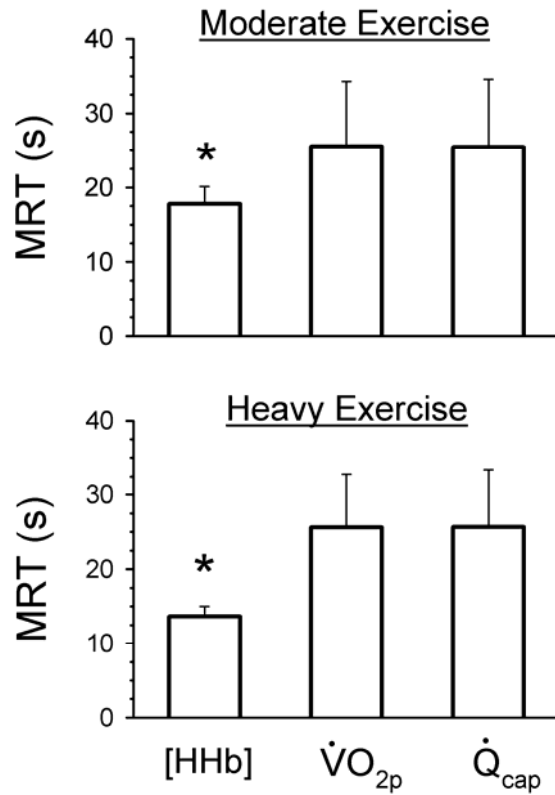


Figure 3.5. Overall kinetics (mean response time, MRT) of deoxy-hemoglobin concentration ([HHb]), pulmonary $\dot{V}O_2$ and muscle capillary blood flow (\dot{Q}_{cap}). For pulmonary $\dot{V}O_2$ MRT represents the time constant of the primary component of the response (Eq. 2). The data are mean \pm S.D. (Error bars). *Significantly different from $\tau_p \dot{V}O_2$ and MRT- \dot{Q}_{cap} ($P < 0.05$).

Figure 3.6. Relationship between kinetics of blood flow and O₂ uptake.

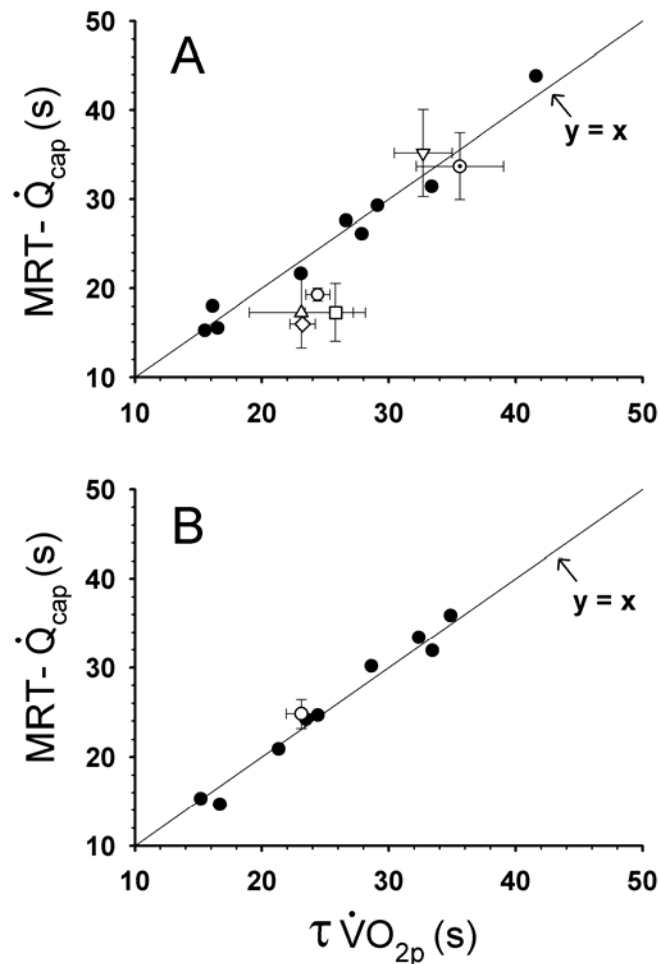


Figure 3.6. Relationship between mean response time of muscle capillary blood flow ($MRT-\dot{Q}_{cap}$) and time constant of pulmonary $\dot{V}O_2$ ($\tau\dot{V}O_{2p}$; primary component) for moderate (*A*; $r = 0.99$, $P < 0.001$) and heavy exercise (*B*; $r = 0.99$, $P < 0.001$). Also shown are the means \pm s.e.m. (symbol \pm error bars) from previous studies investigating the relationship between muscle blood flow and muscle $\dot{V}O_2$. In (*A*) and (*B*) *solid line* represents line of identity. *A*) *closed circles*, present study; *open circle dotted*, cycling (Grassi *et al.*, 1996); *open triangle down*, knee-extension (Koga *et al.*, 2005); *open square*, dog gastrocnemius (Grassi *et al.*, 1998); *open triangle up*, knee-extension (MacDonald *et al.*, 1998); *open circle*, forearm exercise (Hughson *et al.*, 1996); *open diamond*, rat spinotrapezius (Behnke *et al.*, 2002a). *B*) *closed circles*, present study; *open circle*, dog gastrocnemius (Grassi *et al.*, 2000). Note that for the present study and the studies of MacDonald *et al.* (1998) and Koga *et al.* (2005), $\tau\dot{V}O_2$ corresponds to the time

constant of primary component of pulmonary $\dot{V}O_2$. For Hughson *et al.* (1996) the data shown represents the results of arm exercise below heart level. In Grassi *et al.* (1998), $\tau\dot{V}O_2$ and MRT- \dot{Q} were calculated from the reported $t_{50\%}$ and for Grassi *et al.* (2000), they correspond to the reported $\tau + TD$ of $\dot{V}O_2$ and \dot{Q}_m , respectively.

**CHAPTER 4 - Effects of altered nitric oxide availability on rat
muscle microvascular oxygenation during contractions**

Summary

The present study was developed to explore the role of nitric oxide (NO) in controlling microvascular O₂ pressure (PO_{2mv}) at rest and during contractions (1 Hz). We hypothesized that at the onset of contractions sodium nitroprusside (SNP) would raise PO_{2mv} and slow the kinetics of PO_{2mv} change whereas L-nitro arginine methyl ester (L-NAME) would decrease PO_{2mv} and speed its kinetics. The spinotrapezius muscle of female Sprague-Dawley rats (n = 7, body mass = 298 ± 10 g) was superfused with SNP (300 μM) and L-NAME (1.5 mM) and measured PO_{2mv} (phosphorescence quenching). SNP decreased mean arterial pressure (92 ± 5 mmHg) below that of control (CON, 124 ± 4 mmHg) and L-NAME (120 ± 4 mmHg) conditions. SNP did not raise PO_{2mv} at rest but it did elevate the PO_{2mv}-to-MAP ratio (50% increase, *P* < 0.05) and slow the kinetics by lengthening the time delay (TD, 14.0 ± 5.0 s) and time constant (τ, 24.0 ± 10.0 s) of the response compared with CON (TD, 8.4 ± 3.3 s; τ, 16.0 ± 4.5 s, *P* < 0.05 vs. SNP). L-NAME decreased PO_{2mv} at rest and tended to speed τ (10.1 ± 3.8 s, *P* = 0.1), while TD (8.1 ± 1.0 s) was not significantly different. L-NAME also caused PO_{2mv} to fall transiently below steady-state contracting values. These results indicate that NO availability can significantly affect PO_{2mv} at rest and during contractions and suggests that PO_{2mv} derangements in aging and chronic disease conditions may potentially result from impairments in NO availability.

Introduction

To power oxidative phosphorylation and minimize reliance on finite energy sources during muscle contractions O_2 must be transported from the lungs to the mitochondria. The penultimate step in this pathway, which may be limiting during exercise, is at the capillary-myocyte barrier (Wagner, 1996). The O_2 pressure (PO_2) gradient, i.e. the PO_2 difference between the capillary or microvascular blood and that in the intramyocyte space, is the exclusive driving force for O_2 flux into the myocyte (Fick's law of diffusion). Thus, if microvascular PO_2 (PO_{2mv}) falls below that necessary to drive a given O_2 flux, muscle O_2 uptake ($\dot{V}O_2$) will be compromised and a greater reliance will be placed upon substrate-level phosphorylation (e.g. creatine phosphate) and anaerobic glycolysis for ATP requirements (Hogan *et al.*, 1992).

Microvascular PO_2 is determined by the matching of muscle O_2 delivery ($\dot{Q}O_2$) and $\dot{V}O_2$, i.e., $\dot{Q}O_2/\dot{V}O_2$. At the onset of muscle contractions, when $\dot{V}O_2$ is rising at its fastest rate, $\dot{Q}O_2$ must rise in proportion to $\dot{V}O_2$ in order to limit or constrain the fall of PO_{2mv} which would compromise muscle oxidative function. In healthy young muscles at the onset of contractions, PO_{2mv} remains at or close to resting levels for 10-20 s (time delay, TD) before decreasing exponentially to a steady-state level that is determined by the muscle fiber type as well as the stimulation characteristics (Behnke *et al.*, 2001; Behnke *et al.*, 2002a; Behnke *et al.*, 2003; McDonough *et al.*, 2005). This profile is thought to reflect a biphasic increase of $\dot{Q}O_2$ that is superimposed upon a monoexponential $\dot{V}O_2$ response (MacDonald *et al.*, 1998; Shoemaker & Hughson, 1999; Behnke *et al.*, 2001; Kindig *et al.*, 2002b; Ferreira *et al.*, 2005b; Koga *et al.*, 2005). In marked contrast to this healthy response, aging (Behnke *et al.*, 2005) and disease conditions such as chronic heart failure [CHF; (Diederich *et al.*, 2002)] and diabetes (Behnke *et al.*, 2002b) are characterized by a much faster fall of PO_{2mv} following the onset of contractions. Moreover, in old individuals and these disease conditions PO_{2mv} decreases transiently below its end-contraction value in contrast to the monoexponential PO_{2mv} profile seen in young healthy muscles. In this context, PO_{2mv} may achieve very low levels either transiently or for the duration of the contractions bout. In both instances the PO_{2mv} , which constitutes the upstream pressure facilitating mitochondrial O_2 delivery, is compromised and this is likely to contribute to the slowed $\dot{V}O_2$ kinetics characteristic of these conditions (Meakins & Long, 1927; Riley *et al.*, 1994; Regensteiner *et al.*, 1998; Hepple *et al.*, 1999; Bell *et al.*, 1999; Scheuermann *et al.*, 2002).

Amongst the numerous mechanisms that increase $\dot{Q}O_2$ in the contracting muscle, the muscle pump, nitric oxide (NO), cyclooxygenase, endothelial-derived hyperpolarizing factor, and contraction-induced metabolites (including H^+ , K^+ and CO_2) as well as conducted vasodilation (Segal, 2000; Tschakovsky & Sheriff, 2004) have been considered important. There

are likely to be interspecies variations in the relative importance of these mechanisms, however, NO-mediated vasodilation has been demonstrated to be crucial in sustaining the exercise hyperemia seen in running rats (Hirai *et al.*, 1995) and the cardiac output in horses (Bailey *et al.*, 2000). Moreover, aging (Taddei *et al.*, 1995; Woodman *et al.*, 2002; Tanabe *et al.*, 2003), CHF (Drexler *et al.*, 1992; Hirai *et al.*, 1995; Varin *et al.*, 1999), and diabetes (De Vriese *et al.*, 2000; Bagi & Koller, 2003) are all associated with a downregulation of endothelial function and/or endothelial NO production. In addition to its effects on $\dot{Q}O_2$, NO has an important role in modulating mitochondrial oxidative phosphorylation (Brown, 2000). Accordingly, blockade of nitric oxide synthase speeds the kinetics of $\dot{V}O_2$ in humans (Jones *et al.*, 2003; Jones *et al.*, 2004b) and horses (Kindig *et al.*, 2001; Kindig *et al.*, 2002a) but not in the dog gastrocnemius muscle (Grassi *et al.*, 2005).

Therefore, the purpose of the present investigation was to explore the role of NO on the $\dot{Q}O_2$ -to- $\dot{V}O_2$ matching (as assessed from measurements of PO_{2mv}) across the rest-to-contractions transition. Specifically, we tested the hypothesis that at the onset of contractions: 1. increasing NO availability via sodium nitroprusside superfusion would elevate resting and contracting PO_{2mv} and slow the dynamic fall of PO_{2mv} . 2. L-NAME induced decrease of NO availability would reduce resting and contracting PO_{2mv} and speed the dynamic fall of PO_{2mv} . We further hypothesized that L-NAME would induce a transient lowering of PO_{2mv} below the steady-state value that would be qualitatively similar to that seen in conditions associated with reduced NO availability, e.g., aging, CHF and diabetes.

Methods

Animals: Seven female Sprague-Dawley rats (body mass 298 ± 10 g) were used in this investigation. Rats were maintained on a 12:12-h light-dark cycle and received water and food *ad libitum*. Upon completion of the study, each animal was euthanized with pentobarbital sodium. All procedures described herein were approved by the Kansas State University Institutional Animal Care and Use Committee (IACUC).

Surgical Preparation: The animals were anaesthetized with pentobarbital sodium (50 mg kg^{-1} I.P., to effect) and placed on a heating pad to maintain a constant body temperature (~ 38 °C) throughout the experimental protocol. The left carotid artery was cannulated (Polyethylene-50, Intra-Medic tubing, Clay Adams, Sparks, MD, USA) for infusion of the phosphorescent probe palladium *meso*-tetra (4-carboxyphenyl) porphyrin dendrimer (R2; 15 mg/kg), monitoring of arterial blood pressure (Digi-Med BPA model 200, Louisville, KY, USA) and blood withdrawal. Arterial blood was sampled after completion of the experimental protocol to determine blood gas, pH, and plasma lactate (Nova Stat Profile M, Waltham, MA, USA), as well as systemic haematocrit (Adams Micro-Hematocrit reader, Clay Adams, Parsipanny, NJ, USA).

The skin and overlying fascia of the mid-dorsal region of the rat was reflected back to expose the right spinotrapezius muscle. The spinotrapezius is a postural muscle that originates on the lower thoracic and upper lumbar region closely associated with the vertebral column and inserts on the scapula. The muscle and surrounding tissue were kept moist with a Krebs-Henseleit bicarbonate-buffered solution (4.7 mM KCl, 2.0 mM CaCl_2 , 2.4 mM MgSO_4 , 131 mM NaCl, and 22 mM NaHCO_3) equilibrated with 5 % CO_2 -95 % N_2 at 38 °C and covered with Saran Wrap (Dow, Indianapolis, IN, USA) between stimulation periods.

Muscle stimulations: Electrical stimulation of the muscle was conducted (1 Hz; 4-6 V; 2 ms pulse duration) to elicit twitch muscle contractions using a Grass S88 stimulator (Quincy, MA, USA) for 3 min. These stimulation parameters have been shown to elicit an increase in blood flow of $\sim 240\%$ and increase in $\dot{V}\text{O}_2$ of $\sim 350\%$ (Behnke *et al.*, 2002a). To elicit muscle contractions, stainless steel plate electrodes (2.5 mm diameter) were sutured to the rostral (cathode) and caudal region (anode) of the muscle using 6-0 sutures. The sutures were necessary to avoid changes in electrode position upon superfusion of the muscle.

Experimental Protocol: Upon completion of the surgery, the phosphor R2 was infused via the arterial cannula approximately 15 min before the first stimulation period for measurement

of PO_2mv (see below). The spinotrapezius muscle was superfused with Krebs-Henseleit (CON), SNP (300 μ M in Krebs-Henseleit) and L-NAME (1.5 mM in Krebs-Henseleit). These concentrations were established based on preliminary experiments. All solutions were maintained at $\sim 38^\circ\text{C}$. The dose of SNP was titrated to avoid a decrease in MAP below 60-70 mmHg at any time. Sodium nitroprusside displayed an effect on MAP of rapid onset, while L-NAME did not affect MAP suggesting that a physiologically relevant leakage of L-NAME into the systemic circulation did not occur. The order of treatment was SNP, CON and L-NAME. The SNP trial was always first to minimize the total procedure time and any potential transient vasoconstriction induced by suturing of electrodes to the muscle, while L-NAME was the last treatment due to its long half-life that prevented randomization of CON and L-NAME conditions. Prior to stimulation the muscle was superfused for a total of 15-20 min with each solution (average flow rate 1-2 $\text{ml}\cdot\text{min}^{-1}$). A 10 min period was allowed between the end of muscle stimulation and start of superfusion with CON and L-NAME solutions. After the end of the SNP trial the muscle was superfused with Krebs-Henseleit for 25-30 min (i.e., 10 min constantly flushing of the muscle to wash out SNP, plus 15-20 min to replicate the drug treatments). It is noteworthy that preliminary experiments showed no order effect on any parameter of PO_2mv kinetics (Eq. 1) when the muscles were allowed to recover for 25-30 min (Ferreira, Padilla, Williams, Hageman, Musch and Poole, unpublished findings). The total procedure time (i.e. surgery and stimulation periods) did not exceed 4 hours.

Microvascular PO_2 measurements: Microvascular PO_2 (PO_2mv) was measured using the phosphorescence quenching method. As described previously (Behnke *et al.*, 2001; Behnke *et al.*, 2002a; Geer *et al.*, 2002), the phosphorescence quenching technique used to determine PO_2mv is based upon the Stern-Volmer relationship (Rumsey *et al.*, 1988) which describes quantitatively the O_2 dependence of the phosphorescent probe (i.e. R2). As a non-toxic dendrimer (Lahiri *et al.*, 1993), the R2 probe is bound to albumin at 38°C and pH 7.4, and is uniformly distributed in the plasma providing a signal corresponding to the volume-weighted O_2 pressure in the microvascular compartment [principally the PO_2 within the capillary space, which volumetrically constitutes the major intramuscular vascular space (Poole *et al.*, 1995)]. In addition to binding to albumin, R2 is negatively charged which helps facilitate restriction of the compound to the vascular space (Poole *et al.*, 2004). We used values for the quenching constant and lifetime of phosphorescence decay in the absence of O_2 for R2 of 409 $\text{mmHg}\cdot\text{s}^{-1}$ and 601 μs , respectively (Lo *et al.*, 1997; Pawlowski & Wilson, 1992).

Microvascular PO_2 was determined using a Frequency Domain Phosphorometer (PMOD 1000, Oxygen Enterprises Ltd, Philadelphia, PA, USA) at 2s intervals. The common end of the

bifurcated light guide was placed 2-3 mm above the medial region of the spinotrapezius (i.e. superficial to the dorsal surface) with the excitation light focused on a ~2 mm diameter circle. Movement of the light guide (or animal) was avoided to monitor the same sampling site throughout the experiment. On a few occasions, repositioning of the phosphorometer light guide was necessary in order to sample PO₂mv from precisely the same location of the spinotrapezius muscle. The phosphorometer employs a sinusoidal modulation of the excitation light (524 nm) at frequencies between 100 Hz and 20 kHz, which permits phosphorescence lifetime measurements from 10 μs to ~2.5 ms. Ten scans (100 ms) were performed in the single frequency mode to acquire the resultant lifetime of the phosphorescence (700 nm) (Vinogradov *et al.*, 2002).

Curve-fitting of PO₂mv dynamics: The dynamics of PO₂mv were described by nonlinear regression analysis using commercial software packages (SigmaPlot 7.01, Systat Software, CA, USA). Goodness of fit was determined via three criteria: 1) the coefficient of determination (r²), 2) the sum of the squared residuals (i.e. χ²), and 3) visual inspection. The equation used to describe the kinetics of PO₂mv was

$$\begin{aligned} \text{PO}_2\text{mv}_{(t)} = & \text{PO}_2\text{mv}_{(\text{baseline})} - \Delta\text{PO}_2\text{mv}_{(\text{primary})} [1 - e^{-(t-\text{TD}_1)/\tau_1}] && \text{(primary component)} && (1) \\ & + \Delta\text{PO}_2\text{mv}_{(\text{secondary})} [1 - e^{-(t-\text{TD}_2)/\tau_2}] && \text{(secondary component)} \end{aligned}$$

where baseline corresponds to precontraction PO₂mv, and Δ is the amplitude of the PO₂mv response. The time constants are indicated as τ₁ and τ₂, and TD₁ and TD₂ are the independent time delays of the respective responses. For monoexponential responses only the primary component was used to describe the data. An equation including the primary and secondary components was used whenever we observed a consistent decrease in PO₂mv below its end-contraction value. While we are not certain that the secondary component is exponential this fitting procedure has been successfully used in previous studies allowing an excellent description of the data (see above) to examine the overall kinetics of PO₂mv (Behnke *et al.*, 2002b; Diederich *et al.*, 2002; Behnke *et al.*, 2003; Behnke *et al.*, 2005). The results from curve fitting were then used to calculate the nadir and end-stimulation PO₂mv.

Statistics: Means were compared with one-way ANOVA, while the Student-Newman-Keuls test was used for *post-hoc* analysis. Statistical significance was accepted at *P* < 0.05. All tests were conducted with commercially available software (SigmaStat 3.0, Systat Software, CA, USA). Data are reported as mean ± SEM.

Results

Arterial O₂ saturation was $93 \pm 1 \%$, systemic haematocrit $41.0 \pm 0.77 \%$, arterial blood pH 7.45 ± 0.01 and plasma lactate $1.6 \text{ mmol}\cdot\text{L}^{-1}$. Mean arterial pressure (MAP) decreased significantly during superfusion with SNP ($92 \pm 5 \text{ mmHg}$), while MAP for Control ($124 \pm 4 \text{ mmHg}$) and during the superfusion with L-NAME ($120 \pm 4 \text{ mmHg}$) were not significantly different.

The PO_{2mv} response was substantially different for Control, SNP and L-NAME both qualitatively (Figs. 4.1 and 4.2A) and quantitatively (Figs. 4.2B and 4.3). Baseline PO_{2mv} was significantly lower during L-NAME compared to Control and SNP (Fig. 4.3), while no significant difference was seen for SNP vs. Control. However, when normalized for changes in MAP a significant difference was observed for both SNP and L-NAME compared to Control (Fig. 4.2B). Specifically, before muscle stimulations the PO_{2mv}-to-MAP ratio was 50% higher during SNP and 30% lower during L-NAME compared to Control, which demonstrates that a substantial drug effect was achieved. At the end of stimulation PO_{2mv} was significantly higher during SNP, while L-NAME decreased PO_{2mv} significantly compared to Control (Fig. 4.3).

The overall dynamics of PO_{2mv}, represented by the MRT, were slower during SNP compared to Control (Fig. 4.3). Specifically, we observed a longer time delay (TD) during SNP vs. Control and a slower time constant (τ) of PO_{2mv} (Fig. 4.3). Thus, the MRT (TD + τ) was significantly longer for SNP vs. Control. In contrast, L-NAME tended to speed the kinetics of PO_{2mv} compared to Control (similar TD with a tendency for significantly faster τ ; $P = 0.1$) and led to a transient PO_{2mv} decrease below the final contracting steady-state PO_{2mv} (Figs. 4.1-4.2). This response was characterized by a better fit of the L-NAME response with a two-component model as opposed to the one-component model in all animals studied. In marked contrast, the best fit for the Control response of only one animal (out of seven) was achieved with a two-component model. For unknown reasons one animal demonstrated an apparently linear increase in PO_{2mv} of delayed onset ($\sim 100 \text{ s}$) during the Control trial. The ΔPO_{2mv} (Baseline - Nadir) appeared to be lower for SNP vs. Control and L-NAME but the P value for ANOVA did not reach the a priori established significance level ($P = 0.10$). In this context, the nadir PO_{2mv} was significantly increased by SNP vs. Control ($17.4 \pm 1.2 \text{ mmHg}$ vs. $13.0 \pm 0.8 \text{ mmHg}$; $P < 0.05$), whereas the nadir PO_{2mv} was lower during L-NAME ($6.3 \pm 0.8 \text{ mmHg}$) compared to Control and SNP (both $P < 0.05$). Altogether, the PO_{2mv} data indicate that SNP and L-NAME substantially altered the dynamics of the $\dot{Q}\text{O}_2$ -to- $\dot{V}\text{O}_2$ ratio following the onset of muscle stimulations.

Discussion

The most important original finding of the present investigation is that NO availability exerts a major influence over the ability to sustain PO_{2mv} at rest and during contractions in the mixed-fiber type spinotrapezius muscle. Specifically, in accordance with our first and second hypotheses increasing NO availability with SNP raised PO_{2mv} (increased $\dot{Q}O_2/\dot{V}O_2$ ratio) during contractions whereas decreasing NO availability with L-NAME reduced PO_{2mv} at rest and during contractions. In addition, SNP slowed whereas L-NAME speeded the kinetics of PO_{2mv} at the onset of contractions. However, in contrast to our hypothesis SNP did not increase PO_{2mv} in resting muscle when compared to control. We believe that this effect resulted from SNP “leakage” into the systemic circulation which lowered the MAP. It is pertinent that SNP increased the PO_{2mv}/MAP ratio significantly as seen in Figure 4.2. These results demonstrate that interventions that increase NO production and availability (e.g., exercise training) have the potential to increase PO_{2mv} in contracting muscle. By the same token, conditions that decrease NO production, and therefore availability, are expected to reduce PO_{2mv} at rest and during muscle contractions. These effects on PO_{2mv} are important because this variable provides the driving force for blood-myocyte O_2 transport.

Correspondence with Existing Literature: The PO_{2mv} profiles from the control stimulations resembled closely those demonstrated previously in the spinotrapezius muscle from female Sprague-Dawley rats in our laboratory (Behnke *et al.*, 2001; Behnke *et al.*, 2002a; Diederich *et al.*, 2002). Accordingly, at the onset of contractions there was a significant delay (TD) where PO_{2mv} remained at or close to resting baseline values followed by an exponential fall to the contracting steady state.

To our knowledge there are no published data on the effects of either SNP or L-NAME on PO_{2mv} in muscle. Compared with the control conditions in the present investigation, SNP slowed (increased TD, τ and MRT) whereas L-NAME tended to speed (decreased τ and MRT, $P = 0.1$) the overall PO_{2mv} response. Moreover, L-NAME induced a pronounced fall in baseline PO_{2mv} and distinctly altered the shape of the PO_{2mv} response curve by driving PO_{2mv} transiently below its steady-state level which necessitated use of a double exponential model to fit the data (Fig. 4.1B). A similar transient fall of PO_{2mv} below contracting steady-state levels at the onset of contractions has been found previously in the spinotrapezius muscle of old rats (Behnke *et al.*, 2005), Type I diabetic rats (Behnke *et al.*, 2002b) and rats with CHF (Diederich *et al.*, 2002). In addition, PO_{2mv} kinetics are speeded in Type I diabetes [shorter TD and MRT (Behnke *et al.*, 2002b)] and moderate CHF [shorter τ and MRT (Diederich *et al.*, 2002)].

Mechanistic Bases for effects of Sodium Nitroprusside and L-NAME on PO_{2mv} : With SNP superfusion it was not possible to prevent a systemic vasodilation that reduced MAP significantly from ~ 120 to 90 mmHg. Based on the assumption that the reduced MAP would decrease blood flow and therefore $\dot{Q}O_2$ in proportion to the driving pressure and that the O_2 dissociation curve is linear across the range of PO_{2mv} measured, we corrected the resting PO_{2mv} for changes in MAP. This is conceptually similar to calculations of vascular conductance and the results of this normalization (Fig. 4.2B) suggest that had MAP remained at control levels resting PO_{2mv} would have been $\sim 50\%$ higher during SNP compared to control values, which is indirect evidence for substantial vasodilation of arteriolar resistance vessels.

The kinetics of PO_{2mv} reflect the dynamic matching between $\dot{Q}O_2$ and $\dot{V}O_2$. Therefore, alterations in the temporal profile of increase in either $\dot{Q}O_2$ or $\dot{V}O_2$ will affect the kinetics of PO_{2mv} . Sodium nitroprusside will cause vascular smooth muscle relaxation and increase vascular conductance possibly leading to faster increase in $\dot{Q}O_2$. Moreover, augmented NO availability inhibits mitochondrial function directly and also by competing with O_2 at the binding site on cytochrome oxidase [e.g., (Shen *et al.*, 1994; Brown, 2000)]. Thus, the increased TD and slowed τ may have resulted from both an impairment of mitochondrial oxidative function (slower $\dot{V}O_2$ kinetics) and faster increase in $\dot{Q}O_2$ during contractions. The compelling weight of evidence suggests that the early increase in $\dot{Q}O_2$ (Phase I) is mediated by either a muscle pumping effect and/or a rapid vasodilation (Tschakovsky & Sheriff, 2004). In this regard it is pertinent that Dobson & Gladden (2003) and Hamman *et al.* (2003) have both been unable to demonstrate the presence of a muscle pumping effect during contractions where the muscle is pre-vasodilated with adenosine. Furthermore, increased NO availability may inhibit the production and/or action of endothelium-derived hyperpolarizing factor (EDHF, an important vasodilator pathway) (Nishikawa *et al.*, 2000). This would support the notion that the prolongation of TD and slowing of τ resulted from impaired $\dot{V}O_2$ rather than faster $\dot{Q}O_2$, at least across the first few seconds of contractions.

In contrast to SNP, L-NAME superfusion did not alter MAP and at least by this criterion did not alter the perfusion pressure to the spinotrapezius muscle. However, within the spinotrapezius muscle itself the decreased PO_{2mv} at rest and more rapid fall at the onset of contractions indicated a reduced $\dot{Q}O_2$ - $\dot{V}O_2$ ratio and a faster increase of $\dot{V}O_2$ relative to $\dot{Q}O_2$ compared with control conditions. Whereas in contracting human muscle the role of NO-mediated vasodilation as the principal determinant of the $\dot{Q}O_2$ kinetics (Radegran & Saltin, 1999) and steady-state $\dot{Q}O_2$ (Joyner & Dietz, 1997) has been questioned, there is solid evidence that NO contributes significantly to resting and contracting muscle blood flow and thus $\dot{Q}O_2$ in rats [e.g., (Hirai *et al.*, 1995)]. In addition, the removal or reduction of inhibitory effects of NO on

mitochondrial oxidative function and thus $\dot{V}O_2$ must be considered. Specifically, NO blockade: 1. speeds $\dot{V}O_2$ kinetics at the onset of exercise in horses (Kindig *et al.*, 2001; Kindig *et al.*, 2002a) and humans (Jones *et al.*, 2003; Jones *et al.*, 2004a; Jones *et al.*, 2004b) but not in canine muscle (Grassi *et al.*, 2005), and 2. increases $\dot{V}O_2$ at rest and during contractions (Shen *et al.*, 1994). The present investigation is the first to demonstrate that NO availability is critical for preserving the balance between $\dot{Q}O_2$ and $\dot{V}O_2$ such that the magnitude of the fall of PO_{2mv} at the onset of contractions is constrained.

As mentioned previously, the dynamic profiles of $\dot{Q}O_2$ and $\dot{V}O_2$ at the onset of contractions are different (Shoemaker & Hughson, 1999; Kindig *et al.*, 2002b). The dynamics of $\dot{Q}O_2$ are biphasic with a close-to-instantaneous Phase I followed after several seconds by a slower Phase II that elevates $\dot{Q}O_2$ to the steady state. In contrast, $\dot{V}O_2$ begins to increase essentially instantaneously from contractions onset in a close-to-monoexponential fashion (Behnke *et al.*, 2002a; Grassi *et al.*, 2002). Behnke *et al.* (2002a) and Ferreira *et al.* (2005a) have modeled the effects of altering the magnitude and kinetics of $\dot{Q}O_2$ on either PO_{2mv} or venous O_2 content. Accordingly, several scenarios can account for the biphasic PO_{2mv} (undershoot) that was apparent at the onset of contractions in the L-NAME condition. These can be summarized as a slower increase and reduced amplitude of $\dot{Q}O_2$ during Phase I and/or Phase II. In each of these conditions, accelerated $\dot{V}O_2$ kinetics and a greater steady-state $\dot{V}O_2$ response will exacerbate the lowering of PO_{2mv} across the transition. Some insight into which of the above scenarios may be producing the PO_{2mv} profile observed herein with L-NAME may be derived from consideration of whether NO-induced vasodilation contributes to Phase I or Phase II of the $\dot{Q}O_2$ response. Based on the results of Behnke *et al.* (2002a) and Ferreira *et al.* (2005a) the similar time delay, but faster time constant of PO_{2mv} for L-NAME vs. Control, suggest that L-NAME caused a dynamic $\dot{Q}O_2$ -to- $\dot{V}O_2$ mismatch primarily during Phase II of the $\dot{Q}O_2$ response. As discussed above, Phase I is thought to be mediated by a muscle pumping effect and/or rapid vasodilation (Tschakovsky & Sheriff, 2004). Sheriff & Hakeman (2001) demonstrated that L-NAME attenuated the increase in vascular conductance from 2-10 s following the onset of exercise in treadmill-running dogs. However, the dynamic profile of increase in \dot{Q} of running dogs is different from that observed in the rat-spinotrapezius muscle (Kindig *et al.*, 2002b). The latter has a biphasic response that more closely resembles the exercise hyperemia seen in exercising humans (Shoemaker & Hughson, 1999). Thus, it is possible that in the spinotrapezius muscle NO-mediated vasodilation is a secondary response of delayed onset contingent upon shear stress-induced deformation of the vascular endothelium in addition to reduction of tonic sympathetic vasoconstriction that may be fiber-type dependent (sympatholysis, Thomas & Victor 1998).

Implications for understanding Vascular Control in Health and Disease: The demonstration herein that NO synthase inhibition can reduce muscle PO_2mv at rest and during contractions raises the possibility that derangements in NO availability might underlie the altered PO_2mv profiles noted in aged muscle (Behnke *et al.*, 2005) and that of individuals with Type I diabetes (Behnke *et al.*, 2002b) and CHF (Diederich *et al.*, 2002). Each of these conditions is associated with endothelial dysfunction and/or reduced endothelial NO synthase [aging, (Woodman *et al.*, 2002; Tanabe *et al.*, 2003); Type I diabetes (Bagi & Koller, 2003); CHF, (Hirai *et al.*, 1995; Didion & Mayhan, 1997)]. However, there is evidence that other sources of NO, notably neuronal and inducible NO synthase (nNO synthase and iNO synthase), may be regulated differently such that their contribution to intracellular NO availability is increased and contributes to pathological inflammatory effects (Hambrecht *et al.*, 1999; Adams *et al.*, 2003; Bojunga *et al.*, 2004; Gielen *et al.*, 2005) at the same time that vascular NO is reduced. Thus it is conceivable that, unlike in the present investigation where L-NAME might have simultaneously decreased O_2 delivery and increased O_2 demand, pathological dysfunction in the NO synthase family may decrease both $\dot{Q}O_2$ and $\dot{V}O_2$ (via increased NO-mediated inhibition of mitochondrial function). This would help reduce the disequilibrium between $\dot{Q}O_2$ and $\dot{V}O_2$ and constrain the fall in PO_2mv . However, as evident from the PO_2mv undershoot seen in these conditions the matching between $\dot{Q}O_2$ and $\dot{V}O_2$ found in healthy muscle is not restored. One consequence of this is that blood-myocyte O_2 flux will be decreased and any resultant decrease in intracellular PO_2 is expected to reduce intracellular energy levels (Wilson *et al.*, 1977).

Model Considerations: Electrical stimulation induces a fiber recruitment pattern very different from that found in vivo, and the balance of mechanisms that increase \dot{Q} and therefore $\dot{Q}O_2$ may be very different from that found during voluntary exercise in humans. However, the profile of PO_2mv demonstrated in this and many other investigations [e.g., (Behnke *et al.*, 2001; Behnke *et al.*, 2002a; Behnke *et al.*, 2002b; McDonough *et al.*, 2005)] resembled closely that of femoral venous PO_2 (Grassi *et al.*, 1996; Bangsbo *et al.*, 2000) and also estimates of muscle O_2 saturation assessed via near infrared spectroscopy in humans (Burnley *et al.*, 2002; DeLorey *et al.*, 2003; Grassi *et al.*, 2003).

The superfusion of pharmacological agents directly over the muscle is expected to minimize systemic effects because the active compounds would exert their effects within the spinotrapezius muscle with hopefully only minor systemic leakage through the circulation. Notwithstanding this, there was some leakage of SNP into the systemic circulation which caused a fall of MAP. The normalization procedure used in Figure 4.2 attempts to allow for the

influence of this effect on muscle \dot{Q} by recognizing that the lowered MAP will reduce \dot{Q} and thus $\dot{Q}O_2$ at any given level of vascular conductance. This was not a problem with L-NAME as evidenced by the unchanged MAP maintained during superfusion of this compound. Thus, the effects of L-NAME could be investigated herein without the confounding systemic effects on tonic sympathetic vasoconstriction that may have masked the effects of L-NAME in previous studies [for discussion see (Hirai *et al.*, 1995)].

It is recognized (and discussed above) that NO affects $\dot{Q}O_2$ and $\dot{V}O_2$ at different levels and in different directions. It is possible, in a far more invasive preparation, to quantify the effect of altered NO availability on $\dot{Q}O_2$ and $\dot{V}O_2$ independently. Unfortunately, the procedures necessary for making those measurements impose a severe risk of compromising the preparation and we therefore elected to examine the effects of altered NO availability unencumbered by more intrusive experimental interventions. Hence, for the present investigation, we elected to focus on the principal criterion of blood-myocyte O_2 transfer, PO_{2mv} .

Conclusions

Despite the plethora of vasodilatory mechanisms that facilitate an increased blood flow and oxygen delivery ($\dot{Q}O_2$) at the onset of muscle contractions, in electrically-stimulated rat spinotrapezius muscle the NO pathway appears to represent an integral component of the $\dot{Q}O_2$ -to- $\dot{V}O_2$ matching, during the steady-state and transitional phase of muscle contractions, that ensures maintenance of a high PO_{2mv} . Decreases in NO availability that may occur in aged muscle or secondary to chronic diseases such as diabetes or CHF have the potential to cause the altered PO_{2mv} profiles and reduced O_2 driving pressure described for those conditions (Behnke *et al.*, 2002b; Behnke *et al.*, 2005; Diederich *et al.*, 2002). Mechanistically, the decrease of PO_{2mv} induced by diminished NO availability described herein may initiate a cascade of responses that impair muscle performance including a reduced blood-myocyte O_2 flux, lowered intracellular PO_2 and decreased cellular energy levels.

Figure 4.1. Microvascular PO₂ response from a representative animal

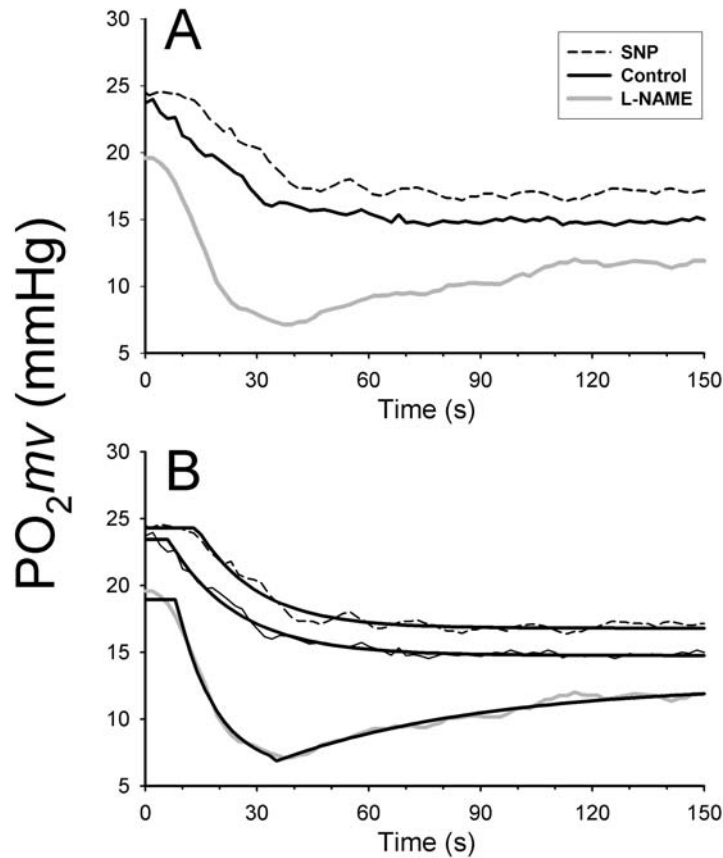


Figure 4.1. Microvascular PO₂ response from a representative animal under control, sodium nitroprusside (SNP) and L-NAME (L-nitro arginine methyl ester). Panel A presents the raw data. Panel B shows the same response as in *A* with best regression fit (solid thick lines). Time zero denotes onset of muscle contractions. Compared with the Control response (mean response time, MRT = 24 s) PO₂mv dynamics were slower during SNP (MRT = 29 s), while during L-NAME PO₂mv kinetics were speeded (MRT = 19 s) and PO₂mv fell transiently below the end contractions value. The increase in PO₂mv after reaching its nadir occurs as a consequence of $\dot{V}O_2$ approaching the steady-state (or diminished rate of increase) while $\dot{Q}O_2$ continues to increase towards its final steady-state value (i.e., slower kinetics of $\dot{Q}O_2$ vs. $\dot{V}O_2$).

Figure 4.2. Microvascular PO₂ response normalized to mean arterial pressure.

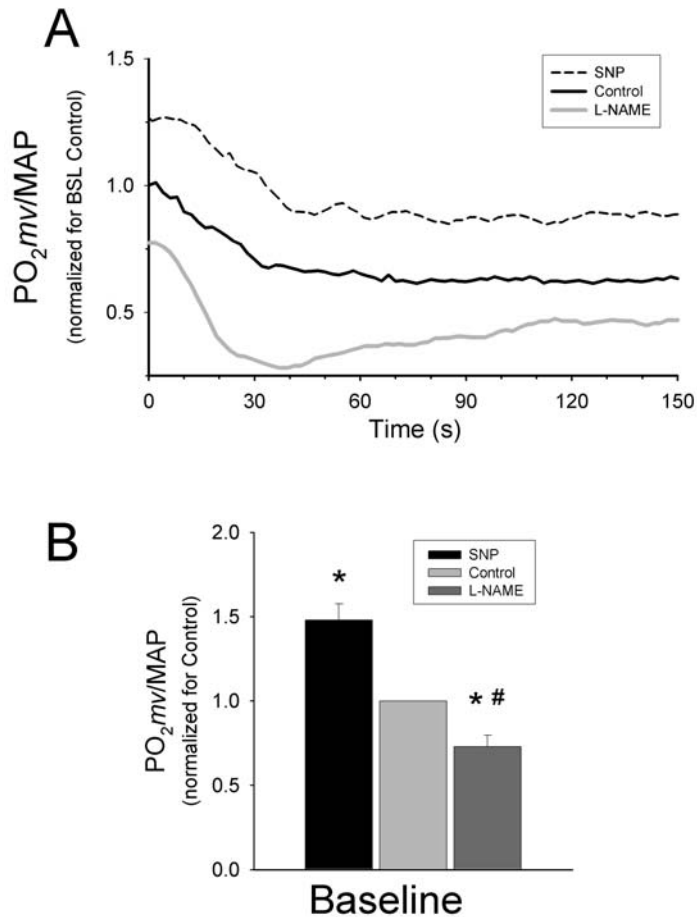


Figure 4.2. Panel A: Microvascular PO₂ response from Figure 4.1 normalized to mean arterial pressure (MAP) during each treatment. In addition, to illustrate and facilitate visualization of the effects of SNP and L-NAME on PO₂mv responses the data were normalized to the baseline (BSL, pre-contracting) value of PO₂mv/MAP during superfusion with Krebs-Henseleit (Control). **Panel B:** Ratio of microvascular PO₂-to-MAP for all seven rat spinotrapezius muscles. The data are normalized to Control values. * Significantly different from Control. # Significantly different from SNP.

Figure 4.3. Kinetics of microvascular PO₂.

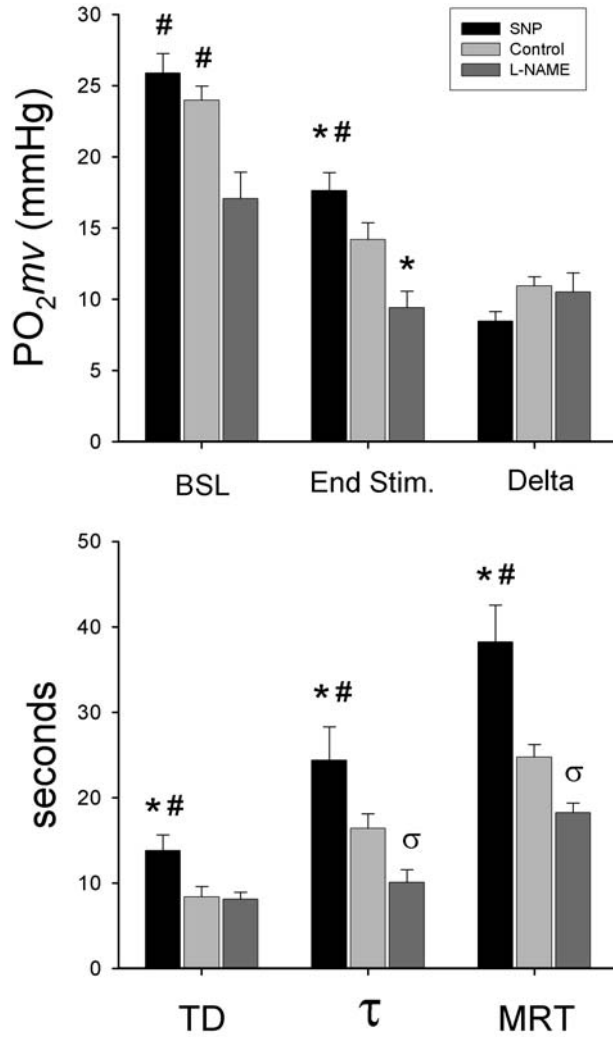


Figure 4.3. Kinetic parameters describing the microvascular PO₂ (PO₂mv) response at rest and in response to 1 Hz stimulation. BSL, Baseline; Δ , decrease in PO₂mv from baseline to nadir; End Stim., end of stimulation; TD, time delay; τ , time constant; MRT, mean response time (TD + τ). * $P < 0.05$ vs. Control; # $P < 0.05$ vs. L-NAME; σ $P = 0.10$ vs. Control.

**CHAPTER 5 - Frequency domain characteristics and filtering of
blood flow following the onset of exercise: implications for kinetics
analysis**

Summary

Typically, the kinetics of blood flow (BF) are determined with data processing methods that yield poor kinetics characterization (i.e., large confidence intervals). In this study we examined the validity and usefulness of a low pass filter (LP_{FILTER}) to reduce point-to-point variability and enhance parameter estimation of the kinetics of BF. Computer simulations were used to determine the power spectrum (Fast Fourier Transform) of simulated responses. In addition, we studied the leg BF response to a single transition in four subjects during supine knee-extension exercise using three methods of data processing [Beat-by-Beat, average of 3 cardiac cycles ($AVG_{3 \text{ BEATS}}$) and LP_{FILTER}]. Femoral artery blood velocity was measured by Doppler ultrasound [and converted to flow using resting values of femoral artery diameter]. The power spectrum of BF, which contained the kinetics information (≤ 0.2 Hz) did not overlap with the main sources of 'noise' (muscle contraction and cardiac cycle) in either simulated responses or Doppler measurements. For the data from 4 subjects, there were no significant differences between the parameter estimates for a 2 exponential fitting function using Beat-by-Beat, $AVG_{3 \text{ BEATS}}$ and LP_{FILTER} ($P > 0.05$). However, LP_{FILTER} (cutoff = 0.2 Hz) resulted in a significantly lower standard error of the estimate (SEE) for all parameters ($P < 0.05$). The means \pm SD for the SEE of time-related parameters for Beat-by-Beat, $AVG_{3 \text{ BEATS}}$ and LP_{FILTER} were: time constant-phase 1 = 5.0 ± 1.1 s, 4.5 ± 2.1 s and 0.3 ± 0.2 s; time delay-phase 2 = 17.8 ± 7.9 s, 12.8 ± 7.5 s and 1.4 ± 1.4 s; time constant-phase 2 = 15.8 ± 4.6 s, 9.9 ± 2.9 s and 1.1 ± 0.5 s, respectively. In conclusion, LP_{FILTER} appeared to be a valid procedure providing the highest signal-to-noise ratio while maintaining original data density. This resulted in better kinetic characterization of BF response (i.e., smallest confidence interval for parameter estimates).

Introduction

The redundancy of processes associated with the muscle blood flow response to exercise (Laughlin & Korzick, 2001; Clifford & Hellsten, 2004) has necessitated the use of kinetics analysis to across the rest-to-exercise transition to discern the relative contribution or importance of select vasodilatory mechanisms. In this context, Doppler ultrasound has been used to measure the dynamics of blood flow response in humans (Shoemaker *et al.*, 1994) and animals (Buckwalter *et al.*, 1998). In spite of good signal acquisition (i.e., little measurement error), these measurements are characteristically ‘noisy’ during exercise due to cardiac cycle and contraction-induced oscillations in blood flow (Lutjemeier *et al.*, 2005) (see Fig 5.1). This is relevant for data interpretation because to make physiological inferences from kinetic parameters and to compare the effects of interventions on control processes it is paramount that the confidence interval for parameter estimation be as narrow as possible. In general, the signal-to-noise ratio and density of data across the transition phase (see *Discussion*) are the main factors affecting the confidence of parameter estimation of kinetics responses (Lamarra *et al.*, 1987).

The kinetics of blood flow are characterized by a fast increase (Phase 1) followed by a slower response beginning ~10-20 s after the onset of exercise (Phase 2) [rev (Shoemaker & Hughson, 1999)]. This biphasic characteristic and rapid early response increases the sensitivity of parameter estimation (and the confidence interval) to the method used for kinetics analysis. Several methods have been used to pre-process the raw data [e.g., beat-by-beat (Fukuba *et al.*, 2004) and contraction-relaxation cycle (Saunders *et al.*, 2005)]. Beat-by-beat data has a temporal resolution that seems adequate for determining blood flow kinetics; however, the low signal-to-noise ratio leads to unacceptably high confidence intervals for the resulting parameter estimates. Conversely, averaging the blood flow response over a contraction-relaxation cycle will improve the signal-to-noise ratio, but with the undesirable effect of reducing the density of data across the transition phase, which might prevent adequate determination of the fast responding processes (Phase 1). Ensemble-averaging of multiple exercise replicates has also been used to improve the signal-to-noise ratio and accentuate the kinetic features [e.g., (MacDonald *et al.*, 1998; Koga *et al.*, 2005; Saunders *et al.*, 2005)]. However, to achieve acceptable confidence intervals for ‘noisy’ responses such as blood flow, it may be necessary to ensemble-average an unreasonable number of transitions (see *Discussion*) (Lamarra, 1990). This would severely limit the utility of this approach in scenarios like patient evaluation where only a limited number of transitions are feasible.

To date there is no method that achieves an optimal balance between signal-to-noise ratio and data density to accentuate the underlying kinetics of blood flow and, consequently, provide

narrow confidence intervals of parameter estimates. In this context, filtering the blood flow data in the frequency-domain might be an alternate option to time-domain filtering (beat-by-beat and contraction-relaxation cycle); however, this approach requires minimal overlap between the frequency spectrum of the underlying kinetics response and the main sources of ‘noise’ in blood flow. To the best of our knowledge, the frequency-domain characteristics of the oscillatory components of blood flow and the underlying kinetic response have not been determined.

The purpose of the present study was to examine the validity and usefulness of filtering blood flow data in the frequency-domain prior to characterizing the kinetic response. We hypothesized that the main sources of ‘noise’ in blood flow during exercise would be muscle contraction and cardiac cycle (Walloe & Wesche, 1988; Radegran & Saltin, 1998; Lutjemeier *et al.*, 2005) (for example see Fig. 5.1), and that the frequency content of these oscillations would not overlap with the frequency range of the slower processes determining the underlying kinetics response because, in general, contraction frequency and heart rate are high-frequency processes. This would permit the application of a low pass filter to the raw Doppler blood flow data in which the higher frequencies associated with muscle contraction and cardiac cycle would be eliminated. The advantage of this filtering procedure would be a lower standard error of the estimate for the parameters of frequency-domain filtered data compared to those obtained with time-domain methods, representing a substantial improvement in the confidence interval for each kinetic parameter.

Methods

Computer simulations: The dynamic (and biphasic) increase in blood flow following the onset of exercise was simulated with exponential equations. The default parameter values for simulations were Baseline = 0.5 a.u., $A_1 = 2$ a.u., $A_2 = 3$ a.u., $\tau_1 = 2$ s, $TD_2 = 15$ s and $\tau_2 = 15$ s (see Eq. 1), similar to a previous computer modeling study (Ferreira *et al.*, 2005a). For simulations of responses without noise the physiologically relevant parameter values are A_1 as percentage of total amplitude ($A_{tot} = A_1 + A_2$), τ_1 , TD_2 and τ_2 . For these parameters our default values are in agreement with results observed in healthy subjects (Radegran & Saltin, 1998; MacDonald *et al.*, 1998; Saunders *et al.*, 2005).

The oscillations in leg blood flow superimposed on the underlying kinetics response were simulated by a sinusoidal function [$y(t) = A \cdot \sin(360 t / T)$], where A = mean-to-peak amplitude and T = period of oscillations (i.e., $T = 1/f$ where f is frequency of oscillations). The known sources of oscillations at rest and exercise are cardiac frequencies (Radegran & Saltin, 1998), very low frequency oscillations (Wray *et al.*, 2004) and muscle contraction (Walloe & Wesche, 1988; Radegran & Saltin, 1998; Lutjemeier *et al.*, 2005). For both heart rate ($100 \text{ beats} \cdot \text{min}^{-1}$, $f = 1.67$ Hz) and muscle contraction (40 min^{-1} , $f = 0.67$ Hz) we simulated $A = 2$ a.u., which represented oscillations equal to 80% of the simulated increase in blood flow from rest-to-exercise. The mean-to-peak amplitude of the very low frequency oscillations (6 min^{-1} , $f = 0.1$ Hz) was arbitrarily set as 0.5 a.u.. In addition, we simulated the existence of random noise (range - 0.75 to 0.75 a.u.) on blood flow measurements. The oscillatory components and random noise were added to the underlying simulated biphasic increase in 'mean' blood flow to qualitatively approximate the raw data of Doppler ultrasound measurements during rest and exercise. It is important to note that a constant heart rate was simulated for the rest-to-exercise transition. Clearly, these simulations are an oversimplification of the real blood flow response; however, they permit examination of the effects of known sources of noise on the time- and frequency-domain characteristics of leg blood flow response to exercise.

Human studies: The experiments were conducted in 4 healthy individuals (2 men and 2 women, age 28 ± 9.0 yrs and body mass 65.8 ± 13.8 kg). The protocol was explained in detail to each subject, who signed a consent form after reading a description of the study. The subjects were familiarized with the exercise protocol from participation in previous studies in the laboratory. The study was approved by the Institutional Review Board for Research Involving Humans Subjects at Kansas State University.

The protocol consisted of supine single-leg knee-extension exercise (2 min rest + 6 min exercise) performed at a light-to-moderate work rate so as to achieve a steady state of cardiovascular variables. The knee-extension exercise was performed at a contraction rate of 40 min^{-1} . To maintain the desired cadence the subjects were aided by the signal from a metronome, which was started at the beginning of the resting period to avoid anticipatory responses. Subjects performed one rest-to-exercise transition. One subject returned to the laboratory on two different days (in addition to the initial visit) to complete several transitions to the same work rate as performed on the first day in order to establish reproducibility. In two visits the subject performed two transitions, with 25-30 min of recovery between each transition, yielding a total of 5 exercise bouts (three days) at the same work rate.

Femoral artery blood velocity (BV) was measured by pulsed-wave Doppler ultrasound (Model 500V, Multigon Industries, Mt Vernon, NY) using a 4-MHz probe with fixed angle of insonation of 45° and full gate width. The Doppler probe was placed above the common femoral artery of the right (exercising) leg $\sim 2\text{-}3$ cm proximal to the femoral artery bifurcation. The probe position was determined by echo-Doppler ultrasound. The audio signal was processed and converted to velocity as described in detail by Lutjemeier et al. (2005). The data were collected at 200 Hz and stored for offline analysis. To calculate beat-by-beat blood velocity (and flow), the 200 Hz data were integrated over each R-R interval of the ECG determined by a modified Lead I configuration. Femoral artery diameter was measured at rest by echo-Doppler ultrasound (Vivid 3-Pro, GE) with a 7.5-MHz linear probe. Previous studies have shown that femoral artery diameter did not change significantly during exercise (Radegran, 1997; DeLorey *et al.*, 2004c; MacDonald *et al.*, 1998). Thus, resting diameter was used to calculate leg blood flow (LBF), where $\text{LBF} = \text{BV} \cdot \pi r^2$ (BV in $\text{cm} \cdot \text{s}^{-1}$ and r is femoral artery radius in cm) and was multiplied by 0.06 to convert from $\text{ml} \cdot \text{s}^{-1}$ to $\text{L} \cdot \text{min}^{-1}$.

Spectral Analysis and Filtering: A fast Fourier transform [FFT, Cooley-Tukey's algorithm - Hanning window (Yamamoto & Hughson, 1993)] was used to examine the frequency domain (spectral) characteristics of the simulated and directly measured blood flow response to exercise. Spectral analyses were done on data sets with 15 s of rest and 180 s of exercise (rest-to-exercise transition). This time window included $\sim 90\text{-}120$ s of 'steady state'. The Fourier transform assumes stationary data and inclusion of the dynamic increase in blood flow violates this assumption. However, this analysis was important to establish the range of spectral frequencies containing information on the biphasic kinetics of blood flow (see Results) and to determine the cutoff frequency for filtering the data.

The spectral analysis of blood flow responses (computer simulations and *in vivo* measurements) demonstrated that the frequency range containing the kinetics information did not overlap with higher frequency ‘noise’ such as those induced by heart rate and muscle contraction (see Results). Thus, a frequency-domain filtering procedure was used to eliminate the higher frequency noise (i.e., low pass filter). The filtering was done using a default low pass function of SigmaPlot (lowpass.xfm - SigmaPlot 2001, Systat Software Inc, CA). The cutoff for filtering was titrated to produce the lowest ‘noise’ while retaining data with frequencies fundamental for describing the biphasic kinetics of blood flow. To examine the effects of filtering on the underlying kinetics response we applied the low pass filter (LP_{FILTER}) on computer simulated data, filtering out frequencies ≥ 0.1 and 0.2 Hz (i.e., eliminating 99.9% and 99.8% of high frequencies, respectively, for 200 Hz data). The cutoff frequency determined by this analysis was then used for filtering the raw Doppler blood flow data for kinetics analysis.

Kinetics Analysis: The raw Doppler data from 5 transitions of one subject were time aligned to the onset of exercise and ensemble-averaged to produce a single data set. For these transitions, a low pass filter (LP_{FILTER} ; cutoff $f = 0.2$ Hz) was then applied to the 200 Hz ensemble-averaged data. Finally, the data were resampled at 10 Hz for nonlinear regression analysis, i.e., from the 200 Hz data set we retrieved every 20th datum). The resampling was necessary because using a personal computer for curve-fitting of a single response with 36,000 data points (180 s at 200 Hz) with a 2 exponential model would usually take 30-45 min and frequently lock up the computer before achieving the convergence criteria of the nonlinear regression. Importantly, for data sets in which the curve-fitting could be successfully completed at 200 Hz we observed that the parameter estimates of blood flow kinetics (see Eq. 1 below) for 10 Hz (resampled) data were, within round-off error, almost identical to the 200 Hz data. The Beat-by-Beat data were interpolated (zero-order interpolation) at 10 Hz and ensemble-averaged for analysis of blood flow kinetics.

The kinetics of blood flow for a single transition of each subject (visit 1) were determined for the Beat-by-Beat, average of 3 consecutive beats ($AVG_{3 \text{ BEATS}}$) and LP_{FILTER} of raw Doppler data. For the latter, the Doppler data (200 Hz) were filtered and resampled at 10 Hz as described above. The time course of leg blood flow was determined by nonlinear regression using a least-squares technique (SigmaPlot 2001, Jandel Scientific). A two-component model was used to describe the response (Shoemaker *et al.*, 1996b; MacDonald *et al.*, 1998; Radegran & Saltin, 1998; Koga *et al.*, 2005)

$$\begin{aligned} \text{LBF} = \text{LBF}_{\text{BSL}} + A_1 \cdot (1 - e^{-(t-\text{TD1})/\tau_1}) & \quad (\text{Phase 1}) \\ + A_2 \cdot (1 - e^{-(t-\text{TD2})/\tau_2}) & \quad (\text{Phase 2}) \end{aligned} \quad (1)$$

where BSL = baseline, A = amplitude, TD = time delay, and τ = time constant of each phase of the LBF response. The nonlinear regression results of interest for this study were the parameter estimate (PE) describing the LBF kinetics, and the standard error of the estimate (SEE) for each parameter, which describes the confidence of parameter estimation. A reduction in the SEE represents a decrease, and therefore improvement in the confidence interval for estimation of kinetic parameters.

Statistical Analysis: The PE and SEE for blood flow kinetics were determined from nonlinear regression analysis (Marquadt-Levenberg algorithm, SigmaPlot 7.01, Systat Software) of data pre-processed with the three different methods (Beat-by-Beat, $\text{AVG}_3 \text{ BEATS}$ and $\text{LP}_{\text{FILTER}}$). The SEE for Beat-by-Beat, $\text{AVG}_3 \text{ BEATS}$ and $\text{LP}_{\text{FILTER}}$ were compared by one-way ANOVA. The Fisher-LSD test was used for *post-hoc* analysis. Significance was declared when $P < 0.05$. Data are presented as mean \pm standard deviation.

Results

The time- and frequency-domain characteristics of the simulated blood flow response are shown in Fig. 5.2. The spectral analysis of simulated blood flow + ‘noise’ identified the three simulated oscillatory components (as expected) and a lower frequency component (in the range 0 to 0.1 Hz), which appeared to contain the information about the underlying kinetics response. However, filtering the data by removing frequencies greater than 0.1 Hz distorted the simulated blood flow (Fig. 5.3). As shown in Table 1, we observed that within the range of kinetic parameters previously described for blood flow response in healthy subjects (Radegran & Saltin, 1998; MacDonald *et al.*, 1998; Saunders *et al.*, 2005) a cutoff frequency of 0.2 Hz retained sufficient frequency information so as to accurately characterize the biphasic kinetics of blood flow including the transitional changes at exercise onset (Fig. 5.3, lower inset) and the Phase I-II transition (Fig. 5.3, upper inset).

To further examine the validity of our simulations and establish reproducibility we determined the frequency characteristics of the raw Doppler data from a single-transition and from 5 transitions ensemble averaged (Fig. 5.4). The power spectrum of these responses qualitatively resembled the computer simulations. Moreover, the overall frequency-domain characteristics of each transition were grossly similar (Fig. 5.5). The primary effect of ensemble-averaging several transitions was a reduction in the power of components with frequencies > 0.1 Hz (Fig. 5.4B), which is in effect qualitatively similar to a low-pass filter with cutoff of ~ 0.1 to 0.2 Hz.

The effects of LP_{FILTER} on the raw Doppler data ensemble-averaged are shown in Fig. 6. As predicted by the computer simulations, the LP_{FILTER} eliminated the primary sources of ‘noise’ and revealed the underlying biphasic increase in LBF. This noise-reducing effect was greater than that achieved by ensemble-averaging five transitions (after 10 Hz interpolation) of Beat-by-Beat data (Fig. 5.6C). The LP_{FILTER} was applied to each of the five transitions and their kinetics were determined (Table 5.1). For each of the 5 transitions the overall kinetics (mean response time, MRT) of leg blood flow after LP_{FILTER} were virtually identical to the corresponding raw (unfiltered) Doppler data when both were analyzed by a monoexponential function (Table 5.2). These results demonstrate that LP_{FILTER} did not slow the overall kinetics of blood flow, which is a concern with any filtering procedure. The CV for baseline and steady state blood flow was $<10\%$, which is similar to a previous study in our laboratory (Lutjemeier *et al.*, 2005). However, the CV for each kinetic (i.e., time-dependent) parameter ranged from 12 to 67%, suggesting substantial day-to-day variability.

The mean work rate for a single transition performed by 4 subjects was 10.3 ± 2.6 W, which elicited a mean heart rate equal to 89.0 ± 9.4 bpm and leg blood flow of 1.32 ± 0.23 L \cdot min $^{-1}$ at the steady state of exercise. A representative response showing the three methods of data processing used for kinetics analysis (Beat-by-Beat, $AVG_{3\text{ BEATS}}$ and LP_{FILTER}) is depicted in Fig. 5.7. The parameter estimates describing the blood flow response for each method were not significantly different (Table 5.3). However, the SEE for each parameter was significantly lower for LP_{FILTER} compared to Beat-by-Beat and $AVG_{3\text{ BEATS}}$ (Fig. 5.8). The LP_{FILTER} method decreased the SEE by 85-95% compared to Beat-by-Beat and $AVG_{3\text{ BEATS}}$.

Discussion

In the present study we examined, for the first time, the time and frequency domain characteristics of arterial blood flow responses following the onset of exercise. The principal and novel findings were that the low frequency range (< 0.5 Hz) of the power spectrum contained the information necessary to describe the biphasic kinetics of blood flow adjustment, and that the primary sources of ‘noise’ in Doppler measurements (muscle contraction and cardiac cycle) occurred at higher frequencies, and thus did not overlap with the frequency spectrum of the blood flow kinetics. These observations provided the bases for applying a low pass filter (cutoff = 0.2 Hz) to the Doppler blood flow data. For single rest-exercise transitions, the LP_{FILTER} method produced the lowest noise with highest temporal resolution compared to processing the data as Beat-by-Beat and $AVG_3 \text{ BEATS}$. The implications for kinetics analysis were a significant reduction in the standard error of the estimate and, therefore, improvement in the 95% confidence interval for each kinetic parameter.

The ensemble averaging of blood flow from several similar transitions to reduce the sample-to-sample variation and improve kinetic parameter estimation is made under the premise that the sample-to-sample variation has a normal distribution (i.e., Gaussian or ‘white’ noise); however, the frequency analysis of raw Doppler data suggests that the variability in blood flow is non-white noise. Even though we have not performed a thorough analysis of time-domain ‘noise’ distribution as previously done for pulmonary $\dot{V}O_2$ and PCr (Lamarra *et al.*, 1987; Rossiter *et al.*, 2000), a fundamental characteristic of ‘white (Gaussian) noise’ is the uniform distribution of power in the frequency spectrum. Therefore, the non-Gaussian properties of blood flow noise were evidenced by distinct peaks encountered in the power spectrum associated with muscle contraction and cardiac cycle (Fig. 5.4), which agreed nicely with the results from computer simulations (Fig. 5.2). For Doppler measurements, the ‘noise’ related to muscle contraction showed a narrow frequency range, suggesting small variations in contraction frequency, and the greatest power spectral density. In contrast, the spectral characteristics of oscillations induced by cardiac cycle demonstrated a wide frequency range, which reflected the dynamic increase in heart rate following the onset of exercise (rest 60 ± 3.1 bpm, exercise 89 ± 9.4 bpm). The most important observation, however, was that the contraction and cardiac cycle ‘noise’ did not overlap with the power spectrum describing the underlying dynamic increase in blood flow. This is a pre-requisite to apply the LP_{FILTER} because in the presence of overlap the cutoff frequency necessary to eliminate the primary sources of noise would also filter out frequency components essential to describe the underlying kinetics and, therefore, distort the response (e.g., Fig. 5.3). Based on comparison of kinetics of simulated and filtered responses

(Table 5.1 and Fig. 5.3) we chose a cutoff frequency = 0.2 Hz for LP_{FILTER} because a lower cutoff (e.g., 0.1 Hz) distorted the phase 1 of blood flow leading to results that differed by more than 10% from the simulated value. However, we acknowledge that the ‘optimal’ cutoff frequency for LP_{FILTER} will vary according to the underlying kinetics of blood flow (Table 5.1); thus, the cutoff frequency must be tailored to the characteristics of each type of response.

On the basis of the non-Gaussian distribution of blood flow noise it is possible that ensemble averaging might actually enhance the underlying oscillatory characteristic induced by muscle contraction and cardiac cycle instead of eliminating these oscillations and improve the signal-to-noise ratio for kinetics analysis. However, we observed that ensemble-averaging 5 transitions substantially reduced the ‘noise’ in the raw Doppler data (Fig. 5.4A). This might be explained by the fact that after time alignment of each transition for the onset of exercise the occurrence of muscle contraction and heart beat are not superimposable from test-to-test due to the within-subject variability of heart rate (baseline, steady state and dynamics) and timing of muscle contraction. In the frequency domain, averaging several like transitions reduced the power spectrum of high frequency components. This was evidenced by a 75% reduction in the area under 0.6 to 0.7 Hz and a 60% reduction for 1.10 to 1.50-Hz, but a similar area under the frequency spectrum for 0 to 0.2 Hz (Fig. 5.4B). Thus, ensemble averaging blood flow data worked in a manner similar to, but less effective than, a low pass filter in diminishing the sample-to-sample variability.

To eliminate or reduce the ‘noise’ of blood flow measurements so as to improve the precision of estimating the kinetic parameters of blood flow, investigators have used different approaches for data processing [beat-by-beat (MacDonald *et al.*, 1998; Fukuba *et al.*, 2004; Koga *et al.*, 2005), 1 s time bins (Shoemaker *et al.*, 1996b; Shoemaker *et al.*, 1994) and averaging over a contraction-relaxation cycle (Shoemaker *et al.*, 1996a; Radegran & Saltin, 1998; Saunders *et al.*, 2005)]. These strategies are based on the observations of Lamarra *et al.* (1987), who defined the confidence interval for τ or TD (K_1) as

$$K_1 = \hat{L} \frac{S_0}{\Delta Y_{\text{SS}}} \quad (2)$$

where S_0 is the standard deviation of the fluctuations around the mean (‘noise’), ΔY_{SS} is the amplitude of increase in the investigated variable from baseline to steady state exercise (‘signal’) and \hat{L} is determined by the time \hat{L} constant and data density. Therefore, decreasing the standard deviation by averaging data over longer time bins (Osada, 2004; Shoemaker *et al.*, 1996c) will improve (i.e., decrease) the confidence interval of parameter estimation. However, these averaging procedures have the limitation of decreasing the temporal resolution for kinetics

analysis (i.e., increase in \hat{L}), which is frequently overlooked in the context of kinetics analysis.

The kinetics of blood flow following the onset of exercise are biphasic (Eq. 1) with an initial fast component ($\tau_1 \sim 1-5$ s) followed by a slower response ($\tau_2 \sim 10-40$ s) that starts or emerges 10-30 s after the start of exercise [rev. (Shoemaker & Hughson, 1999)]. The fast phase 1 of blood flow appears to be crucial for maintaining adequate O₂ delivery following the onset of exercise (Ferreira *et al.*, 2005a); therefore, these kinetics need to be adequately characterized. The theoretical predictions of Lamarra *et al.* (1987) indicated that for a fixed noise and sampling frequency, the confidence interval of τ improves as the kinetics becomes slower due to the increase in density of data across the transition phase. This has direct implications for investigation of blood flow kinetics because the rapidity of the early response (τ_1) and phase 1-phase 2 transition (TD₂ in Eq. 1), and the relatively low amplitude of phase 1 ($\sim 50\%$ of total for moderate exercise) requires high sampling frequencies to determine the biphasic kinetics with acceptable degree of confidence. In this setting, the 95% CI of the kinetic parameters will be very sensitive to the averaging procedure. This was demonstrated in the present study by comparing three methods (Beat-by-Beat, AVG_{3 BEATS} and LP_{FILTER}) to process the blood flow data prior to kinetics analysis.

The simplest and most logical averaging of blood flow data is over a cardiac cycle (Beat-by-Beat); however, the resulting profile has a low signal-to-noise ratio (CV = 33%, Fig. 5.7A) that results in large SEE for kinetic parameters (Fig. 5.8) and in some occasions has masked the biphasic nature of the blood flow response to exercise (Fukuba *et al.*, 2004). In the present study, the Beat-by-Beat method demonstrated a waxing and waning of the ‘noise’ in blood flow (Fig. 5.7A) likely because the heart beat occurred during muscle relaxation at some points generating large oscillations in flow, but at other periods the cardiac cycle coincided with muscle contraction generating small oscillations (Walloe & Wesche, 1988; Radegran & Saltin, 1998; Osada, 2004; Lutjemeier *et al.*, 2005) (e.g., Fig. 5.1). The procedure of averaging over longer time bins is of diminishing return because the decrease in the standard deviation (S_0) is counterbalanced by a reduction in data density (leading to an increase in \hat{L} , see Eq. 2). Accordingly, AVG_{3 BEATS} showed a small decrease in the SEE that was not significantly different from Beat-by-Beat for most kinetic parameters (Fig. 5.8); however, with inclusion of more subjects these differences would probably reach significance. In contrast to time-domain filtering, LP_{FILTER} provided an excellent combination of a decrease in blood flow ‘noise’ while maintaining high temporal resolution for kinetics description (which would tend to minimize \hat{L} in Eq. 2). These effects were confirmed by the very low SEE of each kinetic parameter (Fig. 5.8). For all parameters the SEE of LP_{FILTER} was significantly lower than Beat-by-Beat and AVG_{3 BEATS}, demonstrating a substantial improvement in the 95% CI.

The improvement in the 95% CI is relevant for comparison of kinetic parameters between separate transitions, and becomes more critical when investigators are limited to single-transitions such as in pharmacological and clinical studies of blood flow kinetics [e.g. Shoemaker *et al.*, 1996a; Shoemaker *et al.*, 1999]. However, a shortcoming of single transitions is the potential for within-day and day-to-day variability of the “true” underlying kinetic parameters for a given subject. Even with good compromise between signal-to-noise ratio and data density obtained by LP_{FILTER}, we observed a large within-subject variability of kinetic parameters determined for 5 transitions collected over three days (Table 5.1). This suggests that ensemble-averaging of multiple transitions may still be necessary to minimize variability and accentuate the underlying physiological response. For the subject that repeated 5 transitions, we also compared the effects of LP_{FILTER} to beat-by-beat data (10-Hz interpolated) ensemble-averaged. As previously shown (Lamarra *et al.*, 1987; Rossiter *et al.*, 2000), the effects of ensemble-averaging data with low signal-to-noise ratio on the 95% CI is limited because the latter will be improved by a factor of $1/\sqrt{n}$, where n is the number of repetitions (Lamarra *et al.*, 1987; Rossiter *et al.*, 2000). For example, for the blood flow response shown in Fig. 5.6, in order to obtain a 95% CI for beat-by-beat data (10-Hz interpolated) similar to that achieved with LP_{FILTER} for a given parameter (τ or TD), it would be necessary to average approximately 225 more transitions (estimated from Lamarra *et al.*, 1987). This further emphasizes the advantage of using LP_{FILTER} to process blood flow data for kinetics analysis irrespective of using single or multiple transitions ensemble-averaged (Figs. 5.6-5.8).

The present analysis was conducted with supine one-leg knee extension exercise of moderate intensity at 40 contractions·min⁻¹, thus, the possibility to extrapolate our results to different exercise modes, intensities and contraction frequencies must be considered. Compared to our results for supine knee-extension exercise, other exercise modes may result in differences in amplitude and kinetics of the blood flow response. From the perspective of frequency analysis the total amplitude of blood flow response is a “dc shift” located at 0 Hz on the power spectrum and, thus, would not be affected by LP_{FILTER}. Hence, the major concern for extrapolating our results to other exercise modalities, intensities or contraction frequencies is the kinetics (i.e., time-dependent characteristics) of the adjustment in blood flow. Specifically, situations where blood flow kinetics are substantially faster than examined herein will require higher cutoff frequencies to avoid distortion of the kinetic response (Table 5.1 and Fig. 5.3). With regard to contraction frequency, the applicability of our results will depend on the effects of contraction frequency on blood flow kinetics. If we assume, for example, that BF kinetics are independent of contraction frequency, our data would suggest that ~15 contractions·min⁻¹ (or 0.25 Hz) is the lower limit to be able to apply the LP_{FILTER} with a cutoff = 0.2 Hz (i.e., eliminating the frequency

components $\geq 12 \text{ min}^{-1}$). However, there is no upper limit for contraction frequency because $\text{LP}_{\text{FILTER}}$ will eliminate all high frequency components. Likewise, heavy exercise is characterized by the existence of a slow increase in blood flow after phase 2 (Koga *et al.*, 2005; Poole *et al.*, 1991), which will not limit the use of $\text{LP}_{\text{FILTER}}$ because the frequency components describing this process are lower than 0.2 Hz (i.e., time constant longer than the kinetics of phase 2) and, thus, retained after applying the $\text{LP}_{\text{FILTER}}$. Therefore, the filtering procedure used in the present study should be valid for different exercise modes and intensities. However, for low contraction frequencies the most appropriate cutoff frequency will depend on the effects of contraction frequency on blood flow kinetics.

As for blood flow, there has been great interest in the kinetics of minute ventilation, pulmonary O_2 uptake (DeLorey *et al.*, 2004c; Fukuba *et al.*, 2004; Koga *et al.*, 2005; Lamarra *et al.*, 1987; Rossiter *et al.*, 2000) and phosphocreatine (from ^{31}P -MRS) (e.g., Rossiter *et al.*, 2000). Is it possible to use the $\text{LP}_{\text{FILTER}}$ to reduce the noise of pulmonary O_2 uptake or phosphocreatine and thereby decrease the number of trials needed to improve the confidence of kinetics analysis? These variables have Gaussian distribution of noise (Lamarra *et al.*, 1987; Rossiter *et al.*, 2000), thus, we anticipate uniform distribution of noise on their frequency spectrum, suggesting that application of the $\text{LP}_{\text{FILTER}}$ might be possible. However, it would require a different strategy of data processing because, for example, pulmonary O_2 uptake data is a time series where each breath is a discrete event of variable duration, in contrast to the analog blood flow using Doppler ultrasound, which can be evenly sampled in time.

Limitations: In the current study we assumed constant femoral artery diameter from rest to exercise to calculate blood flow from Doppler measurements of blood velocity. However, as mentioned above, femoral artery diameter did not change significantly during knee-extension exercise (Radegran, 1997; DeLorey *et al.*, 2004c; MacDonald *et al.*, 1998).

It was outside the scope of our study to establish a generic cutoff frequency for low pass filtering of blood flow data for kinetics analysis. However, we observed that using a cutoff = 0.5 Hz dramatically reduced the ‘noise’ observed for direct measurements of blood flow while the fast responding characteristics of simulated responses were preserved. In fact, a cutoff frequency = 0.5 Hz also resulted in very low standard error of estimate for the kinetic parameters of blood flow from 5 transitions ensemble-averaged (1.0 - 4.7 % for 0.5 Hz vs. 0.4 - 3.5 % for 0.2 Hz, see Table 5.4) but investigators must keep in mind that this cutoff frequency would only be appropriate for exercise performed with a muscle contraction frequency greater than 30 min^{-1} (see above).

The large within-subject variability of blood flow kinetics (Table 5.2) poses a limitation for using a single transition to compare the effects of Beat-by-Beat, $AVG_{3\text{ BEATS}}$ and LP_{FILTER} on the SEE of kinetic parameters. Although the variability might be attributed to Doppler measurement errors (Gill, 1985), careful inspection of the velocity waveforms did not reveal any loss of signal or noise in the transition phase. Furthermore, the intra-subject variability for kinetics of multiple transitions will not affect our comparison of Beat-by-Beat, $AVG_{3\text{ BEATS}}$ and LP_{FILTER} for a single transition because the same data set was used for each method.

Conclusion

In summary, we have demonstrated that the low-frequency range (≤ 0.5 Hz) of the power spectrum contained the information necessary to describe the kinetics of blood flow, the main sources of ‘noise’ in Doppler measurements of blood velocity were muscle contraction and heart rate, and that these did not overlap with the frequency spectrum of the biphasic kinetics. Moreover, ensemble-averaging several like transitions had an effect qualitatively similar to, but less effective than, a low pass filter (i.e., reduce/eliminate high frequency noise). These observations suggest that LP_{FILTER} was a valid procedure to pre-treat blood flow data for kinetics analysis. In this setting, LP_{FILTER} yielded the highest signal-to-noise ratio and temporal resolution compared to beat-by-beat data and the average of 3 consecutive beats, which resulted in significantly lower standard error of the estimate for all kinetic parameters describing the blood flow response. The direct consequence was a substantial improvement in the 95% confidence interval of each kinetic parameter.

Table 5.1. Effects of simulated parameters on cutoff frequency for low pass filter.

	Parameter	Frequency (Hz)	Difference (%)
τ_1 (s)	0.5	0.5	0.02 - 7.3
	1	0.3	0.11 - 5.0
	2	0.2	0.09 - 3.1
	3	0.2	0.06 - 1.5
A_1 (% A_{tot})	20	0.2	0.02 - 2.6
	40	0.2	0.09 - 3.1
	60	0.2	0.20 - 3.1
	80	0.2	0.29 - 3.2
TD_2 (s)	5	0.3	0.03 - 2.6
	10	0.2	0.15 - 4.6
	15	0.2	0.09 - 3.1
	20	0.2	0.06 - 2.7

Default parameters for simulated blood flow kinetics are $BSL = 0.5$ a.u., $A_1 = 2$ a.u., $A_2 = 3$ a.u., $\tau_1 = 2$ s, $TD_2 = 15$ s and $\tau_2 = 15$ s (see Eq. 1 for definition of parameters). $A_{tot} = A_1 + A_2$. Frequency refers to the cutoff frequency of low pass filter necessary to describe the kinetics with resulting parameters differing $\leq 10\%$ of simulated response. $\text{Difference (\%)} = \left| \frac{PAR_{SIM} - PE_{CF}}{PAR_{SIM}} \right| \cdot 100$, where PAR_{SIM} is simulated parameter value and PE_{CF} is parameter estimate determined by curve fitting the filtered response. Note that these results are independent of the absolute values of A_1 and A_2 .

Table 5.2. Kinetics parameters of leg blood flow for a single subject.

Parameter	Transitions					CV (%)	Ensemble average
	1	2	3	4	5		
BSL (L·min⁻¹)	0.39	0.40	0.48	0.42	0.45	9.2	0.43
A₁ (L·min⁻¹)	0.73	0.92	0.76	0.82	0.50	20.9	0.72
A₂ (L·min⁻¹)	0.37	0.30	0.54	0.40	0.56	25.9	0.42
EX_{SS} (L·min⁻¹)	1.48	1.49	1.78	1.61	1.51	8.2	1.56
τ₁ (s)	4.05	10.0	3.23	4.71	1.63	67.0	4.22
TD₂ (s)	22.1	20.0	22.4	16.4	19.8	11.9	20.2
τ₂ (s)	9.0	10.6	24.6	19.9	15.2	40.9	14.7
MRT (s)	14.5	14.3	22.6	14.4	23.3	26.4	16.5
MRT_{RD} (s)	14.6	14.6	22.5	14.1	23.3	26.6	16.6

BSL refers to baseline, A = amplitude, EX_{SS} = exercise steady state, τ = time constant, TD = time delay and MRT = mean response time. Subscripts (1) and (2) indicate each phase of the blood flow response while RD is raw data (200 Hz). “Ensemble average” depicts the kinetic parameters for five transitions ensemble averaged, not the average of parameters shown for transitions 1-5. All kinetics descriptions, except for MRT_{RD}, were determined after low pass filtering of the respective data set.

Table 5.3. Parameter estimates describing the kinetics of blood flow for a single transition.

BSL (L·min⁻¹)			A₁ (L·min⁻¹)			A₂ (L·min⁻¹)		
B-B	AV	LP_{FI}	B-B	AV	LP_{FI}	B-B	AV	LP_{FI}
0.39	0.40	0.39	0.44	0.40	0.41	0.19	0.23	0.21
0.39	0.39	0.39	0.42	0.41	0.42	0.43	0.44	0.42
0.41	0.41	0.40	0.58	0.57	0.63	0.55	0.56	0.54
0.38	0.38	0.39	0.65	0.70	0.73	0.46	0.41	0.37
0.39	0.39	0.39	0.52	0.52	0.55	0.41	0.41	0.39
τ₁ (s)			TD₂ (s)			τ₂ (s)		
B-B	AV	LP_{FI}	B-B	AV	LP_{FI}	B-B	AV	LP_{FI}
2.84	1.36	1.72	10.5	6.3	11.1	26.1	31.4	19.5
2.04	1.11	1.36	19.4	18.5	20.7	34.9	36.6	33.1
3.63	3.08	4.78	14.1	13.1	15.2	44.5	46.4	50.3
3.19	3.93	4.04	15.0	19.3	22.0	12.8	9.8	8.9
2.9	2.4	3.0	14.7	14.3	17.3	29.6	31.0	28.0

Individual results from each method used to pre-process the data from single transitions for kinetics analysis. B-B = Beat-by-Beat, AVG_{3BEATS} = average blood flow for three consecutive cardiac cycles, LP_{FILTER} = low pass filter cutoff 0.2 Hz. Bottom row for each parameter is mean (SD). See Table 5.1 for further abbreviations.

Table 5.4. Effects of cutoff frequency on kinetics parameters of leg blood flow for five transitions ensemble averaged.

Parameter	Frequency			
	0.2 Hz		0.5 Hz	
	PE (SEE)	% PE	PE (SEE)	% PE
BSL (L·min ⁻¹)	0.43 (0.002)	0.44	0.42 (0.004)	1.02
A ₁ (L·min ⁻¹)	0.72 (0.006)	0.81	0.73 (0.009)	1.24
A ₂ (L·min ⁻¹)	0.42 (0.005)	1.23	0.42 (0.007)	1.73
τ_1 (s)	4.22 (0.15)	3.47	4.36 (0.21)	4.71
TD ₂ (s)	20.2 (0.27)	1.35	20.0 (0.39)	1.94
τ_2 (s)	14.7 (0.32)	2.14	14.9 (0.44)	2.93

PE = parameter estimate, SEE = standard error of estimate. % PE = SEE·100/PE (conceptually similar to coefficient of variation). See Table 5.2 for abbreviations. Note that PE values are similar when using a cutoff frequency of 0.2 and 0.5 Hz. Even though the SEE for 0.5 Hz is slightly greater than for 0.2 Hz the values are very low (< 5%), which is not achieved with Beat-by-Beat and AVG_{3BEATS} (see Fig. 5.8).

Figure 5.1. Raw data during rest-to-exercise transition.

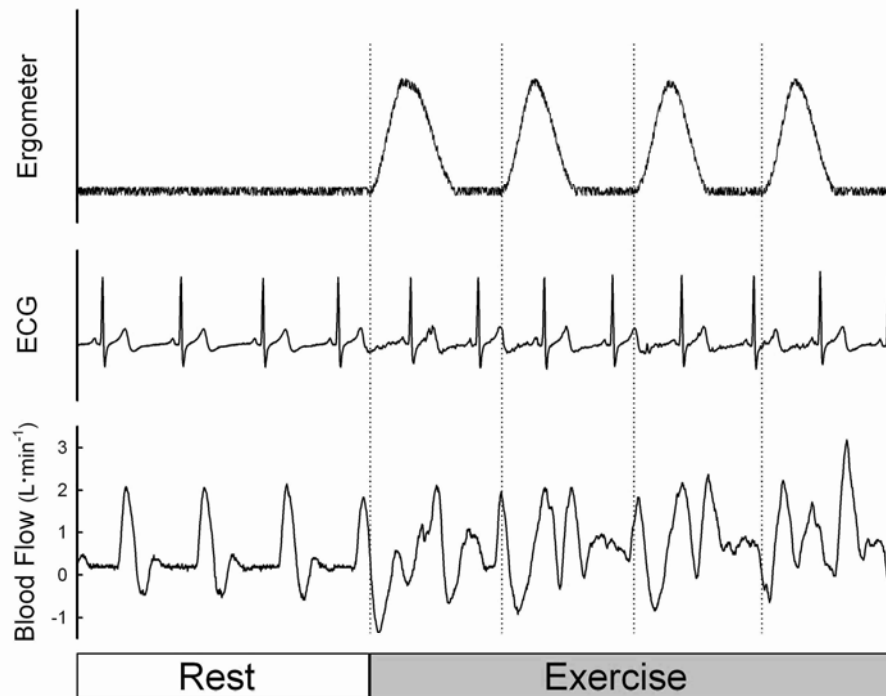


Figure 5.1. Raw waveforms of lever arm displacement from knee-extension ergometer (Ergometer), electrocardiogram (ECG) and blood velocity (converted to blood flow) during the rest-to-exercise transition. At rest, heart beats are the primary source of high-frequency oscillations in blood flow whereas during exercise oscillations are determined by the interaction between cardiac cycle and muscle contractions.

Figure 5.2. Time- and frequency-domain characteristics of simulated blood flow.

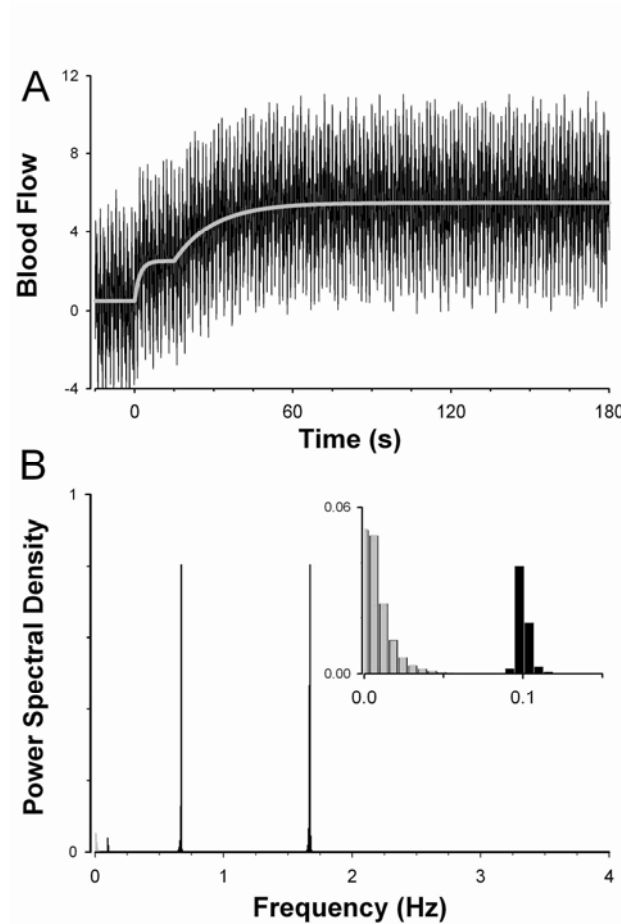


Figure 5.2. Time- and frequency-domain characteristics of simulated blood flow. *A)* Simulated blood flow in the time-domain ($\tau_1 = 2$ s, $TD_2 = 15$ s, $\tau_2 = 15$ s as from *Eq. 1*). The underlying biphasic increase in blood flow is depicted by the *gray line*. *Solid (black) line* shows the simulated response after the oscillatory components (very low frequency, heart rate and muscle contraction) and random noise were superimposed on the underlying kinetics. *B)* Frequency-domain characteristics of simulated blood flow. *Black bars*, power spectrum of solid (black) line in *A*; *Gray bars*, power spectrum of gray line in *A*. *Inset*: Panel (*B*) with scales expanded. As expected, the very low frequency (6 min^{-1} ; 0.1-Hz), muscle contraction (40 min^{-1} ; $\sim 0.67 \text{ Hz}$) and heart rate (100 bpm ; $\sim 1.67 \text{ Hz}$) oscillations were retrieved by the frequency analysis. Note that the lower-frequency spectrum (i.e., $< 0.1 \text{ Hz}$) contains most of the information describing the underlying biphasic response (*B, Inset*).

Figure 5.3. Effects of low-pass filtering on the kinetics of simulated blood flow.

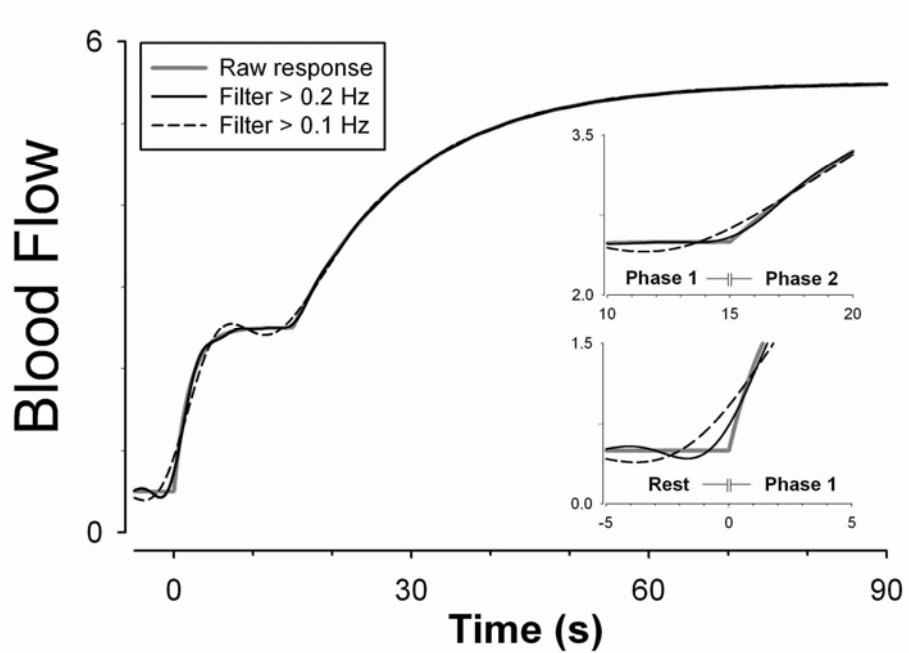


Figure 5.3. Effects of low-pass filtering on the kinetics of simulated blood flow. Filtering data with frequencies greater than 0.1 Hz distorted the early increase in blood flow and the Phase 1-Phase 2 transition. The underlying kinetics of blood flow ($\tau_1 = 2$ s, $TD_2 = 15$ s, $\tau_2 = 15$ s as from Eq. 1) were preserved by low-pass filtering with a cutoff frequency = 0.2 Hz. *Inset*, scales expanded to facilitate visualization of the effects of LP_{FILTER} on the rest-to-exercise (*bottom inset*) and Phase 1-to-Phase 2 transitions (*top inset*).

Figure 5.4. Time- and frequency-domain characteristics of raw Doppler data.

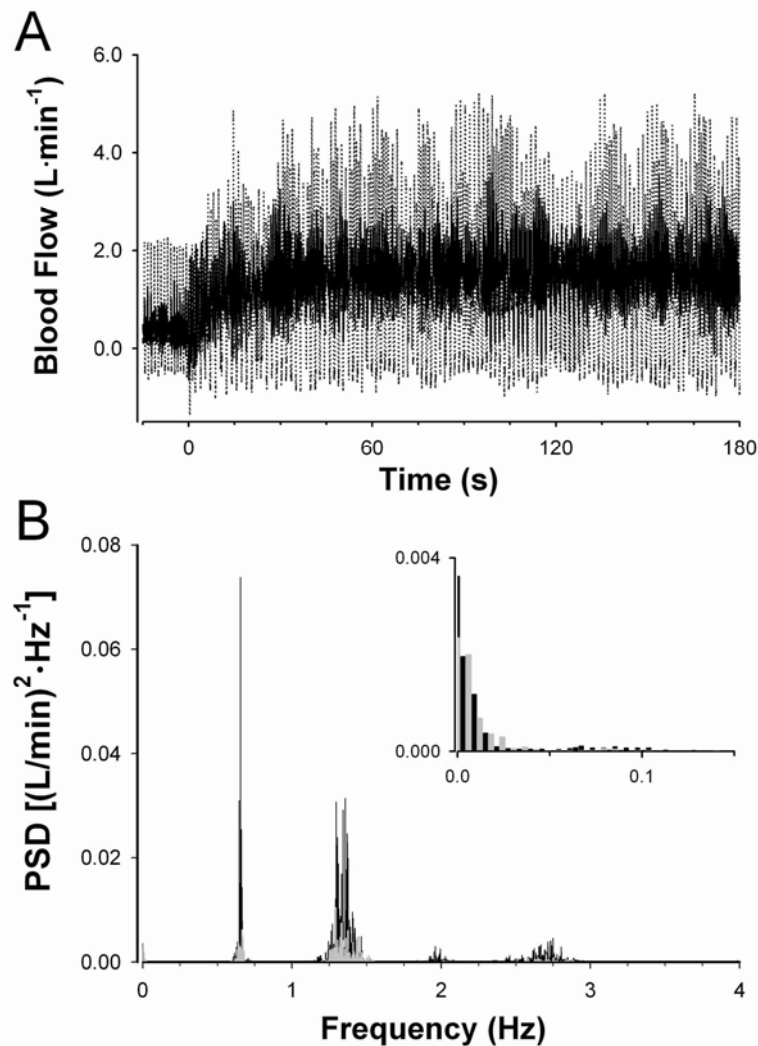


Figure 5.4 Time- and frequency-domain characteristics of raw Doppler data. *A)* Leg blood flow (LBF) in the time-domain (sampling frequency 200-Hz). *Dotted line*, LBF of a single transition. *Solid line*, LBF of 5 transitions ensemble-averaged. Note the similarity between Doppler measurements and simulated response (Fig. 5.1*A*) and the increase in signal-to-noise ratio when several transitions are averaged. *B)* Power spectral density (PSD) of responses shown in *A*. *Black bars*, power spectrum of a single transition (*dotted line* in *A*); *Gray bars*, power spectrum of 5 transitions ensemble-averaged (*solid line* in *A*). *Inset*: Panel (*B*) with scales expanded. The main sources of ‘noise’ (oscillations) on the Doppler LBF data were muscle contraction (40 min^{-1} ; $\sim 0.67 \text{ Hz}$) and heart rate [60-90 bpm; $\sim 1.0 - 1.5 \text{ Hz}$ (from rest-to-

exercise)]. Other higher frequency components reflect the harmonics of the fundamental frequencies of contraction and heart rate. Note that the primary effect of ensemble-averaging was a reduction in the 'noise' present at frequencies greater than 0.1 Hz, while the power at frequencies <0.1 Hz is relatively similar to those of a single transition (*B, Inset*).

Figure 5.5. Power spectral density of leg blood flow.

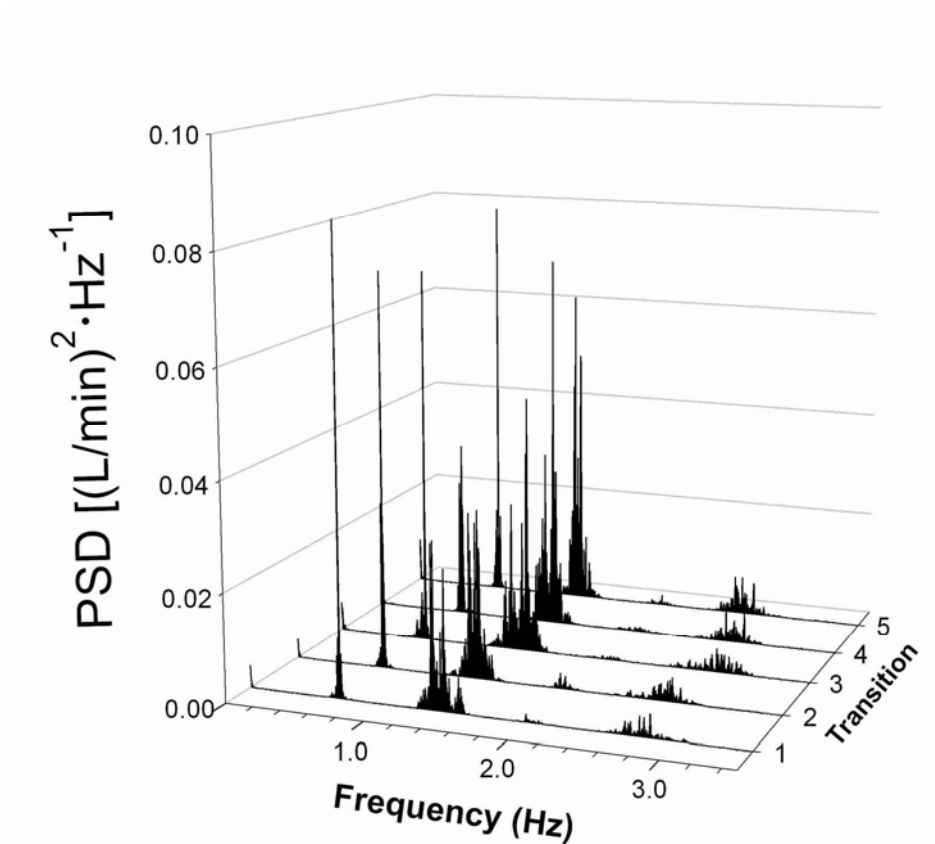


Figure 5.5. Power spectral density (PSD) of leg blood flow response to five transitions to the same work rate by one subject. Note that the power spectral characteristics are qualitatively similar for each transition. The kinetic parameters for these transitions are shown in Table 5.1.

Figure 5.6. Representative leg blood flow response (5 transitions averaged).

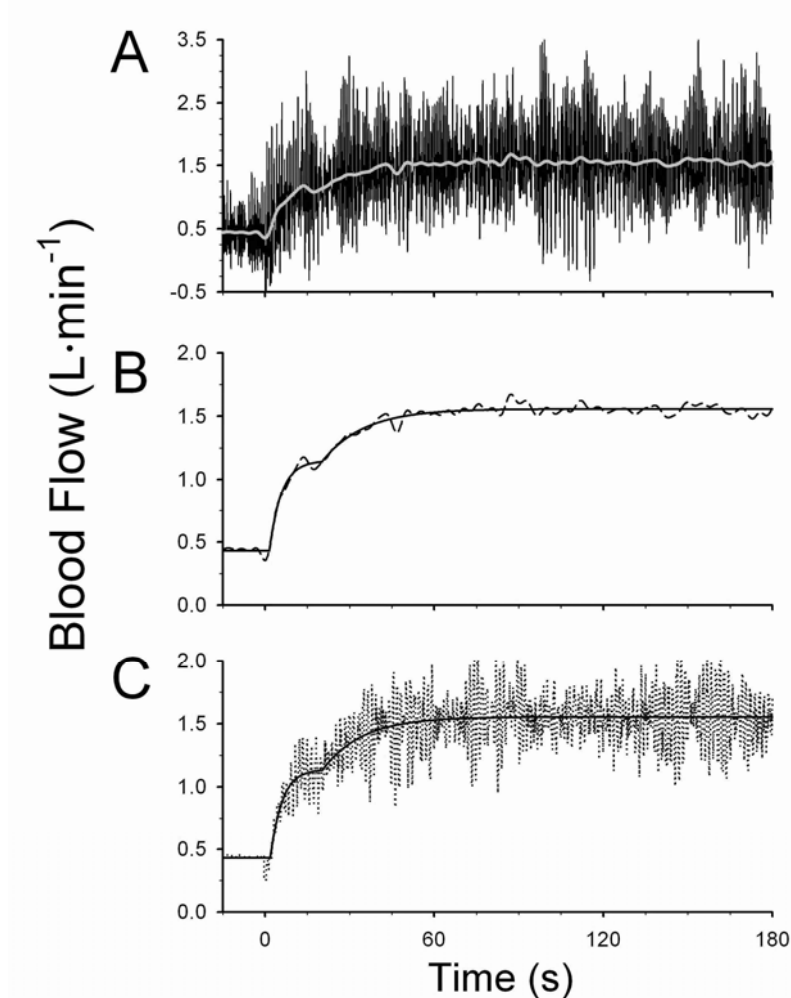


Figure 5.6. Leg blood flow response in one subject for five rest-to-exercise transitions ensemble-averaged. *A)* Raw Doppler blood flow data (sampling frequency 200 Hz) (*solid line*) and after low-pass filter (LP_{FILTER}; *gray line*). *B)* Raw Doppler data shown in *(A)* after LP_{FILTER} and resampled at 10 Hz (*Dashed Line*). *C)* Beat-by-Beat blood flow data (10 Hz interpolated and ensemble averaged). In *(B)* and *(C)*, solid line represents the best regression fit. The Beat-by-Beat (10 Hz interpolated) procedure substantially reduces the noise compared to the raw data (solid line in *A*); however, the signal-to-noise ratio is not optimal for kinetics analysis. The improvement in signal-to-noise ratio is noticeable for LP_{FILTER} where the standard deviation (‘noise’) of steady state blood flow was reduced by ~ 85 % compared to Beat-by-Beat.

Figure 5.7. Representative leg blood flow response (1 transition).

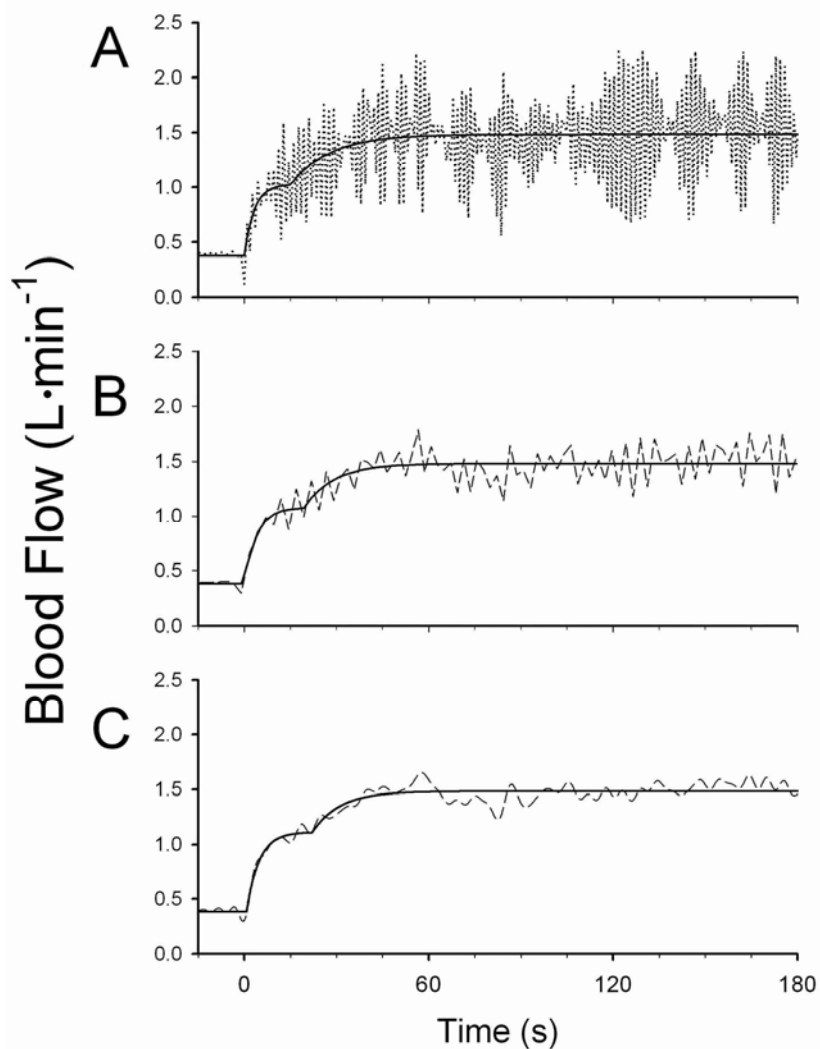


Figure 5.7. Leg blood flow response for a single transition of a representative subject. (A) Beat-by-Beat, (B) Average of 3 beats ($AVG_3\ BEATS$), and (C) low-pass filter (LP_{FILTER}). *Solid line*, best regression fit of each response. $AVG_3\ BEATS$ reduced the noise at the expense of decreasing the data density, which is equivalent to a lower sampling frequency. In contrast, LP_{FILTER} produced the lowest noise with highest temporal resolution. The consequences of these effects on kinetics analysis are shown in Fig. 5.8.

Figure 5.8. Results of SEE for each parameter describing the kinetics of blood flow.

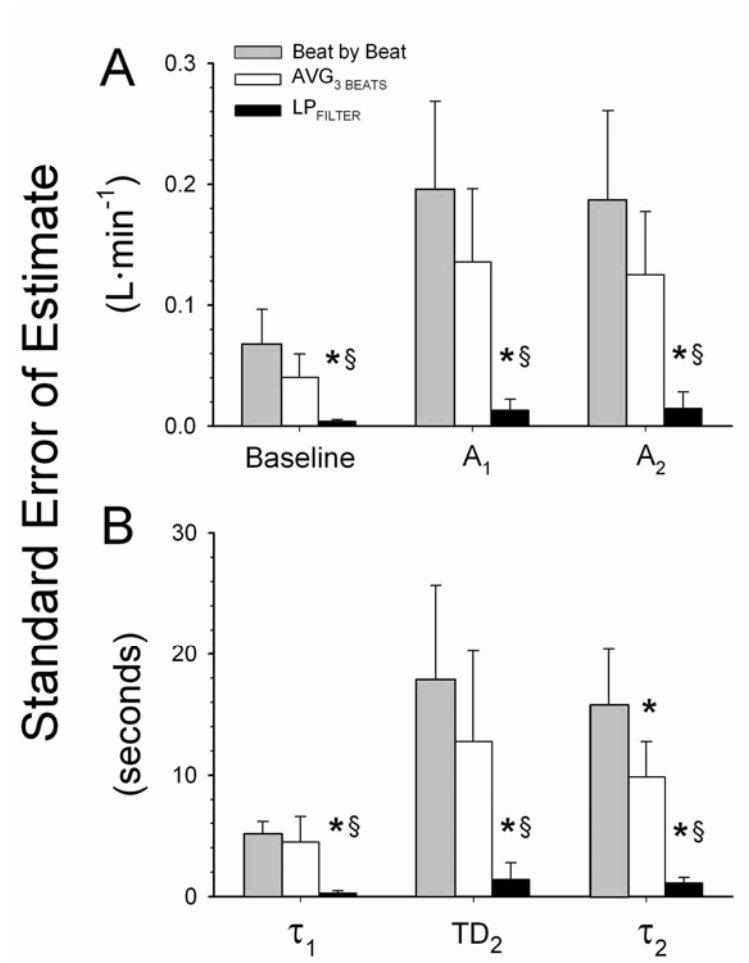


Figure 5.8. Standard error of the estimate (SEE) for each parameter describing the kinetics of blood flow when using three methods for pre-processing the data of single transitions for 4 subjects. Parameters are from *Eq. 1* where A = amplitude, τ = time constant, and TD = time delay of each phase of the blood flow response. $AVG_{3\text{ BEATS}}$ = average of 3 consecutive heart beats, LP_{FILTER} = low pass filter (cutoff frequency = 0.2 Hz). *Significantly different ($P < 0.05$) from Beat-by-Beat. § Significantly different from $AVG_{3\text{ BEATS}}$ ($P < 0.01$). Note that LP_{FILTER} dramatically reduces the SEE for each parameter, and therefore improves the confidence for determining the kinetics of blood flow.

CHAPTER 6 - Conclusions

Integrating the studies described in this dissertation, we conclude that the dynamics of muscle O₂ delivery are similar to the kinetics of muscle O₂ uptake following the onset of exercise based on both computer simulations and *in vivo* estimates. Moreover, our studies demonstrated that the temporal profile of muscle microvascular oxygenation (or microvascular O₂ pressure) is determined by the interaction of a biphasic increase in O₂ delivery and a monoexponential kinetics of O₂ uptake. Specifically, the early (first 15-20 s) rapid increase in O₂ delivery is mandatory to maintain an elevated driving force for capillary-myocyte O₂ transfer during the period when O₂ uptake is increasing at its fastest rate. Nitric oxide is an essential component of this response, where diminished nitric oxide availability speeded the dynamics of microvascular O₂ pressure causing a decrease to substantially lower values, resembling downregulatory or pathological responses seen in aging and chronic diseases, that may impair capillary gas exchange. Altogether our results emphasize the importance of characterizing the kinetics of blood flow, specially the initial phase, with good confidence in order to understand the mechanisms which govern the dynamic matching of O₂ delivery and uptake during exercise. Application of a low-pass filter to Doppler blood flow data improved the signal-to-noise ratio yielding narrow confidence intervals of parameter estimates that are necessary to draw definitive conclusions regarding putative mechanisms controlling blood flow (or O₂ delivery) kinetics.

References

- Adams, V., Spate, U., Krankel, N., Schulze, P.C., Linke, A., Schuler, G., & Hambrecht, R.** (2003). Nuclear factor-kappa B activation in skeletal muscle of patients with chronic heart failure: correlation with the expression of inducible nitric oxide synthase. *Eur J Cardiovasc Prev Rehabil* **10**, 273-277.
- Bagi, Z. & Koller, A.** (2003). Lack of nitric oxide mediation of flow-dependent arteriolar dilation in type I diabetes is restored by sepiapterin. *J Vasc Res* **40**, 47-57.
- Bailey, J.K., Kindig, C.A., Behnke, B.J., Musch, T.I., Schmid-Schoenbein, G.W., & Poole, D.C.** (2000). Spinotrapezius muscle microcirculatory function: effects of surgical exteriorization. *Am J Physiol Heart Circ Physiol* **279**, H3131-H3137.
- Bangsbo, J., Krstrup, P., Gonzalez-Alonso, J., Boushel, R., & Saltin, B.** (2000). Muscle oxygen kinetics at onset of intense dynamic exercise in humans. *Am J Physiol Regul Integr Comp Physiol* **279**, R899-R906.
- Barstow, T.J., Lamarra, N., & Whipp, B.J.** (1990). Modulation of muscle and pulmonary O₂ uptakes by circulatory dynamics during exercise. *J Appl Physiol* **68**, 979-989.
- Barstow, T.J. & Mole, P.A.** (1987). Simulation of pulmonary O₂ uptake during exercise transients in humans. *J Appl Physiol* **63**, 2253-2261.
- Beaver, W.L., Wasserman, K., & Whipp, B.J.** (1986). A new method for detecting anaerobic threshold by gas exchange. *J Appl Physiol* **60**, 2020-2027.
- Behnke, B.J., Barstow, T.J., Kindig, C.A., McDonough, P., Musch, T.I., & Poole, D.C.** (2002a). Dynamics of oxygen uptake following exercise onset in rat skeletal muscle. *Respir Physiol Neurobiol* **133**, 229-239.
- Behnke, B.J., Delp, M.D., Dougherty, P.J., Musch, T.I., & Poole, D.C.** (2005). Effects of aging on microvascular oxygen pressures in rat skeletal muscle. *Respir Physiol Neurobiol* **146**, 259-268.
- Behnke, B.J., Kindig, C.A., McDonough, P., Poole, D.C., & Sexton, W.L.** (2002b). Dynamics of microvascular oxygen pressure during rest-contraction transition in skeletal muscle of diabetic rats. *Am J Physiol Heart Circ Physiol* **283**, H926-H932.
- Behnke, B.J., Kindig, C.A., Musch, T.I., Koga, S., & Poole, D.C.** (2001). Dynamics of microvascular oxygen pressure across the rest-exercise transition in rat skeletal muscle. *Respir Physiol* **126**, 53-63.

Behnke, B.J., Kindig, C.A., Musch, T.I., Sexton, W.L., & Poole, D.C. (2002c). Effects of prior contractions on muscle microvascular oxygen pressure at onset of subsequent contractions. *J Physiol* **539**, 927-934.

Behnke, B.J., McDonough, P., Padilla, D.J., Musch, T.I., & Poole, D.C. (2003). Oxygen exchange profile in rat muscles of contrasting fibre types. *J Physiol* **549**, 597-605.

Belardinelli, R., Barstow, T.J., Nguyen, P., & Wasserman, K. (1997). Skeletal muscle oxygenation and oxygen uptake kinetics following constant work rate exercise in chronic congestive heart failure. *Am J Cardiol* **80**, 1319-1324.

Bell, C., Paterson, D.H., Kowalchuk, J.M., & Cunningham, D.A. (1999). Oxygen uptake kinetics of older humans are slowed with age but are unaffected by hyperoxia. *Exp Physiol* **84**, 747-759.

Bojunga, J., Dresar-Mayert, B., Usadel, K.H., Kusterer, K., & Zeuzem, S. (2004). Antioxidative treatment reverses imbalances of nitric oxide synthase isoform expression and attenuates tissue-cGMP activation in diabetic rats. *Biochem Biophys Res Commun* **316**, 771-780.

Brown, G.C. (2000). Nitric oxide as a competitive inhibitor of oxygen consumption in the mitochondrial respiratory chain. *Acta Physiol Scand* **168**, 667-674.

Buckwalter, J.B., Ruble, S.B., Mueller, P.J., & Clifford, P.S. (1998). Skeletal muscle vasodilation at the onset of exercise. *J Appl Physiol* **85**, 1649-1654.

Burnley, M., Doust, J.H., Ball, D., & Jones, A.M. (2002). Effects of prior heavy exercise on $\dot{V}O_2$ kinetics during heavy exercise are related to changes in muscle activity. *J Appl Physiol* **93**, 167-174.

Clifford, P.S. & Hellsten, Y. (2004). Vasodilatory mechanisms in contracting skeletal muscle. *J Appl Physiol* **97**, 393-403.

Costes, F., Barthelemy, J.C., Feasson, L., Busso, T., Geysant, A., & Denis, C. (1996). Comparison of muscle near-infrared spectroscopy and femoral blood gases during steady-state exercise in humans. *J Appl Physiol* **80**, 1345-1350.

De Vriese, A.S., Verbeuren, T.J., Van, d., V, Lameire, N.H., & Vanhoutte, P.M. (2000). Endothelial dysfunction in diabetes. *Br J Pharmacol* **130**, 963-974.

DeLorey, D.S., Kowalchuk, J.M., & Paterson, D.H. (2003). Relationship between pulmonary O_2 uptake kinetics and muscle deoxygenation during moderate-intensity exercise. *J Appl Physiol* **95**, 113-120.

DeLorey, D.S., Kowalchuk, J.M., & Paterson, D.H. (2004a). Effect of age on O_2 uptake kinetics and the adaptation of muscle deoxygenation at the onset of moderate-intensity cycling exercise. *J Appl Physiol* **97**, 165-172.

DeLorey, D.S., Kowalchuk, J.M., & Paterson, D.H. (2004b). Effects of Prior Heavy-Intensity Exercise on Pulmonary O₂ Uptake and Muscle Deoxygenation Kinetics in Young and Older Adult Humans. *J Appl Physiol* **97**, 998-1005.

DeLorey, D.S., Shaw, C.N., Shoemaker, J.K., Kowalchuk, J.M., & Paterson, D.H. (2004c). The effect of hypoxia on pulmonary O₂ uptake, leg blood flow and muscle deoxygenation during single-leg knee-extension exercise. *Exp Physiol* **89**, 293-302.

Didion, S.P. & Mayhan, W.G. (1997). Effect of chronic myocardial infarction on in vivo reactivity of skeletal muscle arterioles. *Am J Physiol* **272**, H2403-H2408.

Diederich, E.R., Behnke, B.J., McDonough, P., Kindig, C.A., Barstow, T.J., Poole, D.C., & Musch, T.I. (2002). Dynamics of microvascular oxygen partial pressure in contracting skeletal muscle of rats with chronic heart failure. *Cardiovasc Res* **56**, 479-486.

Dobson, J.L. & Gladden, L.B. (2003). Effect of rhythmic tetanic skeletal muscle contractions on peak muscle perfusion. *J Appl Physiol* **94**, 11-19.

Drexler, H., Hayoz, D., Munzel, T., Hornig, B., Just, H., Brunner, H.R., & Zelis, R. (1992). Endothelial function in chronic congestive heart failure. *Am J Cardiol* **69**, 1596-1601.

Ferrari, M., Binzoni, T., & Quaresima, V. (1997). Oxidative metabolism in muscle. *Philos Trans R Soc Lond B Biol Sci* **352**, 677-683.

Ferreira, L.F., Poole, D.C., & Barstow, T.J. (2005a). Muscle blood flow - O₂ uptake interaction and their relation to on-exercise dynamic of O₂ exchange. *Respir Physiol Neurobiol* **147**, 91-103.

Ferreira, L.F., Townsend, D.K., Lutjemeier, B.J., & Barstow, T.J. (2005b). Muscle capillary blood flow kinetics estimated from pulmonary O₂ uptake and near-infrared spectroscopy. *J Appl Physiol* **98**, 1820-1828.

Fukuba, Y., Ohe, Y., Miura, A., Kitano, A., Endo, M., Sato, H., Miyachi, M., Koga, S., & Fukuda, O. (2004). Dissociation between the time courses of femoral artery blood flow and pulmonary $\dot{V}O_2$ during repeated bouts of heavy knee extension exercise in humans. *Exp Physiol* **89**, 243-253.

Geer, C.M., Behnke, B.J., McDonough, P., & Poole, D.C. (2002). Dynamics of microvascular oxygen pressure in the rat diaphragm. *J Appl Physiol* **93**, 227-232.

Gielen, S., Adams, V., Linke, A., Erbs, S., Mobius-Winkler, S., Schubert, A., Schuler, G., & Hambrecht, R. (2005). Exercise training in chronic heart failure: correlation between reduced local inflammation and improved oxidative capacity in the skeletal muscle. *Eur J Cardiovasc Prev Rehabil* **12**, 393-400.

Gill, R.W. (1985). Measurement of blood flow by ultrasound: accuracy and sources of error. *Ultrasound Med Biol* **11**, 625-641.

Gorczynski, R.J., Klitzman, B., & Duling, B.R. (1978). Interrelations between contracting striated muscle and precapillary microvessels. *Am J Physiol* **235**, H494-H504.

Grassi, B., Gladden, L.B., Samaja, M., Stary, C.M., & Hogan, M.C. (1998). Faster adjustment of O₂ delivery does not affect $\dot{V}O_2$ on-kinetics in isolated in situ canine muscle. *J Appl Physiol* **85**, 1394-1403.

Grassi, B., Hogan, M.C., Greenhaff, P.L., Hamann, J.J., Kelley, K.M., Aschenbach, W.G., Constantin-Teodosiu, D., & Gladden, L.B. (2002). Oxygen uptake on-kinetics in dog gastrocnemius in situ following activation of pyruvate dehydrogenase by dichloroacetate. *J Physiol* **538**, 195-207.

Grassi, B., Hogan, M.C., Kelley, K.M., Aschenbach, W.G., Hamann, J.J., Evans, R.K., Patillo, R.E., & Gladden, L.B. (2000). Role of convective O₂ delivery in determining $\dot{V}O_2$ on-kinetics in canine muscle contracting at peak $\dot{V}O_2$. *J Appl Physiol* **89**, 1293-1301.

Grassi, B., Hogan, M.C., Kelley, K.M., Howlett, R.A., & Gladden, L.B. (2005). Effects of nitric oxide synthase inhibition by L-NAME on oxygen uptake kinetics in isolated canine muscle in situ. *J Physiol* **568**, 1021-1033.

Grassi, B., Pogliaghi, S., Rampichini, S., Quaresima, V., Ferrari, M., Marconi, C., & Cerretelli, P. (2003). Muscle oxygenation and pulmonary gas exchange kinetics during cycling exercise on-transitions in humans. *J Appl Physiol* **95**, 149-158.

Grassi, B., Poole, D.C., Richardson, R.S., Knight, D.R., Erickson, B.K., & Wagner, P.D. (1996). Muscle O₂ uptake kinetics in humans: implications for metabolic control. *J Appl Physiol* **80**, 988-998.

Grassi, B., Quaresima, V., Marconi, C., Ferrari, M., & Cerretelli, P. (1999). Blood lactate accumulation and muscle deoxygenation during incremental exercise. *J Appl Physiol* **87**, 348-355.

Gratton, E., Fantini, S., Franceschini, M.A., Gratton, G., & Fabiani, M. (1997). Measurements of scattering and absorption changes in muscle and brain. *Philos Trans R Soc Lond B Biol Sci* **352**, 727-735.

Hamann, J.J., Buckwalter, J.B., & Clifford, P.S. (2004a). Vasodilatation is obligatory for contraction-induced hyperaemia in canine skeletal muscle. *J Physiol* **557**, 1013-1020.

Hamann, J.J., Buckwalter, J.B., Clifford, P.S., & Shoemaker, J.K. (2004b). Is the blood flow response to a single contraction determined by work performed? *J Appl Physiol* **96**, 2146-2152.

Hamann, J.J., Valic, Z., Buckwalter, J.B., & Clifford, P.S. (2003). Muscle pump does not enhance blood flow in exercising skeletal muscle. *J Appl Physiol* **94**, 6-10.

Hambrecht, R., Adams, V., Gielen, S., Linke, A., Mobius-Winkler, S., Yu, J., Niebauer, J., Jiang, H., Fiehn, E., & Schuler, G. (1999). Exercise intolerance in patients with chronic heart failure and increased expression of inducible nitric oxide synthase in the skeletal muscle. *J Am Coll Cardiol* **33**, 174-179.

Hepple, R.T., Liu, P.P., Plyley, M.J., & Goodman, J.M. (1999). Oxygen uptake kinetics during exercise in chronic heart failure: influence of peripheral vascular reserve. *Clin Sci (Lond)* **97**, 569-577.

Hirai, T., Zelis, R., & Musch, T.I. (1995). Effects of nitric oxide synthase inhibition on the muscle blood flow response to exercise in rats with heart failure. *Cardiovasc Res* **30**, 469-476.

Hogan, M.C., Arthur, P.G., Bebout, D.E., Hochachka, P.W., & Wagner, P.D. (1992). Role of O₂ in regulating tissue respiration in dog muscle working in situ. *J Appl Physiol* **73**, 728-736.

Hueber, D.M., Franceschini, M.A., Ma, H.Y., Zhang, Q., Ballesteros, J.R., Fantini, S., Wallace, D., Ntziachristos, V., & Chance, B. (2001). Non-invasive and quantitative near-infrared haemoglobin spectrometry in the piglet brain during hypoxic stress, using a frequency-domain multidistance instrument. *Phys Med Biol* **46**, 41-62.

Hughson, R.L. (2003). Regulation of blood flow at the onset of exercise by feed forward and feedback mechanisms. *Can J Appl Physiol* **28**, 774-787.

Hughson, R.L., Shoemaker, J.K., Tschakovsky, M.E., & Kowalchuk, J.M. (1996). Dependence of muscle $\dot{V}O_2$ on blood flow dynamics at onset of forearm exercise. *J Appl Physiol* **81**, 1619-1626.

Hughson, R.L., Tschakovsky, M.E., & Houston, M.E. (2001). Regulation of oxygen consumption at the onset of exercise. *Exerc Sport Sci Rev* **29**, 129-133.

Jones, A.M., Wilkerson, D.P., & Campbell, I.T. (2004a). Nitric oxide synthase inhibition with L-NAME reduces maximal oxygen uptake but not gas exchange threshold during incremental cycle exercise in man. *J Physiol* **560**, 329-338.

Jones, A.M., Wilkerson, D.P., Koppo, K., Wilmschurst, S., & Campbell, I.T. (2003). Inhibition of nitric oxide synthase by L-NAME speeds phase II pulmonary $\dot{V}O_2$ kinetics in the transition to moderate-intensity exercise in man. *J Physiol* **552**, 265-272.

Jones, A.M., Wilkerson, D.P., Wilmschurst, S., & Campbell, I.T. (2004b). Influence of L-NAME on pulmonary O₂ uptake kinetics during heavy-intensity cycle exercise. *J Appl Physiol* **96**, 1033-1038.

Jones, A.M. & Poole, D.C. (2005). Oxygen uptake kinetics in sport, exercise and medicine, 1st ed. Routledge, New York, NY.

Joyner, M.J. & Dietz, N.M. (1997). Nitric oxide and vasodilation in human limbs. *J Appl Physiol* **83**, 1785-1796.

Kindig, C.A., Kelley, K.M., Howlett, R.A., Stary, C.M., & Hogan, M.C. (2003). Assessment of O₂ uptake dynamics in isolated single skeletal myocytes. *J Appl Physiol* **94**, 353-357.

Kindig, C.A., McDonough, P., Erickson, H.H., & Poole, D.C. (2002a). Nitric oxide synthase inhibition speeds oxygen uptake kinetics in horses during moderate domain running. *Respir Physiol Neurobiol* **132**, 169-178.

Kindig, C.A., McDonough, P., Erickson, H.H., & Poole, D.C. (2001). Effect of L-NAME on oxygen uptake kinetics during heavy-intensity exercise in the horse. *J Appl Physiol* **91**, 891-896.

Kindig, C.A., Richardson, T.E., & Poole, D.C. (2002b). Skeletal muscle capillary hemodynamics from rest to contractions: implications for oxygen transfer. *J Appl Physiol* **92**, 2513-2520.

Koga, S., Poole, D.C., Shiojiri, T., Kondo, N., Fukuba, Y., Miura, A., & Barstow, T.J. (2005). A comparison of oxygen uptake kinetics during knee extension and cycle exercise. *Am J Physiol Regul Integr Comp Physiol* **288**, R212-R220.

Lahiri, S., Rumsey, W.L., Wilson, D.F., & Iturriaga, R. (1993). Contribution of in vivo microvascular PO₂ in the cat carotid body chemotransduction. *J Appl Physiol* **75**, 1035-1043.

Lamarra, N. (1990). Variables, constants, and parameters: clarifying the system structure. *Med Sci Sports Exerc* **22**, 88-95.

Lamarra, N., Whipp, B.J., Ward, S.A., & Wasserman, K. (1987). Effect of interbreath fluctuations on characterizing exercise gas exchange kinetics. *J Appl Physiol* **62**, 2003-2012.

Laughlin, M.H. & Armstrong, R.B. (1982). Muscular blood flow distribution patterns as a function of running speed in rats. *Am J Physiol* **243**, H296-H306.

Laughlin, M.H. & Korzick, D.H. (2001). Vascular smooth muscle: integrator of vasoactive signals during exercise hyperemia. *Med Sci Sports Exerc* **33**, 81-91.

Lexell, J., Henriksson-Larsen, K., & Sjostrom, M. (1983). Distribution of different fibre types in human skeletal muscles. 2. A study of cross-sections of whole m. vastus lateralis. *Acta Physiol Scand* **117**, 115-122.

Li, L. & Caldwell, G.E. (1998). Muscle coordination in cycling: effect of surface incline and posture. *J Appl Physiol* **85**, 927-934.

Lo, L., Vinogradov, S.A., Koch, C., & Wilson, D.F. (1997). A new, water soluble, phosphor for oxygen measurements in vivo. *Adv Exp Med Biol* **428**, 651-656.

Lutjemeier, B.J., Miura, A., Scheuermann, B.W., Koga, S., Townsend, D.K., & Barstow, T.J. (2005). Muscle contraction-blood flow interactions during upright knee extension exercise in humans. *J Appl Physiol* **98**, 1575-1583.

MacDonald, M.J., Pedersen, P.K., & Hughson, R.L. (1997). Acceleration of $\dot{V}O_2$ kinetics in heavy submaximal exercise by hyperoxia and prior high-intensity exercise. *J Appl Physiol* **83**, 1318-1325.

MacDonald, M.J., Shoemaker, J.K., Tschakovsky, M.E., & Hughson, R.L. (1998). Alveolar oxygen uptake and femoral artery blood flow dynamics in upright and supine leg exercise in humans. *J Appl Physiol* **85**, 1622-1628.

MacDonald, M.J., Tarnopolsky, M.A., Green, H.J., & Hughson, R.L. (1999). Comparison of femoral blood gases and muscle near-infrared spectroscopy at exercise onset in humans. *J Appl Physiol* **86**, 687-693.

MacDonald, M.J., Tarnopolsky, M.A., & Hughson, R.L. (2000). Effect of hyperoxia and hypoxia on leg blood flow and pulmonary and leg oxygen uptake at the onset of kicking exercise. *Can J Physiol Pharmacol* **78**, 67-74.

Mancini, D.M., Bolinger, L., Li, H., Kendrick, K., Chance, B., & Wilson, J.R. (1994). Validation of near-infrared spectroscopy in humans. *J Appl Physiol* **77**, 2740-2747.

McCully, K.K. & Hamaoka, T. (2000). Near-infrared spectroscopy: what can it tell us about oxygen saturation in skeletal muscle? *Exerc Sport Sci Rev* **28**, 123-127.

McDonough, P., Behnke, B.J., Padilla, D.J., Musch, T.I., & Poole, D.C. (2005). Control of microvascular oxygen pressures in rat muscles comprised of different fibre types. *J Physiol* **563**, 903-913.

Meakins, J. & Long, C. (1927). Oxygen consumption, oxygen debt and lactic acid in circulatory failure. *J Clin Invest* **4**, 273-293.

Mizuno, M., Kimura, Y., Iwakawa, T., Oda, K., Ishii, K., Ishiwata, K., Nakamura, Y., & Muraoka, I. (2003). Regional differences in blood flow and oxygen consumption in resting muscle and their relationship during recovery from exhaustive exercise. *J Appl Physiol* **95**, 2204-2210.

Nishikawa, Y., Stepp, D.W., & Chilian, W.M. (2000). Nitric oxide exerts feedback inhibition on EDHF-induced coronary arteriolar dilation in vivo. *Am J Physiol Heart Circ Physiol* **279**, H459-H465.

Osada, T. (2004). Muscle contraction-induced limb blood flow variability during dynamic knee extensor. *Med Sci Sports Exerc* **36**, 1149-1158.

Pawlowski, M. & Wilson, D.F. (1992). Monitoring of the oxygen pressure in the blood of live animals using the oxygen dependent quenching of phosphorescence. *Adv Exp Med Biol* **316**, 179-185.

Piiper, J., di Prampero, P.E., & Cerretelli, P. (1968). Oxygen debt and high-energy phosphates in gastrocnemius muscle of the dog. *Am J Physiol* **215**, 523-531.

Poole, D.C., Behnke, B.J., McDonough, P., McAllister, R.M., & Wilson, D.F. (2004). Measurement of muscle microvascular oxygen pressures: compartmentalization of phosphorescent probe. *Microcirculation* **11**, 317-326.

Poole, D.C., Schaffartzik, W., Knight, D.R., Derion, T., Kennedy, B., Guy, H.J., Prediletto, R., & Wagner, P.D. (1991). Contribution of excising legs to the slow component of oxygen uptake kinetics in humans. *J Appl Physiol* **71**, 1245-1260.

Poole, D.C., Wagner, P.D., & Wilson, D.F. (1995). Diaphragm microvascular plasma PO₂ measured in vivo. *J Appl Physiol* **79**, 2050-2057.

Radegran, G. (1997). Ultrasound Doppler estimates of femoral artery blood flow during dynamic knee extensor exercise in humans. *J Appl Physiol* **83**, 1383-1388.

Radegran, G. & Saltin, B. (1998). Muscle blood flow at onset of dynamic exercise in humans. *Am J Physiol* **274**, H314-H322.

Radegran, G. & Saltin, B. (1999). Nitric oxide in the regulation of vasomotor tone in human skeletal muscle. *Am J Physiol* **276**, H1951-H1960.

Regensteiner, J.G., Bauer, T.A., Reusch, J.E., Brandenburg, S.L., Sippel, J.M., Vogelsong, A.M., Smith, S., Wolfel, E.E., Eckel, R.H., & Hiatt, W.R. (1998). Abnormal oxygen uptake kinetic responses in women with type II diabetes mellitus. *J Appl Physiol* **85**, 310-317.

Richardson, R.S., Noyszewski, E.A., Kendrick, K.F., Leigh, J.S., & Wagner, P.D. (1995). Myoglobin O₂ desaturation during exercise. Evidence of limited O₂ transport. *J Clin Invest* **96**, 1916-1926.

Richardson, R.S., Poole, D.C., Knight, D.R., Kurdak, S.S., Hogan, M.C., Grassi, B., Johnson, E.C., Kendrick, K.F., Erickson, B.K., & Wagner, P.D. (1993). High muscle blood flow in man: is maximal O₂ extraction compromised? *J Appl Physiol* **75**, 1911-1916.

Richardson, T.E., Kindig, C.A., Musch, T.I., & Poole, D.C. (2003). Effects of chronic heart failure on skeletal muscle capillary hemodynamics at rest and during contractions. *J Appl Physiol* **95**, 1055-1062.

Riley, M., Porszasz, J., Stanford, C.F., & Nicholls, D.P. (1994). Gas exchange responses to constant work rate exercise in chronic cardiac failure. *Br Heart J* **72**, 150-155.

Roach, R.C., Koskolou, M.D., Calbet, J.A., & Saltin, B. (1999). Arterial O₂ content and tension in regulation of cardiac output and leg blood flow during exercise in humans. *Am J Physiol* **276**, H438-H445.

Roca, J., Hogan, M.C., Story, D., Bebout, D.E., Haab, P., Gonzalez, R., Ueno, O., & Wagner, P.D. (1989). Evidence for tissue diffusion limitation of $\dot{V}O_{2\max}$ in normal humans. *J Appl Physiol* **67**, 291-299.

Rossiter, H.B., Howe, F.A., Ward, S.A., Kowalchuk, J.M., Griffiths, J.R., & Whipp, B.J. (2000). Intersample fluctuations in phosphocreatine concentration determined by ³¹P-magnetic resonance spectroscopy and parameter estimation of metabolic responses to exercise in humans. *J Physiol* **528 Pt 2**, 359-369.

Rossiter, H.B., Ward, S.A., Doyle, V.L., Howe, F.A., Griffiths, J.R., & Whipp, B.J. (1999). Inferences from pulmonary O₂ uptake with respect to intramuscular [phosphocreatine] kinetics during moderate exercise in humans. *J Physiol* **518 (Pt 3)**, 921-932.

Rumsey, W.L., Vanderkooi, J.M., & Wilson, D.F. (1988). Imaging of phosphorescence: a novel method for measuring oxygen distribution in perfused tissue. *Science* **241**, 1649-1651.

Saunders, N.R., Pyke, K.E., & Tschakovsky, M.E. (2005). Dynamic response characteristics of local muscle blood flow regulatory mechanisms in human forearm exercise. *J Appl Physiol* **98**, 1286-1296.

Scheuermann, B.W., Bell, C., Paterson, D.H., Barstow, T.J., & Kowalchuk, J.M. (2002). Oxygen uptake kinetics for moderate exercise are speeded in older humans by prior heavy exercise. *J Appl Physiol* **92**, 609-616.

Segal, S.S. (2000). Integration of blood flow control to skeletal muscle: key role of feed arteries. *Acta Physiol Scand* **168**, 511-518.

Seiyama, A., Hazeki, O., & Tamura, M. (1988). Noninvasive quantitative analysis of blood oxygenation in rat skeletal muscle. *J Biochem (Tokyo)* **103**, 419-424.

Shen, W., Xu, X., Ochoa, M., Zhao, G., Wolin, M.S., & Hintze, T.H. (1994). Role of nitric oxide in the regulation of oxygen consumption in conscious dogs. *Circ Res* **75**, 1086-1095.

Sheriff, D.D. & Hakeman, A.L. (2001). Role of speed vs. grade in relation to muscle pump function at locomotion onset. *J Appl Physiol* **91**, 269-276.

Sheriff, D.D., Rowell, L.B., & Scher, A.M. (1993). Is rapid rise in vascular conductance at onset of dynamic exercise due to muscle pump? *Am J Physiol* **265**, H1227-H1234.

Shiotani, I., Sato, H., Sato, H., Yokoyama, H., Ohnishi, Y., Hishida, E., Kinjo, K., Nakatani, D., Kuzuya, T., & Hori, M. (2002). Muscle pump-dependent self-perfusion

mechanism in legs in normal subjects and patients with heart failure. *J Appl Physiol* **92**, 1647-1654.

Shoemaker, J.K., Halliwill, J.R., Hughson, R.L., & Joyner, M.J. (1997).

Contributions of acetylcholine and nitric oxide to forearm blood flow at exercise onset and recovery. *Am J Physiol* **273**, H2388-H2395.

Shoemaker, J.K., Hodge, L., & Hughson, R.L. (1994). Cardiorespiratory kinetics and femoral artery blood velocity during dynamic knee extension exercise. *J Appl Physiol* **77**, 2625-2632.

Shoemaker, J.K. & Hughson, R.L. (1999). Adaptation of blood flow during the rest to work transition in humans. *Med Sci Sports Exerc* **31**, 1019-1026.

Shoemaker, J.K., Naylor, H.L., Hogeman, C.S., & Sinoway, L.I. (1999). Blood flow dynamics in heart failure. *Circulation* **99**, 3002-3008.

Shoemaker, J.K., Naylor, H.L., Pozeg, Z.I., & Hughson, R.L. (1996a). Failure of prostaglandins to modulate the time course of blood flow during dynamic forearm exercise in humans. *J Appl Physiol* **81**, 1516-1521.

Shoemaker, J.K., Phillips, S.M., Green, H.J., & Hughson, R.L. (1996b). Faster femoral artery blood velocity kinetics at the onset of exercise following short-term training. *Cardiovasc Res* **31**, 278-286.

Shoemaker, J.K., Pozeg, Z.I., & Hughson, R.L. (1996c). Forearm blood flow by Doppler ultrasound during test and exercise: tests of day-to-day repeatability. *Med Sci Sports Exerc* **28**, 1144-1149.

Taddei, S., Viridis, A., Mattei, P., Ghiadoni, L., Gennari, A., Fasolo, C.B., Sudano, I., & Salvetti, A. (1995). Aging and endothelial function in normotensive subjects and patients with essential hypertension. *Circulation* **91**, 1981-1987.

Tanabe, T., Maeda, S., Miyauchi, T., Iemitsu, M., Takanashi, M., Irukayama-Tomobe, Y., Yokota, T., Ohmori, H., & Matsuda, M. (2003). Exercise training improves ageing-induced decrease in eNOS expression of the aorta. *Acta Physiol Scand* **178**, 3-10.

Thomas, G.D. & Segal, S.S. (2004). Neural control of muscle blood flow during exercise. *J Appl Physiol* **97**, 731-738.

Tordi, N., Perrey, S., Harvey, A., & Hughson, R.L. (2003). Oxygen uptake kinetics during two bouts of heavy cycling separated by fatiguing sprint exercise in humans. *J Appl Physiol* **94**, 533-541.

Tran, T.K., Sailasuta, N., Kreutzer, U., Hurd, R., Chung, Y., Mole, P., Kuno, S., & Jue, T. (1999). Comparative analysis of NMR and NIRS measurements of intracellular PO₂ in human skeletal muscle. *Am J Physiol* **276**, R1682-R1690.

Tschakovsky, M.E. & Hughson, R.L. (1999). Interaction of factors determining oxygen uptake at the onset of exercise. *J Appl Physiol* **86**, 1101-1113.

Tschakovsky, M.E., Rogers, A.M., Pyke, K.E., Saunders, N.R., Glenn, N., Lee, S.J., Weissgerber, T., & Dwyer, E.M. (2004). Immediate exercise hyperemia in humans is contraction intensity dependent: evidence for rapid vasodilation. *J Appl Physiol* **96**, 639-644.

Tschakovsky, M.E. & Sheriff, D.D. (2004). Immediate exercise hyperemia: contributions of the muscle pump vs. rapid vasodilation. *J Appl Physiol* **97**, 739-747.

Tschakovsky, M.E., Shoemaker, J.K., & Hughson, R.L. (1996). Vasodilation and muscle pump contribution to immediate exercise hyperemia. *Am J Physiol* **271**, H1697-H1701.

Varin, R., Mulder, P., Richard, V., Tamion, F., Devaux, C., Henry, J.P., Lallemand, F., Lerebours, G., & Thuillez, C. (1999). Exercise improves flow-mediated vasodilatation of skeletal muscle arteries in rats with chronic heart failure. Role of nitric oxide, prostanoids, and oxidant stress. *Circulation* **99**, 2951-2957.

Vinogradov, S.A., Fernandez-Seara, M.A., Dupan, B.W., & Wilson, D.F. (2002). A method for measuring oxygen distributions in tissue using frequency domain phosphorometry. *Comp Biochem Physiol A Mol Integr Physiol* **132**, 147-152.

Wagner, P.D. (1996). Determinants of maximal oxygen transport and utilization. *Annu Rev Physiol* **58**, 21-50.

Walloe, L. & Wesche, J. (1988). Time course and magnitude of blood flow changes in the human quadriceps muscles during and following rhythmic exercise. *J Physiol* **405**, 257-273.

Wasserman, K., Whipp, B.J., Koyle, S.N., & Beaver, W.L. (1973). Anaerobic threshold and respiratory gas exchange during exercise. *J Appl Physiol* **35**, 236-243.

Whipp, B.J., Lamarra, N., & Ward, S.A. (1995). Obligatory anaerobiosis resulting from oxygen uptake-to-blood flow ratio dispersion in skeletal muscle: a model. *Eur J Appl Physiol Occup Physiol* **71**, 147-152.

Whipp, B.J., Ward, S.A., Lamarra, N., Davis, J.A., & Wasserman, K. (1982). Parameters of ventilatory and gas exchange dynamics during exercise. *J Appl Physiol* **52**, 1506-1513.

Wilkerson, D.P., Koppo, K., Barstow, T.J., & Jones, A.M. (2004). Effect of prior multiple-sprint exercise on pulmonary O₂ uptake kinetics following the onset of perimaximal exercise. *J Appl Physiol* **97**, 1227-1236.

Wilson, D.F., Erecinska, M., Drown, C., & Silver, I.A. (1977). Effect of oxygen tension on cellular energetics. *Am J Physiol* **233**, C135-C140.

Wilson, J.R., Mancini, D.M., McCully, K., Ferraro, N., Lanoce, V., & Chance, B. (1989). Noninvasive detection of skeletal muscle underperfusion with near-infrared spectroscopy in patients with heart failure. *Circulation* **80**, 1668-1674.

Woodman, C.R., Price, E.M., & Laughlin, M.H. (2002). Aging induces muscle-specific impairment of endothelium-dependent dilation in skeletal muscle feed arteries. *J Appl Physiol* **93**, 1685-1690.

Woodman, C.R., Schrage, W.G., Rush, J.W., Ray, C.A., Price, E.M., Hasser, E.M., & Laughlin, M.H. (2001). Hindlimb unweighting decreases endothelium-dependent dilation and eNOS expression in soleus not gastrocnemius. *J Appl Physiol* **91**, 1091-1098.

Wray, D.W., Fadel, P.J., Keller, D.M., Ogoh, S., Sander, M., Raven, P.B., & Smith, M.L. (2004). Dynamic carotid baroreflex control of the peripheral circulation during exercise in humans. *J Physiol* **559**, 675-684.

Wunsch, S.A., Muller-Delp, J., & Delp, M.D. (2000). Time course of vasodilatory responses in skeletal muscle arterioles: role in hyperemia at onset of exercise. *Am J Physiol Heart Circ Physiol* **279**, H1715-H1723.

Yamamoto, Y. & Hughson, R.L. (1993). Extracting fractal components from time series. *Physica D* **68**, 250-264.

Appendix A - Curriculum Vitae

Leonardo Franklin Ferreira

Address: Department of Anatomy and Physiology, Kansas State University
1600 Denison Ave, 228 Coles Hall
66506-5802, Manhattan, KS - USA
Phone: (785) 532-4476
e-mail: ferreira@ksu.edu

Education

- 2003 - Ph.D. in Physiology (*In Progress*)
Department of Anatomy and Physiology, Kansas State University
- 1999 - 2003 Physical Therapy
Universidade Estadual de Londrina (UEL), Brazil.

Research/Work experience

- 2005 - Research Assistant. Clarenburg Research Laboratory. Dept. Anatomy and Physiology, Kansas State University.

Awards

- 2005 Doctoral Student Award. American College of Sports Medicine - Central States Chapter.
- 2002 3rd Place in the International Symposium of Respiratory Physical Therapy, Brazilian Society of Respiratory Physical Therapy.
- 2000 1st Place in the Undergraduate Research Project of the III Meeting of Scientific Activities of the Universidade do Norte do Paraná.

Memberships: American Physiological Society
American College of Sports Medicine
Brazilian Society of Physiology

Grants:

- 2006 Skeletal muscle microvascular oxygen delivery and fatigue in aging: effects of antioxidants. American Heart Association, Grant-in-Aid, P.I. Musch, T.I. *In review.*
- 2005 Dynamic association between muscle O₂ delivery and uptake: role of nitric oxide and gender differences. American Heart Association, Grant-in-Aid, P.I. Barstow, T.B. Not funded.
- 2003 - 2007 Pre-Doctoral Grant, Ministry of Education CAPES/Brazil, “Dynamics of muscle blood flow, O₂ uptake and muscle microvascular oxygenation during exercise.” US\$ 110,000.

Fellowships:

- 07/2006 Postdoctoral Fellowship, Japan Society for the Promotion of Science, “Muscle blood flow and heterogeneity of microvascular oxygenation kinetics during severe-intensity exercise.” US\$ 6,000.
- 2006 Clarenburg Fellow. Clarenburg Research Laboratory, Dept. of Anatomy & Physiology, College of Veterinary Medicine, Kansas State University. US\$ 1,000
- 2005 Clarenburg Fellow. Clarenburg Research Laboratory, Dept. of Anatomy & Physiology, College of Veterinary Medicine, Kansas State University. US\$ 1,000.
- 2002 - 2003 National Institute of Scientific and Technological Development (CNPq - Brazil), Undergraduate Research Training Grant. “Cardiopulmonary autonomic modulation and exercise capacity of COPD patients.” R\$ 3,000 (~ US\$ 1,000).

2001 - 2002 National Institute of Scientific and Technological Development (CNPq -Brazil), Undergraduate Research Training Grant. "Ventilatory Capacity, O₂ desaturation and exercise performance of COPD patients." R\$ 3,000 (~ US\$ 1,000).

Publications:

Research Papers, peer reviewed

1. Hahn S.A., Ferreira L.F., Williams J., Jansson K., Behnke B.J., Musch T.I., Poole D.C. Downhill running trains the rat spinotrapezius muscle. *J. Appl. Physiol* (In Press)
2. Ferreira L.F., Hageman K.S., Hahn S.A., Williams J., Padilla D.J., Poole D.C., Musch T.I. Muscle microvascular oxygenation in chronic heart failure: role of nitric oxide availability. *Acta Physiol.* 2006; 188:3-13.
3. Ferreira L.F., Padilla D.J., Musch T.I., Poole D.C. Temporal profile of skeletal muscle capillary hemodynamics during recovery from contractions. *J Physiol.* 2006; 573:787-797.
4. Harper A.J., Ferreira L.F., Lutjemeier B.J., Townsend D.K., Barstow T.J. Femoral artery and estimated muscle capillary blood flow kinetics following the onset of exercise. *Exp. Physiol* 2006; 91(4):661-671.
5. Ferreira L.F., Padilla D.J., Williams J., Hageman K.S., Musch T.I., Poole D.C. Effects of altered nitric oxide availability on rat muscle microvascular oxygenation during contractions. *Acta Physiol.* 2006; 186(3): 223-232.
6. Ferreira L.F., McDonough P., Behnke B.J., Musch T.I., Poole D.C. Blood flow and O₂ extraction as a function of O₂ uptake in rat muscles composed of different fiber type. *Respir. Physiol. Neurobiol.* (In press)
7. Ferreira L.F., Harper A.H., Barstow T.J. Frequency-domain characteristics and filtering of blood flow following the onset of exercise: implications for kinetics analysis. *J. Appl. Physiol.* 2006; 100(3): 817-825.

8. Ferreira L.F., Lutjemeier B.J., Townsend D.K., Barstow T.J. Effects of pedal frequency on estimated muscle microvascular O₂ extraction. *Eur. J. Appl. Physiol.* 2006; 96(5): 558-563.
9. Behnke B.J., Padilla D.J., Ferreira L.F., Delp M.D., Musch T.I., Poole D.C. Effects of hypovolemic hypotension on microvascular oxygen pressures in contracting skeletal muscles. *J. Appl. Physiol.* 2006; 100(3):1019-1026.
10. Ferreira L.F., Harper A.H., Townsend D.K., Lutjemeier B.J., Barstow T.J. Kinetics of estimated muscle capillary blood flow during recovery from exercise. *Exp. Physiol.* 2005, 90: 715-726.
11. Ferreira L.F., Poole D.C., Barstow T.J. Muscle blood flow - O₂ uptake interaction and their relation to on-exercise dynamic of O₂ exchange. *Respir. Physiol. Neurobiol.* 2005, 147: 91-103.
12. Ferreira L.F., Townsend D.K., Lutjemeier B.J., Barstow T.J. Muscle capillary blood flow kinetics estimated from pulmonary O₂ uptake and near-infrared spectroscopy. *J. Appl. Physiol.* 2005, 98:1820-1828.
13. Ferreira L.F., Lutjemeier B.J., Townsend D.K., Barstow T.J. Dynamics of skeletal muscle oxygenation during sequential bouts of moderate exercise. *Exp. Physiol.* 2005, 90: 393-401.

Research Papers, *in review*

1. Ferreira L.F., Hueber D.M., Barstow T.J., 2005. Effects of assuming constant optical scattering on measurements of muscle oxygenation by near-infrared spectroscopy during exercise. *J. Appl. Physiol.*

Research Papers, *in preparation*

1. Poole D.C. & Ferreira L.F. Invited Review - Oxygen exchange in the young and old: muscle-vascular-pulmonary coupling. *Exp. Physiol*

2. Ferreira L.F., Williams J., Behnke B.J., Musch T.I., Poole D.C. Capillary hemodynamics in contracting muscles of old rats.

Letters-to-the editor

1. Ferreira L.F., Barstow T.J. Kinetics of muscle oxygen use, oxygen content and blood flow during exercise: Reply. *J. Appl. Physiol.* 2005, 99: 2463-2469.
2. Barstow T.J., Lutjemeier B.J., Ferreira L.F. Kinetics of restoration of arteriolar tone after exercise. *J. Appl. Physiol.* 2005, 99: 775.

Abstracts

1. Ferreira L.F., Padilla D.J., Williams J., Hageman K.S., Musch T.I., Poole D.C. Effects of altered nitric oxide availability on rat muscle microvascular oxygenation during contractions. ACSM 2006.
2. Ferreira L.F., Padilla D.J., Williams J., Hageman K.S., Musch T.I., Poole D.C. Effects nitric oxide on skeletal muscle microvascular O₂ pressure of rats with chronic heart failure. FASEB 2006.
3. Ferreira L.F., Padilla D.J., Williams J., Hageman K.S., Musch T.I., Poole D.C. Effects of altered nitric oxide availability on rat muscle microvascular oxygenation during contractions. ACSM-CSC 2005.
4. Townsend D.K., Haub M.D., Lutjemeier B.J., Ferreira L.F., Harper A.H., Barstow T.J. Dissociation of glucose homeostasis from insulin sensitivity in college-age subjects at risk for type 2 diabetes. ACSM 2005
5. Lutjemeier B.J., Harms C.A., Harper A.H., Ferreira L.F., Townsend D.K., Barstow T.J. Pedal frequency does not alter the cardiac output: $\dot{V}O_2$ relationship during cycling. ACSM 2005

6. Ferreira L.F., Hueber D.M., Lutjemeier B.J., Townsend D.K., Barstow T.J. Muscle oxygenation during incremental exercise and recovery: implications of assuming constant scattering. ACSM 2005
7. Harper A.H., Ferreira L.F., Lutjemeier B.J., Townsend D.K., Barstow T.J. Estimated kinetics of muscle capillary blood flow during recovery from exercise. ACSM 2005
8. Ferreira L.F., Lutjemeier B.J., Townsend D.K., Poole D.C., Barstow T.J. Mechanistic bases for the dynamics of O₂ exchange following the onset of exercise. ACSM-CSC 2004
9. Townsend D.K., Ferreira L.F., Lutjemeier B.J., Barstow T.J. The effects of adipose tissue thickness on near-infrared spectrometry during intra-contraction knee-extension exercise. ACSM 2004
10. Barstow T.J., Ferreira L.F., Lutjemeier B.J., Townsend D.K. Tissue oxygen saturation by NIRS during 60 and 100 rpm ramp tests. ACSM 2004
11. Lutjemeier B.J., Townsend D.K., Ferreira L.F., Barstow T.J. Impact of muscle contraction on arterial blood flow and tissue gas exchange by NIRS. ACSM 2004
12. Ferreira L.F., Lutjemeier B.J., Townsend D.K., Barstow T.J. NIRS-Derived estimate of muscle blood flow kinetics during moderate- and heavy-intensity cycling exercise. ACSM 2004.
13. Ferreira L.F., Brunetto A.F. Adaptation of a mechanically-braked cycle-ergometer to the performance of ramp incremental exercise test. SOCESP 2003 - Brazil.
14. Ferreira L.F., Borges H.L., Lavado E.L., Brunetto A.F. Cardiac versus ventilatory limitation to exercise and ventilation-perfusion mismatch in spinal cord injured patients. SOCESP 2003 - Brazil.
15. Brunetto A.F., Yamaguti W.P.S., Ferreira L.F., Silva B.M., Suzumura E.A. Analysis of lactate production and clearance in patients with chronic obstructive pulmonary disease (COPD). SOBRAFIR 2003 - Brazil.

16. Brunetto A.F., Yamaguti W.P.S., Ferreira L.F., Silva B.M., Suzumura EA. Ventilatory capacity of patients with chronic obstructive pulmonary disease. FESBE 2003 - Brazil.

Presentations

- 07/2006 Skeletal muscle oxygenation during exercise: measurement and interpretation.
Faculty of Human Development, Kobe University, Japan.
- 07/2006 Near-Infrared light scattering in contracting skeletal muscle. Hamamatsu
Photonics Inc., Japan
- 01/2002 Cardiopulmonary exercise testing in COPD patients@ Division of Respiratory
Physical Therapy, Dept. Physical Therapy, Health Sciences Center, Universidade
Estadual de Londrina.